AD-A142 976 LITHIUM CELL REACTIONS(U) GTE LABS INC WALTHAM MA 1/1
W CLARK ET AL. DEC 83 AFWAL-TR-83-2083 F33615-81-C-2070

UNCLASSIFIED F/G 10/3 NL

END
DATE
FILMED
8-84
DTIC

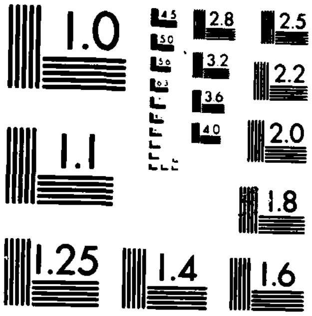

MICROCOPY RESOLUTION TEST CHART
NATIONAL BUREAU OF STANDARDS 1963 A

12

[illegible]83

LITHIUM CELL REACTIONS

[illegible] F. DAMPIER
A. LOMBARDI, T. COLE

GTE LABORATORIES, INCORPORATED
40 SYLVAN ROAD
[illegible]ALTHAM, MASSACHUSETTS 02154

[illegible]ECEMBER 1983

[illegible]NTERIM REPORT FOR PERIOD DECEMBER 1981 - MAY 1983

Approved for public release; distribution unlimited.

AER[illegible] PROPULSION LABORATORY
AIR [illegible]RCE WRIGHT AERONAUTICAL LABORATORIES
AIR [illegible]RCE SYSTEMS COMMAND
[illegible]-PATTERSON AIR FORCE BASE, OHIO 45433

NOTICE

This report has been reviewed by the Office of Public Affairs (ASD/PA) and is releasable to the National Technical Information Service (NTIS). At NTIS, it will be available to the general public, including foreign nations.

This technical report has been reviewed and is approved for publication.

Richard A. Marsh

RICHARD A. MARSH.
Energy Conversion Branch
Aerospace Power Division
Aero Propulsion Laboratory

Wayne S. Bishop

WAYNE S. BISHOP
TAM, Batteries/Fuel Cells
Energy Conversion Branch
Aerospace Power Division
Aero Propulsion Laboratory

FOR THE COMMANDER

J D Reams

JAMES D. REAMS
Chief, Aerospace Power Division
Aero Propulsion Laboratory

"If your address has changed, if you wish to be removed from our mailing list, or if the addressee is no longer employed by your organization please notify AFWAL/POOC-1 W-PAFB, OH 45433 to help us maintain a current mailing list".

Copies of this report should not be returned unless return is required by security considerations, contractual obligations, or notice on a specific document.

REPORT DOCUMENTATION PAGE		READ INSTRUCTIONS BEFORE COMPLETING FORM
1. REPORT NUMBER AFWAL-TR-83-2083	2. GOVT ACCESSION NO. A142976	3. RECIPIENT'S CATALOG NUMBER
4. TITLE (and Subtitle) Lithium Cell Reactions		5. TYPE OF REPORT & PERIOD COVERED Interim Report for Period Dec 81 - May 83
		6. PERFORMING ORG. REPORT NUMBER
7. AUTHOR(s) W. Clark, F. Dampier, A. Lombardi, & T. Cole		8. CONTRACT OR GRANT NUMBER(s) F33615-81-C-2070
9. PERFORMING ORGANIZATION NAME AND ADDRESS GTE Laboratories Inc. 40 Sylvan Road Waltham, MA 02254		10. PROGRAM ELEMENT PROJECT TASK AREA & WORK UNIT NUMBERS PE62203F Project 3145, Task 22 W.U. 96
11. CONTROLLING OFFICE NAME AND ADDRESS Aero Propulsion Laboratory (AFWAL/POOC) Air Force Wright Aeronautical Laboratories (AFSC) Wright-Patterson Air Force Base, Ohio 45433		12. REPORT DATE December 1983
		13. NUMBER OF PAGES 174
14. MONITORING AGENCY NAME & ADDRESS(if different from Controlling Office)		15. SECURITY CLASS. (of this report) Unclassified
		15a. DECLASSIFICATION DOWNGRADING SCHEDULE

16. DISTRIBUTION STATEMENT (of this Report)

Approved for Public Release; Distribution Unlimited

17. DISTRIBUTION STATEMENT (of the abstract entered in Block 20, if different from Report)

18. SUPPLEMENTARY NOTES

19. KEY WORDS (Continue on reverse side if necessary and identify by block number)

Batteries	Thionyl Chloride Batteries
Lithium Batteries	Lithium Cells
Primary Batteries	Thionyl Chloride Cells
Non Rechargeable Batteries	Electrochemical Reactions

20. ABSTRACT (Continue on reverse side if necessary and identify by block number)

The objectives of this program were: (i) investigate reactions occurring in the $Li/SOCL_2$ cell for a range of specified test conditions and (ii) perform detailed analyses for impurities present in cell components, assess the impact of each impurity on cell performance and safety and recommend concentration limits for detrimental impurities. The products of the reduction of $SOCL_2$ were investigated using linear sweep voltammetry (LSV) and constant current coulometry in dimethylformamide (DMF) supporting electrolyte. Voltammetric analysis after 50 to 100% of the $SOCL_2$ had been reduced on platinum or glassy carbon cathodes showed no

DD FORM 1 JAN 73 1473 EDITION OF 1 NOV 65 IS OBSOLETE signs of significant quantities of unstable intermediates with lifetimes from 0.1 to 48 hours. The ~~electroanalyses were carried~~ out in both ~~1.8M LiALCL~~$_4$/SOCL$_2$ neutral electrolyte ~~and 2.0M ALCL$_3$-0.1M LiCL/SOCL$_2$~~ acid electrolyte at 25°C. The decline of the SO$_2$ curent peak and the ~~development~~ of new peaks seen by voltammetry after approximately 12 hours storage ~~were determined~~ as being caused by a slow reaction between SO$_2$, DMF, SOCL$_2$ and possibly ~~LiALCL$_4$~~.

Quantitative infrared spectroscopy demonstrated that substantial amounts of SO$_2$ are absorbed on Shawinigan carbon from 1.8M LiALCL$_4$/SOCL$_2$-SO$_2$ solutions. ~~This new information has implications in understanding~~ cell hazards and in improving performance.

Chemical analyses of the reagents and cell components used in Li/SOCL$_2$ cell construction were carried out as well as cell discharge tests to determine the impact of key impurities on cell performance. The results of voltage delay and discharge tests with 60 Li/SOCL$_2$ cells indicate that up to 100 PPM water can be added to the electrolyte without detrimental effects. At water levels above 100 PPM voltage delay and hydrogen gas evolution can become problems. The results of tests Li/SOCL$_2$ cells containing 5, 20 and 100 PPM of soluble iron indicate that serious voltage delay will occur unless the iron concentration is held to 5 PPM or lower.

Analysis of the ALCL$_3$, LiCL, electrolyte and carbon cathode revealed that the total diethyl ether soluble organic impurities are less than 30 PPM, 100 PPM, 20 PPM and 1 Wt% respectively. Compared to the 7.8 and 7.0 Wt% organic binder present in the Crane and Mead separators, it is clear that the organic impurities present at concentrations below 500 PPM are of negligible importance relative to battery performance or hazards. The most serious problem involving organic impurities involved gas evolution due to a reaction between the organic polymer binder in separators and LiALCL$_4$/SOCL$_2$ electrolyte. The Crane 310 separator used in Li/SOCL$_2$ commercial cells was found to evolve gas for over 500 hours at 25°C and could produce pressure increases in sealed cells.

CONTENTS

LIST OF FIGURES

Figure

LIST OF FIGURES

LIST OF FIGURES

LIST OF FIGURES

LIST OF TABLES

Part I INVESTIGATION OF CHEMICAL, ELECTROCHEMICAL AND PARASITIC REACTIONS IN LITHIUM-THIONYL CHLORIDE CELLS

1.0 INTRODUCTION

The objectives of Part I of the project were to (i) fully investigate reactions occurring in the Li/$SOCl_2$ cell for a range of specified test conditions, and (ii) to perform analyses to identify reactants, intermediates and products generated by the chemical and electrochemical reactions occurring in the cell and to assess their impact upon safety and performance.

The lithium-thionyl chloride (Li/$SOCl_2$) system is one of the highest energy density electrochemical couples under development at the present time (1-4). It has been frequently reported that Li/$SOCl_2$ cells and batteries have exhibited explosive (5-8) behavior while under a variety of conditions such as charging, cell reversal, storage, low temperature discharge and other situations (9). It has been suggested (10) that the spontaneous explosions of partially discharged Li/$SOCl_2$ cells on casual storage may be initiated by reactions involving $SOCl_2$ reduction intermediates. Gas evolution from electrolyte from discharged cells (11), calorimetric (12) and DTA measurements (13) have been cited as evidence which indicates the presence of short lived intermediates of $SOCl_2$ reduction. Thus, information regarding the properties of such intermediates is required if the full benefits of the Li/$SOCl_2$ system in terms of both safety and performance is to be realized.

The performance of the Li/$SOCl_2$ cell using uncatalyzed cathodes at high current densities and/or low temperatures is unacceptable for many military applications (14-16). Improved performance of the $SOCl_2$ cathode has been achieved using noble metal (17) and organometallic (18) catalysts. It is thought that such catalysts may improve the performance of Li/$SOCl_2$ cells at high current densities because the catalysts lead to a more complete and rapid reduction of $SOCl_2$ by facilitating the reduction of difficult to reduce intermediates. It is one purpose of the present study to obtain information on the effect of various catalysts on the mechanism of $SOCl_2$ reduction over a range of specified test conditions. It is expected that this information will be of considerable value in the selection, evaluation and optimization of catalysts for the $SOCl_2$ cathode.

The conditions over which it was planned to investigate the Li/$SOCl_2$ cell reactions involved a test matrix with rates from 1.00 to 100 mA/cm^2, three temperatures −20°, 25 and 75°C, neutral and acid electrolytes and uncatalyzed and Pt catalyzed cathodes. It was also planned to investigate the Li/$SOCl_2$ cell reactions during reversal, cell charging and during storage at 25 and 75°C. Because of certain experimental problems at high rates and high temperatures, the majority of the work was carried out at low and moderate rate at 25°C and below, and only limited exploratory studies were carried out at rates above 20mA/cm^2.

1.1 IN SITU STUDIES OF THIONYL CHLORIDE REDUCTION BY VOLTAMMETRY AND COULOMETRY IN AN ORGANIC SUPPORTING ELECTROLYTE

1.1.1 Background

Electroanalytical techniques and a variety of spectroscopic techniques (IR, Raman, ESR) have been used to analyze the electrolyte from discharged cells to determine the products of the electrochemical reduction of $SOCl_2$. Both techniques have their strengths and weaknesses and it appears that both will be required to determine the composition of the reaction products and intermediates in the Li/$SOCl_2$ cell.

Early investigations (19-21) of $LiALCl_4$/$SOCl_2$ solutions using linear sweep voltammetry (LSV) were limited in scope by passivation of the working electrode due to precipitation of LiCl which is insoluble in $SOCl_2$. More recently, the electrode passivation problem (10, 22) was overcome by using a supporting electrolyte of tetrabutyle ammonium hexafluoraphosphate ($TBAPF_6$) in organic solvents such as dimethylformamide (DMF) in which tetrabutylammonium chloride and S are soluble.

In the present project the reduction of $SOCl_2$ was further investigated in $TBAPF_2$/DMF supporting electrolyte using LSV but the experiments were carried out quantitatively with accuracies up to 6‰2 rather than semi-quantitatively as in the first exploratory study. Using these quantitative LSV procedures the reduction of $SOCl_2$ was investigated using constant current electrolysis on a variety of cathode substrates over a range of current densities, temperatures, overdischarge and storage conditions in both acid and neutral $SOCl_2$ electrolytes. The cathode substrates investigated included glassy carbon, porous Shawinigan carbon, compressed Shawinigan carbon, nickel and platinum. Samples of $SOCl_2$, from hermetically sealed 0.6 Ahr Li/$SOCl_2$ cells discharged at rates from 1 to 10 mA/cm^2 at temperatures from − 20 to 25 °C were also analyzed by LSV in $TBAF_6$/DMF supporting electrolyte. The results are presented in Section 1.2.

1.1.2 Experimental

Voltammetry - The voltammetry experiments were performed using a PAR 173 potentiostat, PAR 178 electrometer probe and PAR 175 function generator with associated ancillary equipment. Data were collected using a Hewlett-Packard/Mosley Model 7001A X-Y recorder, a Tektronix Type 549 storage oscilloscope and a Gould Model 2400S high speed strip chart recorder.

The two compartment H-cell used for voltammetry is shown in Figure 1. Each compartment contained 10 ml of electrolyte to the level indicated in the Figure. A 20 mm fine porosity glass frit (10 μm pore diameter) was used to separate the compartments and prevent passage of material between the working and counter electrode compartments.

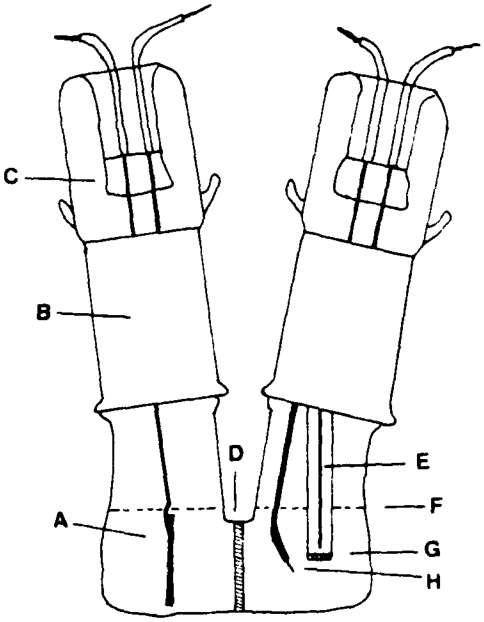

Figure 1: Voltammetry Cell: A, platinum counter electrode; B, 24/40 standard taper joint; C, glass to metal seal; D, 20 mm dia. sintered glass frit; E, Ag/AgCl reference electrode; F, electrolyte level; G, 5 mm dia. sintered glass frit; H, working electrode.

The DMF supporting electrolyte was degassed with argon in the H-cell before the substrates were added. Samples of oxyhalide solutions were added one drop at a time to the DMF supporting electrolyte in the working electrode compartment using a gas tight microliter syringe while the electrodes were completely removed. The cell was then gently agitated with a horizontal motion to dissolve the oxyhalide to prevent overheating and chemical reaction between the oxyhalide and the DMF supporting electrolyte before the next drop was added.

Electrolytes and Electrodes - The dimethylformamide (DMF) used to prepare the supporting electrolyte was Burdick and Jackson "Distilled in Glass" grade. The electrolyte salt, tetrabutylammonium hexafluorophosphate ($N(C_4H_3)_4PF_6$)($TBAPF_8$) was prepared by metathesis of tetrabutylammonium chloride (Aldrich Chemical Co.) and lithium hexaflurophosphate (Ozark Mahoning Co.) following the procedure described by Bowden and Dey (10).

Thionyl chloride (Mobay) was purified according to the method of Friedman and Wetter (23). Aluminum chloride (Fluka, puriss grade) was used without further purification. Lithium chloride (Baker Chemical) was ground in a mortar and dried in vacuo at 160°C for 30 hours. The electrolyte was prepared by dissolving $AlCl_3$ in $SOCl_2$ until solution was complete, then adding excess LiCl. Hydrolysis products (24) were removed by refluxing over lithium for 15-20 hours, which also helped to lower the concentration of iron in the electrolyte. Insoluble materials were removed after processing by filtration.

The platinum working electrodes used for voltammetry were typically made with 0.635 mm dia. Pt wire which was partially insulted using heat shrinkable teflon tubing. Before use, the Pt working electrodes were pretreated by chronic acid followed by a wash with distilled water and air drying. The counter electrode was 1.5 x 2.0 cm Pt foil. The 1 mm dia. AgCl coated Ag wire which was used as a reference electrode was enclosed in a 7 mm dia glass tube with a 5 mm dia. glass frit at the tip. The techniques used to prepare the Ag/AgCl reference electrode and the characteristics of the electrode in $TBAPF_6$/DMF electrolyte are described in Appendix A.

Constant Current Coulometry - The constant current coulometry experiments in DMF electrolyte were carried out in the same type of cell shown in Figure 1 modified in several ways. First, a 4 cm^2 electrolysis electrode of platinum, glassy carbon or other substrate of interest was used in place of the working electrode (H) shown in Figure 1. Second, the solution in the working electrode compartment was stirred during the electrolysis with a Teflon covered magnetic stir bar (3 x 10). At specific times during some of the coulometry experiments the current was interrupted for a short period, the standard taper top with the electrolysis cathode and the reference electrode was removed and a second top with a Pt voltammetry working electrode and a Ag/AgCl reference electrode was inserted into the cell. Voltammetric analyses were then carried out after which, the original set of electrolysis electrodes were replaced and the constant current coulometry continued.

The platinum, nickel and most of the other electrolysis electrodes were of a 1.0 x 2.0 cm rectangular design. The glassy carbon electrode however, was a 7.5 cm long, 6.35 mm diameter cylinder which was masked off with Teflon tape so that only 1.8 cm of the length (area 4 cm^2) was exposed to the electrolyte.

The cells and electrolytes were prepared in a dry room maintained at $<$ 4% relative humidity but $AlCl_3$ and other hygroscopic salts were weighed out inside an argon filled glove box ($<$ 60 ppm H_2O).

1.1.3 Voltammetry of Neutral $SOCl_2$ Electrolyte

A typical voltammogram for 1.8 M $LiAlCl_4/SOCl_2$ electrolyte in $TBAPF_6$/DMF at a platinum working electrode is shown in Figure 2. The large cathodic peak at − 0.75 V is caused by the reduction of $SOCl_2$ and the smaller peak at − 0.95 V is due to SO_2. Work which led to the conclusion that the − 0.95 peak is due to SO_2 is presented in Section 1.1.5. A third peak at − 1.62 V is also observed but the composition of the species undergoing reduction is not yet known with certainty. Data obtained pertaining to the composition of the species reduced at − 1.62 V is discussed in Section 1.1.7.

The sweep of a typical voltammogram such as Figure 2 was begun at the open circuit potential (i.e., approx. 0.18 V vs Ag/AgCl) and then proceeded in the cathodic direction to − 2.55 V vs Ag/AgCl. The direction was then reversed and the sweep proceeded in the anodic direction to approximately 1.00 V at which point the sweep was again reversed and the sweep continued from 1.00 V to the original open circuit potential of approx. 0.18 V where the scan was terminated. This procedure was generally followed throughout Task I but to allow the reduction peaks for $SOCl_2$ to be presented in the greatest detail the portion of the sweep from about 0.2 to 1.0 V has not been shown in most of the figures.

Voltammograms for pure $SOCl_2$ in $TBAPF_6$/DMF supporting electrolyte are shown in Figure 3 and show the same three reduction waves as observed for 1.8 M $LiAlCl_4/SOCl_2$. Thus $LiAlCl_4$ and $AlCl_3$ can be ruled out as possible causes of the reduction wave at − 1.62 V observed for the $LiAlCl_4/SOCl_2$ samples.

A cyclic voltammogram on a Pt electrode in 0.1M $TBAPF_6$/DMF is shown in Figure 4 which demonstrates a clean background.

To use linear sweep voltammetry (LSV) to monitor the concentration of $SOCl_2$ reduction products and intermediates in electrolyte samples from batteries discharged under a variety of conditions, it was required that LSV be carried out to an accuracy of at least 10%. To achieve such an accuracy, techniques were developed to minimize the reaction of $SOCl_2$ electrolyte with DMF and to reproducibly transfer μl quantities of electrolyte (see Section 1.1.2).

The voltammograms for three concentrations of 1.8 M $LiAlCl_4/SOCl_2$ electrolyte in DMF supporting electrolyte are shown in Figure 5. The solid vertical lines in Figure 5 indicate the $SOCl_2$ peak currents. The calibration curve relating peak current to the SOCl$_2$ concentration for 1.8 M LiAlCl$_4$/SOCl$_2$ samples is given in Figure 6. The calibration measurements were fitted to a linear equation by the least squares method and the largest deviation from linearity was 2.4%.

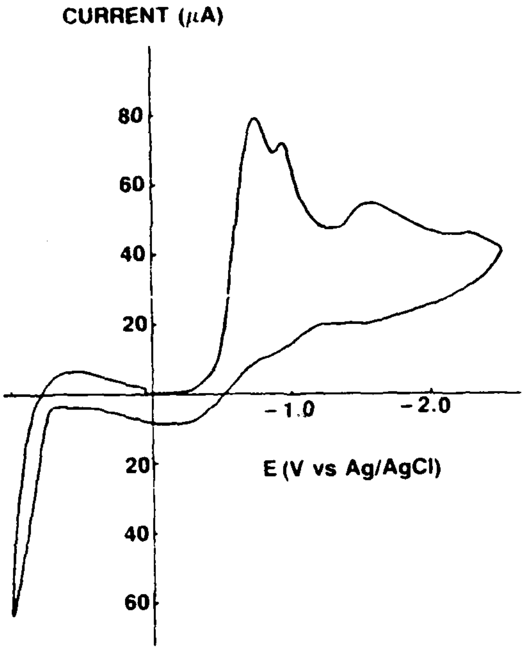

Figure 2: Voltammogram of 5.8μl of 1.8M LiAlCl$_4$/SOCl$_2$ in 10 ml of 0.1 M TBAPF$_6$/DMF at 25 °C on Pt electrode, scan rate 200 mV/sec.

The 5.8μ of sample yielded a DMF solution 6.8 mM in SOCl$_2$.

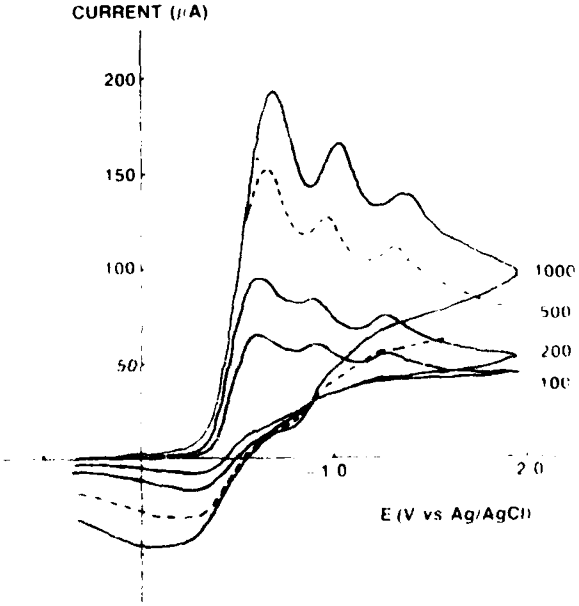

Figure 3: Voltammograms for 13.7 mM of pure SOCl$_2$ in 0.1 M TBAPF$_6$/DMF at 25°C on Pt electrode, at scan rate, from 100 to 1000 mV/sec.

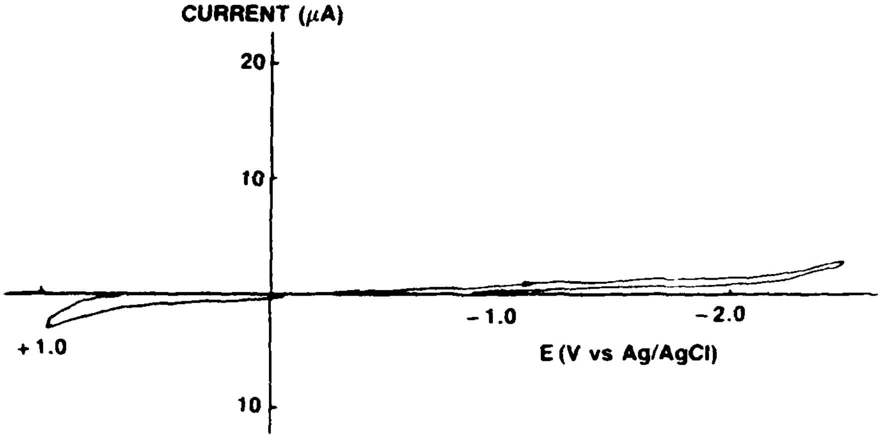

Figure 4: Cyclic voltammogram of 0.1 M $TBAPF_6$ in DMF of Pt electrode, background, scan rate 200 mV/sec.

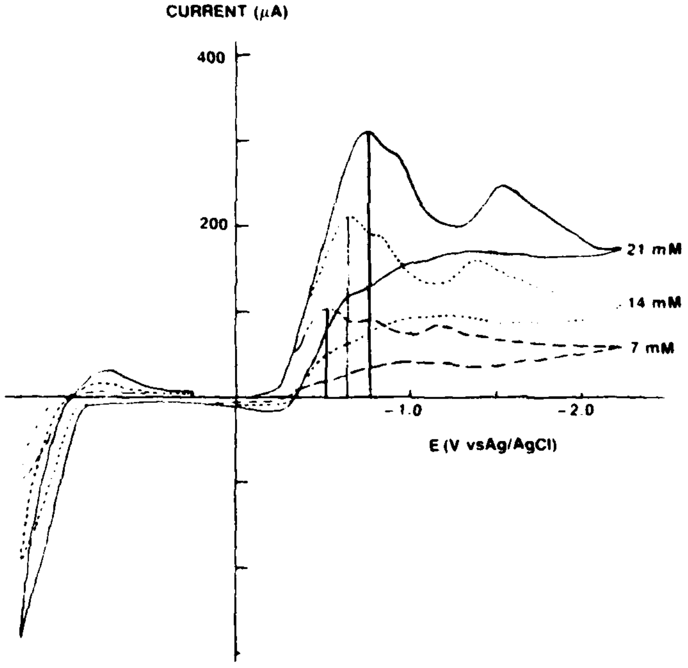

Figure 5: Voltammograms for three samples of 1.8 $LiAlCl_4/SOCl_2$ containing 7, 14 and 21 mM $SOCl_2$, on Pt electrode, in 0.1M $TBAPF_6$/DMF, scan rate 200 mV/sec.

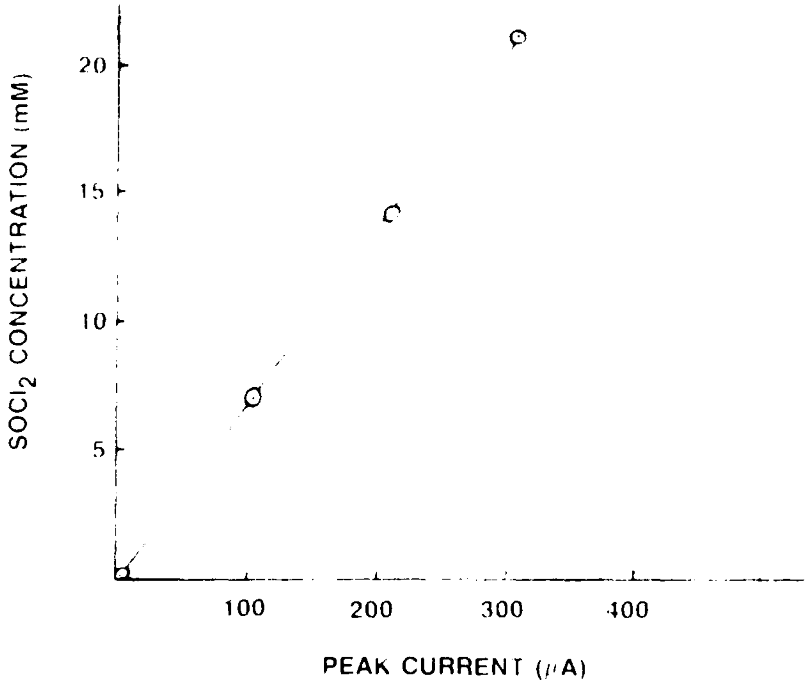

Figure 6: Calibration curve relating peak current by voltammetry to the $SOCl_2$ concentration for 1.8 M $LiAlCl_4/SOCl_2$ samples in 0.1 M $TBAPF_6$/DMF supporting electrolyte.

There has been a dialog in the literature (25, 26) concerning the suitability of DMF as a supporting electrolyte for the analysis of $SOCl_2$ electrolytes because of possible reaction between $SOCl_2$ and DMF. It has been found by LSV analysis that for a 33 mg sample of 1.8 M $LiAlCl_4/SOCl_2$ in 10 ml of DMF supporting electrolyte, the $SOCl_2$ peak current declined 19.7% during 18.5 hrs of storage at 25°C. Neglecting the loss of $SOCl_2$ into the counter electrode compartment, the $SOCl_2$ reaction rate with DMF is less than 1.1%/hr, which is acceptable for the present work.

The effect of the $SOCl_2$ electrolyte sample size on the separation of the SO_2 and $SOCl_2$ peaks during voltammetry at 200 mV/sec is shown in Figures 2 and 5. From a comparison of additional voltammograms not presented here, it was concluded that a sample size of 1.8 M $LiAlCl_4/SOCl_2$ contained approximately 7 mM $SOCl_2$ after being added to the DMF supporting electrolyte gave the best resolution of SO_2 and $SOCl_2$. Whenever possible, it was standard procedure during the present investigation to use samples containing approximately 7 mM $SOCl_2$ in DMF.

The accuracy and reproducibility of the potentials for the $SOCl_2$ and SO_2 peaks is of considerable interest when carrying out quantitative LSV of $SOCl_2$ samples. Abnormal values for the peak potentials are of particular value in identifying problems with the reference electrode, instrumentation or electrolyte contamination. Based on a group of 10 voltammograms, each obtained with fresh 1.8 M $LiAlCl_4/SOCl_2$ electrolyte on different days over a four month period, the peak potentials for $SOCl_2$ and SO_2 were found to be − 0.75 and − 0.95 V respectively vs Ag/AgCl at a 100 mV scan rate with a Pt working electrode. The standard deviations were ± 0.030 and ± 0.039 V respectively. The data from the first two scans for a freshly cleaned Pt working electrode were generally discarded following standard practice (27).

The average open circuit potential (OCP) for the Pt working electrode with 1.8 M $LiAlCl_4/SOCl_2$ samples in $TBAPF_6$/DMF (approximately 7 mM in $SOCl_2$) was 0.18 V vs Ag/AgCl with a standard deviation of 0.11 obtained for 13 samples over a three month period. The variations of the OCP did not correlate with shifts in the potentials of the $SOCl_2$ peaks thus changes in the Ag/AgCl reference electrode potential were ruled out as the cause of the large variations in OCP. Although the exact causes of the OCP variations are not known, it is thought that the variations are due to oxide films on the platinum electrode which are affected by the electrodes history and the cleaning procedures. Discarding the results from the first two scans for each freshly cleaned Pt working electrode was found to improve the reproducibility of the OCP values and the peak currents.

The peak potentials for $SOCl_2$ and SO_2 were − 0.62 and − 0.89 V vs Ag/AgCl respectively in the voltammogram for 13.7 mM of pure $SOCl_2$ shown in Figure 3 for a 200 mV/sec sweep rate. These in principle should agree with the peak potentials of − 0.37 and − 0.65 V for the $SOCl_2$ and SO_2 peaks reported by Bowden and Dey (10). The separation of the $SOCl_2$ and SO_2 peak potentials agree within 10 mV. Thus the differences between the two sets of measurements are likely due to differences in the working electrode geometrics and the design of the reference electrodes.

Dey (10) reported that their Ag/AgCl reference electrode had a potential of 3.30 V vs Li in PF_6= /DMF solutions whereas the Ag/AgCl reference electrodes used in the present work gave a potential of 3.42 V vs a Li reference electrode. Using these two values for the potential of the Ag/AgCl electrode vs Li references, the $SOCl_2$ peak potentials were recalculated as 2.93 and 2.80 V vs Li for the measurements by Dey and the value from Figure 3 respectively. Thus by correcting for differences in the reference electrodes the discrepancy between the $SOCl_2$ peak potentials was reduced from 250 to 130 mV.

1.1.4 Voltammetry of Acid $SOCl_2$ Electrolyte

The 2.0 M $AlCl_3$, 0.10 M $LiCl/SOCl_2$ concentration for the acid electrolyte selected for investigation was chosen based on its favorable characteristics for flow temperature reserve cell applications. A typical voltammogram for the above acid electrolyte in 0.1 M $TBAPF_6$/DMF at a platinum working electrode is shown in Figure 7. The large cathodic peak at − 0.88 V is due to SO_2. Generally the voltammogram is similar to the voltammogram for neutral $SOCl_2$ electrolyte (Figure 2) discussed earlier except that the reduction peaks are shifted about 70 mV more cathodic.

Based on a group of five voltammograms for $SOCl_2$ acid electrolyte at the same concentrations and conditions as the analysis in Figure 7, the average peak potentials for the $SOCl_2$ and SO_2 peaks were − 0.69 and − 0.90 V respectively. The standard deviations were ± 0.055 and ± 0.054 V in the same order.

The voltammograms for three concentrations of 2.0 M $AlCl_3$, 0.10 M $LiCl/SOCl_2$ acid electrolyte in DMF supporting electrolyte are shown in Figure 8. The calibration curve relating peak current to the $SOCl_2$ concentration for the above $SOCl_2$ acid electrolyte is given in Figure 9. The calibration measurements were fitted to a linear equation by the least squares method and the average deviation was 6.18%. The largest deviation was 20.1%.

To permit calculation of the amount of $SOCl_2$ in the acid electrolyte samples, the density of 2.0 M $AlCl_3$, 0.10 M $LiCl/SOCl_2$ was determined using a 25 ml glass pycnometer. The density of the $SOCl_2$ acid electrolyte was found to be 1.69 g/ml at 23°C.

The reaction rate of acid electrolyte with DMF electrolyte was determined by measuring the decline in the $SOCl_2$ peak current by LSV analysis before and after 50 hrs storage. The average reaction rate of the 2.0 M $AlCl_3$, 0.10 M $LiCl/SOCl_2$ electrolyte with DMF at 25°C over the 50 hr period was found to be less than 0.62%/hr for 65 mM $SOCl_2$ in the DMF supporting electrolyte. This compares well with a rate of 1.1%/hr found at 25°C with 1.8 M $LiAlCl_4/SOCl_2$ (see Section 1.1.3).

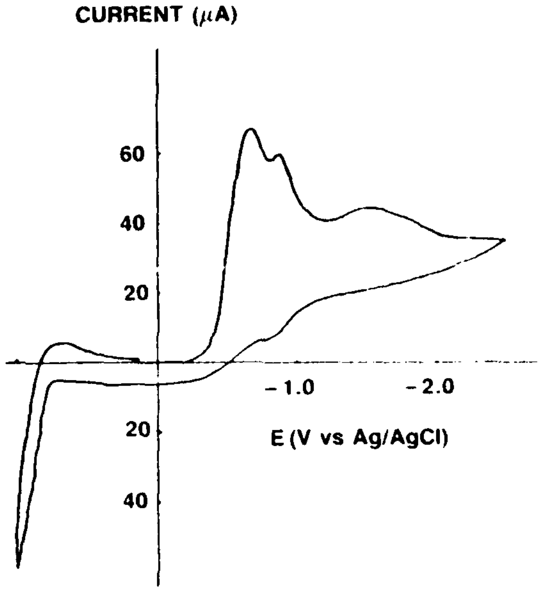

Figure 7: Voltammogram of 10 μl of 2.0 M $AlCl_3$, 0.10 M $TBAPF_6$/DMF at 25°C, on Pt electrode, scan rate 200 mV/sec.

The 10 μl of sample yielded a DMF solution 5.6 mM in $SOCl_2$.

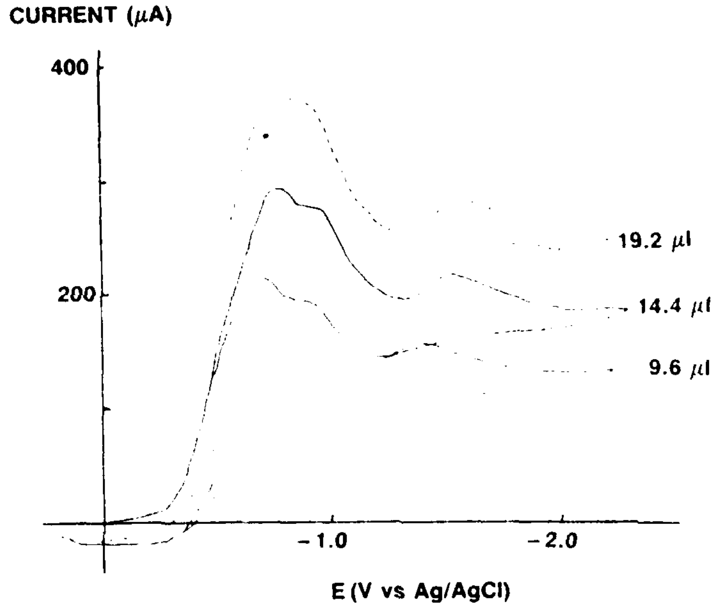

Figure 8: Voltammograms of 9.6, 14.4 and 19.2 μl of 2.0 M AlI_3, 0.10 M $LiCl/SOCl_2$ in 10 ml of 0.1 M $TBAPF_6$/DMF at 25°C, on Pt electrode, scan rate 200 mV/sec.

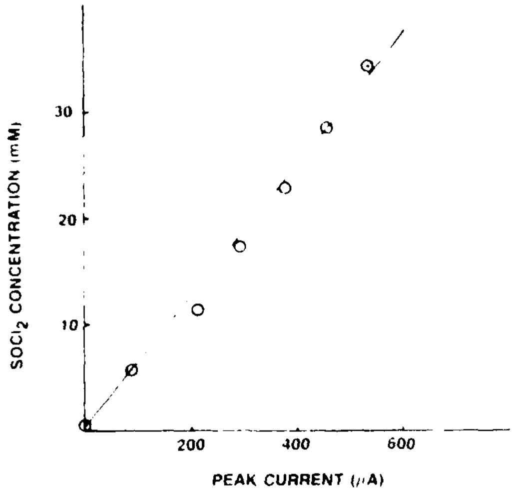

Figure 9: Calibration curve relating peak current by voltammetry to the 2.0 M $AlCl_3$, 0.10 M $LiCl/SOCl_2$ sample size.

1.1.5 Voltammetry of Neutral $SOCl_2$ Electrolyte with added SO_2

Voltammetry of SO_2 in DMF Electrolyte. - The voltammograms for approximately 10 mM SO_2 in 0.1 DMF $TBAPF_6$/supporting electrolyte 18 and 50 hrs after the first scan are given in Figure 10. The peak potentials were at – 0.955 and – 0.960 V respectively. The peak potential and current on the first scan (not shown in Figure $0) were – 0.985 V and 37.8 μA. The crop in the peak current from 37.8 to 29.2 μA during the 50 hr storage period is thought to be primarily due to SO_2 loss by diffusion from the working electrode compartment. The origin of the sharp new peak which developed at – 0.875 V after 50 hrs stand is unknown but it is especially noteworthy since it could be mistaken for a $SOCl_2$ reduction intermediate in samples from discharged $SOCl_2$ cells containing both $SOCl_2$ and SO_2. Intermediates such as SO_2^-, SO, SO_3^{2-} and S_2O^- formed during the reduction of SO_2 in DMF have been investigated by Sawyer and Martin (28) and Gardner, Fouchard and Fawcett (28, 30) in very thorough studies which are too lengthy and complex to be reviewed here.

The – 0.985 V potential recorded for the SO_2 peak on the first scan during the present study compares well with the – 0.81 V SO_2 peak potential reported by Bowden and Dey (10). Comparing the SO_2 peak potentials for the two laboratories on the basis of a Li reference as outlined in Section 1.1.3 to correct for differences in the Ag/AgCl reference electrodes, it was found that the two values were 2.44 V (present work) and 2.49 V (10) vs Li or only 50 mV apart.

Voltammetry of SO_2 in $LiAlCl_4/SOCl_2$ - Voltammograms for approximately 9 mg of f1.8 M $LiAlCl_4/SOCl_2$ with from 0.613 to 4.77 M SO_2 in 10 ml of DMF electrolyte are compared in Figures 11 and 12 with the voltammogram obtained for 1.8 M $LiAlCl_4/SOCl_2$ without added SO_2. These results clearly demonstrate that the second reduction peak at – 0.95 V is due to the reduction of SO_2 and not an intermediate such as $SO.SOCl_2$ as postulated by Bowden and Bey (10).

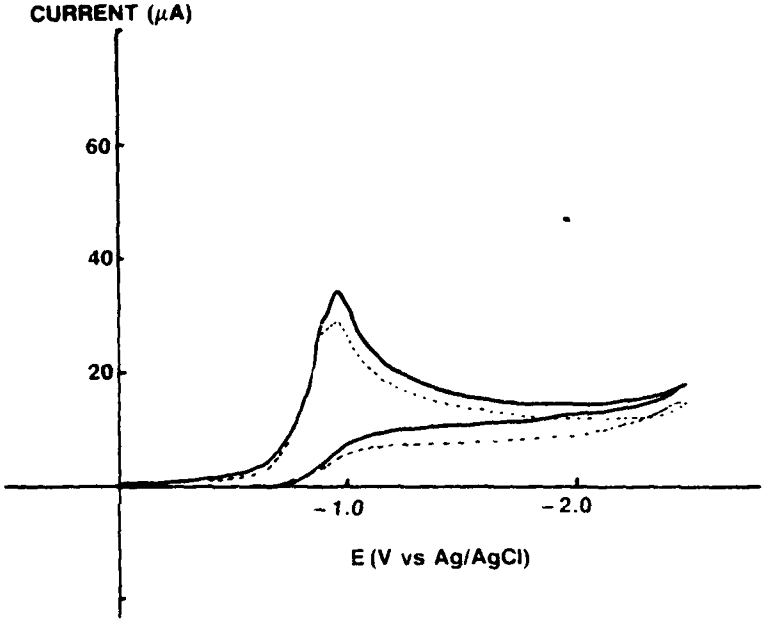

Figure 10: Voltammograms for approximately 10 mM SO_2 in 0.1 M $TBAPF_6/DMF$ at 25°C, 18 and 50 hrs after the first scan, scan rate 200 mV/sec.

(___ ____) after 18 hrs stand
(-----------------) after 50 hrs stand

Similar additional LSV analyses were carried out at ten SO_2 concentrations from 0.61 to 5.86 M in 1.8 M $LiAlCl_4/SOCl_2$ which agree with the results shown in Figures 11 and 12. It should be noted that the solubility of SO_2 in 1.8 M $LiAlCl_4/SOCl_2$ is 4.095 M at 23°C and 3.923 M at 24°C (22). thus the 4.77 M SO_2 solution described in Figure 12 was supersaturated. The exact concentration of SO_2 in the DMF electrolyte after samples of supersaturated SO_2 solutions were added is known with less accuracy (approx ± 5%) because of SO_2 losses due to the effects of Henry's Law.

The SO_2 solutions were prepared by bubbling SO_2 through a known weight of 1.8 M $LiAlCl_4/SOCl_2$ using a glass apparatus fitted with standard taper joints that was cooled with a dry ice bath to approximately − 67°C. The $SOCl_2$ electrolyte was weighed a second time after the SO_2 bubbling was completed and the amount of SO_2 added was computed from the weight gain. The electrolyte was cooled with dry ice primarily to prevent $SOCl_2$ evaporation while the SO_2 was being bubbled through the solution which could cause an error in the calculation of the SO_2 concentration. However, cooling the $SOCl_2$ solution had the secondary benefit of increasing the SO_2 solubility in $SOCl_2$ which decreased the time required to reach saturation. Considerable effort was made during the transfer of the $SO_2/SOCl_2$ solutions to use pipetting techniques which did not cause a partial vacuum above the solutions thereby resulting in SO_2 losses from the solution due to the effects of Henry's Law.

The variations in the SO_2 peak potentials seen in Figures 11 and 12 are largely due to differences in the reference electrode potentials before the $SOCl_2/SOC_2$ samples were added. Correcting for differences in the reference electrode potentials it appears that the SO_2 peak potential shifts at most 30 mV in the cathodic direction with increasing SO_2 concentration up to 3.6 M SO_2.

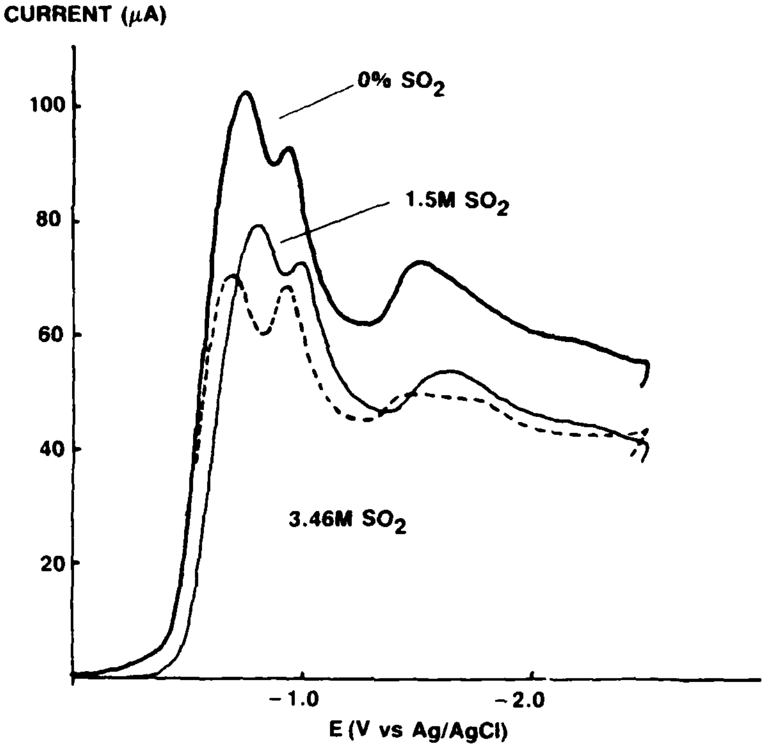

Figure 11: Voltammograms of approximately 9 mg of 1.8 M $LiAlCl_4/SOCl_2$ with 3.46, 1.5 and 0.0 M SO_2 in 10 Ml of 0.1 M $TBAPF_6$/DMF at 25°C, scan rate 200 mV/sec.

The sample sizes were 8.17, 9.89 and 10.2 for the $SOCl_2$ solutions with 3.46, 1.5 and 0.0 M SO_2 respectively.

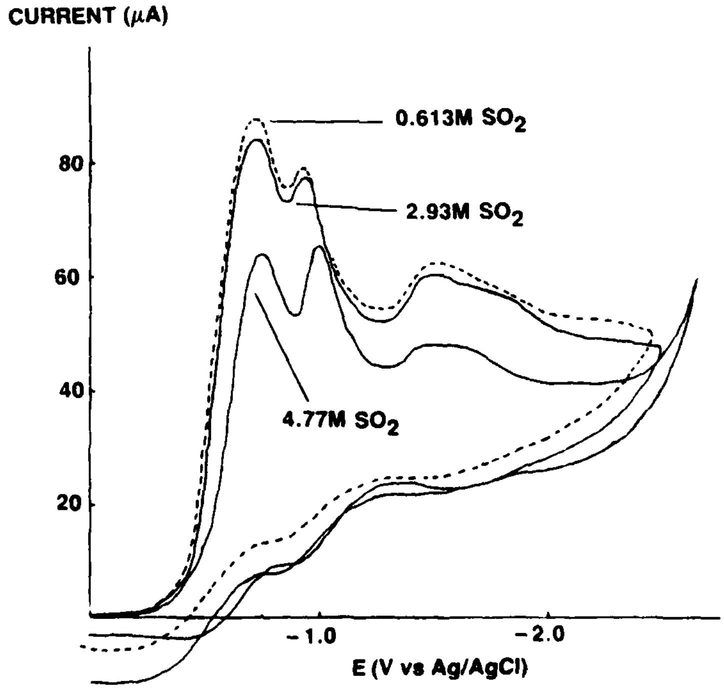

Figure 12: Voltammograms of approximately 9 mg of 1.8 M $LiAlCl_4/SOCl_2$, with 0.613, 2.93 and 4.77 M SO_2 in 10 ml of 0.1 M $TBAPF_6$/DMF at 25°C, scan rate 200 mV/sec.

The 4.77 M SO_2 solution was supersaturated and the concentration is probably only accurate to ± 5%.

Voltammograms of a 1.8 M $LiAlCl_4/SOCl_2$ sample containing 3.5 M SO_2 after 4, 46 and 120 hrs (cf. Figures 13 and 14) show that SO_2 reacts very rapidly in the presence of $LiAlCl_4/SOCl_2$ in DMF supporting electrolyte. In Figure 13 which compares the voltammograms after 0 and 4 hrs of 25° storage the SO_2 peak at − 0.92 V declined and a new peak appeared at − 1.29 V during the 4 hr storage period. After 46 hrs of storage the *new peak increased* and shifted to − 1.21 V (cf. Figure 14) but thereafter the peak current remained steady but the potential continued to shift slightly to − 1.19 V after 120 hrs. The shoulder on the main $SOCl_2$ peak at − 0.67 V which is very prominent after 4 hrs of storage in Figure 13 completely disappeared after 46 hrs of storage which indicates that additional reaction of SO_2 occurred between 4 and 46 hrs of storage.

The composition of the species being produced from SO_2 which reduces at − 1.21 V is not yet fully understood. It is definitely not sulfur which reduces at approximately − 0.72 V and − 0.43 V in DMF at a concentration of 15 mM (cf. Section 1.1.6). It is also not the substance responsible for the − 1.62 V peak for 1.8 M $LiAlCl_4/SOCl_2$ samples (cf. Section 1.1.3)..The − 1.29 V peak is very large, thus it is unlikely that the substance responsible for the − 1.62 V peak in 1.8 M $LiAlCl_4/SOCl_2$ samples is reacting with SO_2. One possible explanation for the new peak at − 1.29 V is that the SO_2 is slowly reacting with $LiAlCl_4/SOCl_2$ and DMF to form adducts such as $LiAlCl_4{\bullet}SO_2{\bullet}SOCl_2$, $LiAlCl_4{\bullet}SO_2{\bullet}DMF$ or $LiAlCl_4{\bullet}SO_2{\bullet}SOCl_2{\bullet}DMF$ which are more difficult to reduce than SO_2. Barbier and coworkers (31) have recently studied $Li/SOCl_2$ battery electrolytes using Raman spectroscopy and have described $LiAlCl_4{\bullet}SOCl_2{\bullet}SO_2$ adducts.

After reviewing the results, it has been concluded that additional voltammetric investigations will probably be required to determine the cause of the reduction peak at − 1.29 V. This additional work would involve LSV analyses with $LiAlCl_4/SOCl_2$, $AlCl_3/SO_2$, $SO_2{\bullet}SOCl_2$ and $LiAlCl_4/SO_2{\bullet}SOCl_2{\bullet}SO_2$ samples in DMF supporting electrolyte.

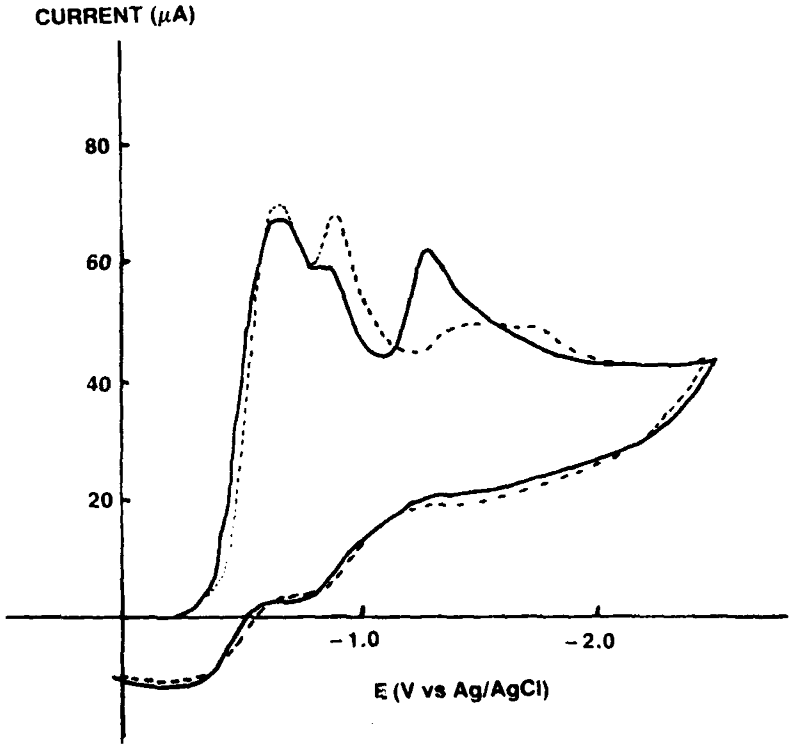

Figure 13: Voltammograms of 8.2 mg of 1.8 M $LiAlCl_4$, 3.5 M $SO_2/SOCl_2$ in 10 ml of 0.1 M $TBAPF_6/DMF$ at 25°C, scan rate 200 mV/sec.

(-----------------) *immediately after electrolyte prepared*
(   ) *after 4 hrs of storage*

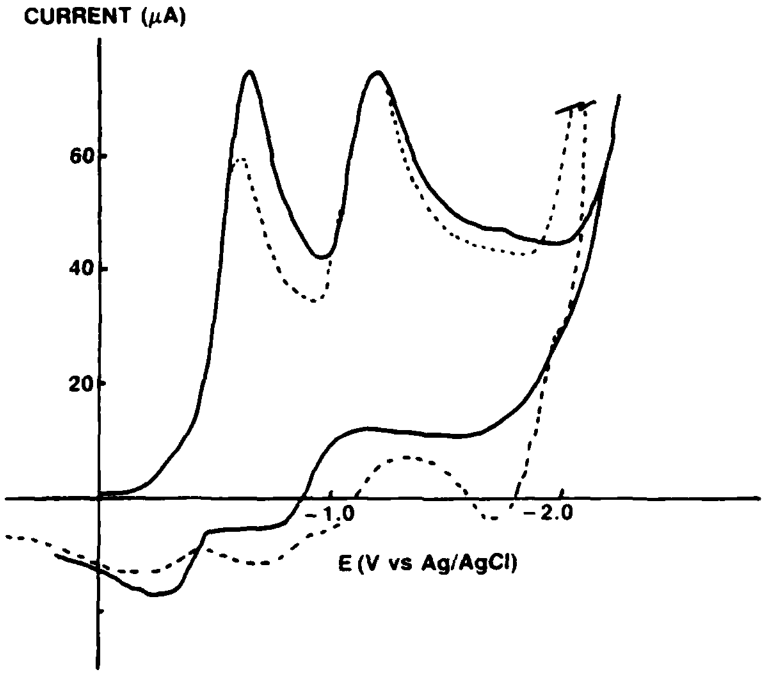

Figure 14: Voltammograms of 8.2 mg of 1.8 M $LiAlCl_4$, 3.5 M $SO_2/SOCl_2$ in 10 ml of 0.1 M $TBAPF_6/DMF$ at 25°C, scan rate 200 mV/sec.

(-----------------) after 46 hrs storage
(__________) after 120 hrs storage

The cause of the large peak at approximately – 1.62 V when 1.8 M $LiAlCl_4/SOCl_2$ samples are analyzed by LSV (cf. Section 1.1.3) is also unresolved at the present time. The – 1.62 V peak does not increase during storage and it may be the second peak of sulfur (see Section 1.1.6) at – 1. 435 V which has shifted. It is possible but less likely that the – 1.62 peak may be due to a product of the reaction of $LiAlCl_4/SOCl_2$ and DMF which is stimulated by the large heat of solvation when single drops of $LiAlCl_4/SOCl_2$ sample are added to the DMF supporting electrolyte. To determine if the – 1.62 V peak is caused this way, tests could be carried out in which approximately 6 μl of $LiAlCl_4/SOCl_2$ would be added to DMF supporting electrolyte at low temperature (e.g. – 20°C) and the electrolyte analyzed by LSV at 25°C. If the heat of solvation during mixing causes a reaction between the DMF and the $LiAlCl_4/SOCl_2$ then the sample prepared at low temperature should give a much smaller peak at – 1.62 V.

Quantitative Voltammetry for SO_2 in $SOCl_2$ Electrolytes. - Accurate values for the amount of SO_2 in $SOCl_2$ electrolyte from discharged cells are required for the present investigation because values lower than the theoretical value would provide information pertaining to the existence of intermediates or other unexpected discharge products. However, the $SOCl_2$ and SO_2 peaks obtained during LSV analysis are only 300 mV apart, the shoulders merge and it is difficult to find a suitable baseline to use to measure the current for the SO_2 peak which is required to calculate the SO_2 concentration. Methods for obtaining baselines to calculate the peak currents for multicomponent systems and multistep charge transfers have been discussed in some detail by Bard and Faulkner (32). The held scan techniques that were evaluated during the present contract closely follow the unpublished approach suggested by Reinmuth described by Bard and Faulkner (32).

The held scan procedure is based on the assumption that the diffusion of $SOCl_2$ and SO_2 occur independently, that the fluxes are additive and the i-E (or i-t) curve for the mixture is the sum of the individual i-E curves of $SOCl_2$ and SO_2. Since the concentration of $SOCl_2$ should fall essentially to zero at potentials just beyond the peak potential Ep (i.e. – 0.75V), the current beyond Ep is independent of potential. To carry out a held scan, the potential sweep was begun at the OCP as usual and proceeded in the cathodic direction to about 60/mV beyond Ep (i.e. – 0.83 V, for n = 2 electrons/molecule reduced) at which point the potential was held constant for 51 seconds. During the scan, the current and potential were recorded on an X-Y recorder and the current was recorded as a function of time on a strip chart recorder. At the end of the period (e.g. 51 sec) during which the potential was held at – 0.83 V, the scan was allowed to proceed in the cathodic direction at 200 mV/sec under the control of the function generator.

In Figure 15 the current-voltage curves obtained during normal and held scan voltammetry are compared for 5.8 μl samples of 1.8 M $LiAlCl_4/SOCl_2$ in DMF supporting electrolyte. Figure 16 shows the held scan voltammogram from Figure 15 with the current versus time decay curve for the $SOCl_2$ peak that was obtained from the strip chart recorder indicated as a dotted line. Figure 17 demonstrates the method in which the current-time curve from the held scan period is superimposed on the normal scan voltammogram to calculate the SO_2 peak current. The vertical line in Figure 17 at – 0.96 V with the arrow between the baseline and the SO_2 peak illustrates the way that the SO_2 peak current is obtained. In this case the SO_2 peak current above the baseline was 9.2 μA.

To use the held scan baseline to compute the SO_2 peak currents for samples from cells with different concentrations of $SOCl_2$, a new baseline curve would be required for each concentration. It would be difficult to obtain experimentally held scan baselines for each new concentration because the scan would have to be held at precisely the same time after the $SOCl_2$ peak and the concentration would have to be duplicated within 3% or better. For such reasons, it was decided to generate new held scan baselines by multiplying the currents point by point for the $SOCl_2$ peak and held scan decay curve in Figure 17 by the ratio of the $SOCl_2$ peak current at the $SOCl_2$ concentration required for the new baseline over the $SOCl_2$ peak current in Figure 17. This procedure does not distort the shape of the $SOCl_2$ curve and the baseline because the current-potential equation for linear sweep voltammograms (cf. pg 217 - ref 32) shows that the current is a simple linear function of the concentration of the electroactive species.

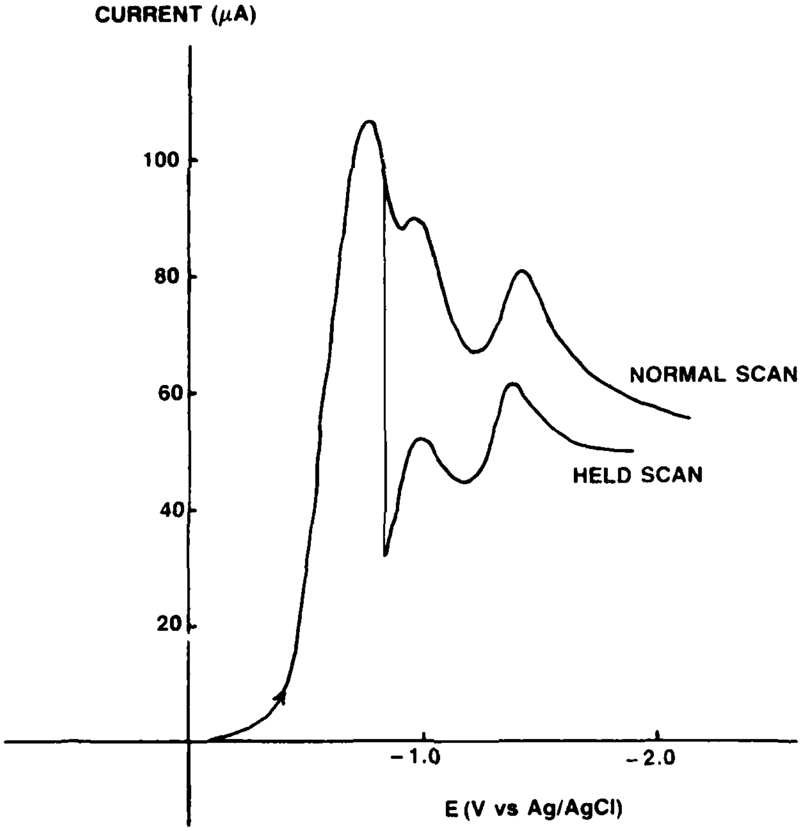

Figure 15: Normal and held scan voltammograms for 5.8 μl of 1.8 M $LiAlCl_4/SOCl_2$ in 10 ml of 0.1 $TBAPF_6$/DMF at 26°C, scan rate 200 mV/sec. The scan was held for 50.9 sec beginning at – 0.83V. The portion of the voltammogram while the potential was stopped at – 0.83 V is shown in Figure 16.

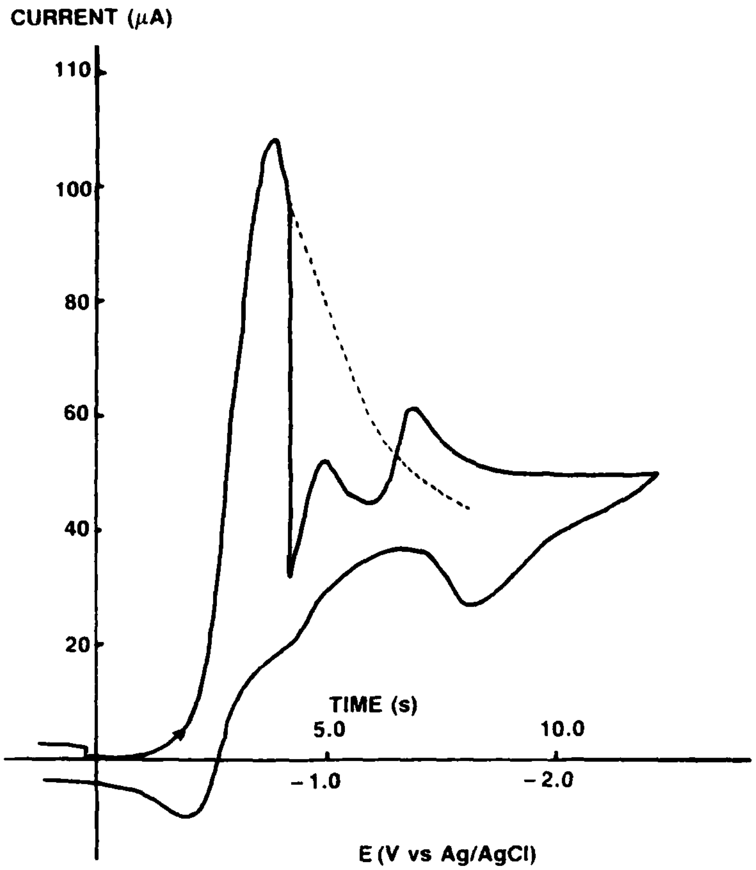

Figure 16: Held scan voltammogram while the potential was stopped at −0.83V and after the scan was continued for 5.8μl of 1.8 M $LiAlCl_4/SOCl_2$ in 10 ml of 0.1 M $TBAPF_6$/DMF at 25°C.

(-----------------) voltammogram while the potential was stopped, current versus time at −0.83 V.

To evaluate the merits of using voltammetry to measure the SO_2 samples, the held scan baseline technique was used to calculate the SO_2 peak currents as a function of concentration using the results in Figures 11 and 12. The SO_2 peak currents depend upon the SO_2 concentration in the DMF supporting electrolyte in the voltammetry cell. Thus, it was necessary to calculate these SO_2/DMF concentrations using the $SO_2/SOCl_2$ concentrations and the sample weights which are listed in Table 1. In Figure 18 the sulfur dioxide peak currents calculated using the held scan baseline are shown as a function of the SO_2/DMF concentration.

Examination of the results in Figure 18 indicates that voltammetry has a low sensitivity and accuracy for the analysis of SO_2 in the presence of large amounts of $SOCl_2$. This low sensitivity is caused by the large amount of $SOCl_2$ in the sample which requires that the voltammogram be carried out with a small sample of $SOCl_2$ to prevent the potentiostat from overloading and going off scale. Such small samples contain small amounts of SO_2 even when saturated with 4.09 M SO_2 at 23 °C. By comparison, a 1.8 M $LiAlCl_4/SOCl_2$ solution is 11.6 M in $SOCl_2$ so that even when saturated with SO_2 the $SOCl_2$ sample is only 35 mole % SO_2. At concentrations much below saturation, the proportion of SO_2 in $SO_2/SOCl_2$ sample is much lower and the accuracy and sensitivity become inadequate for our present requirements.

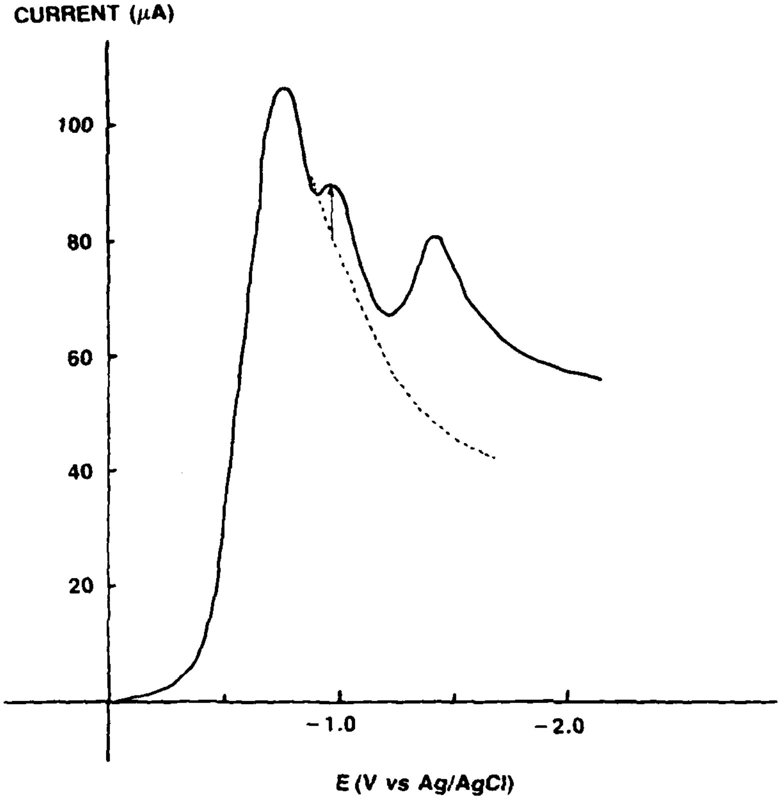

Figure 17: Method of measurement of peak current for SO_2 using the held scan voltammogram while the potential was stopped at −0.83 V.

(________) normal voltammogram for 5.8 μl of 1.8 $LiAlCl_4/SOCl_2$ in 10 ml of DMF supporting electrolyte, from Figure 15.

(----------------) voltammogram while the potential was stopped at −0.83 V, from Figure 16.

TABLE 1

Sulfur Dioxide Concentrations, Sample Sizes and Peak Currents for Voltammetry of $SOCl_2$ Samples in DMF*

Sample No.	Sample Wt. (mg)	Sample SO_2 Concent. (M)	SO_2 Concent. in DMF (mM)	SO_2 Peak Current + (μA)	$SOCl_2$ Concent. in DMF (mM)
1	9.89	1.503	0.855	20.5	6.39
2	8.33	0.613	0.294	22.5	5.57
3	9.68	2.93	1.630	26.5	6.59
4	8.17	3.46	1.626	27.7	4.88
5	10.32	2.35	1.398	23.0	6.45
6	9.32	0.0+ +	0.0	20.0	6.38

*The SO_2 concentrations in the 1.8M $LiAlCl_4/SOCl_2$ samples were calculated assuming no volume change on SO_2 addition

+ The SO_2 peak current was calculated using a held scan baseline. All measurements were at 25°C.

+ + The SO_2 content of sample # was 8.0 . 10^{-4}M as determined by quantitative IR spectroscopy.

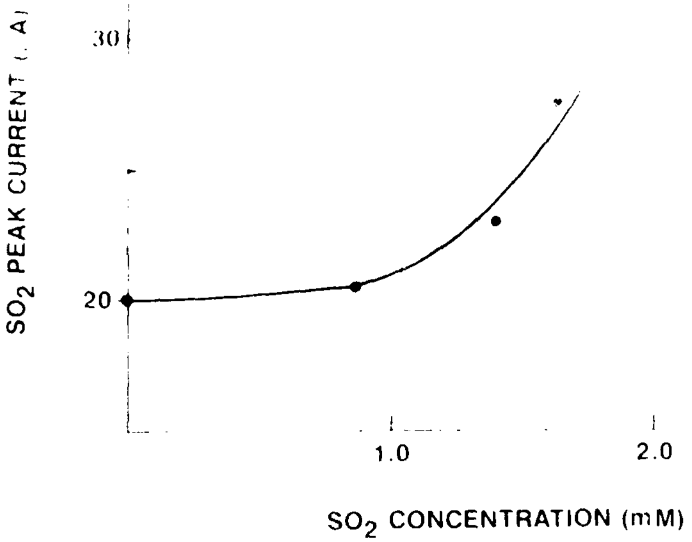

Figure 18: Sulfur dioxide peak currents calculated using held scan baselines as a function of the SO_2 concentration.

The SO_2 concentrations are in 0.1 M $TBAPF_6$/DMF. The SO_2 analyses were carried out in the presence of approximately 6.4 mM $SOCl_2$.

A second serious problem in using voltammetry to analyze for SO_2 quantitatively in the presence of an excess of $SOCl_2$ is that the peak currents for SO_2 and $SOCl_2$ are coupled and the calibration curve changes considerably depending on the $SOCl_2$ concentration in the DMF supporting electrolyte. Thus Figure 18 is a valid calibration curve only for $SO_2/SOCl_2$ samples containing approximately 6.4 mM $SOCl_2$.

In view of the above difficulties involved in the analysis of SO_2 in $SOCl_2$ samples by voltammetry, it has been found that quantitative infrared spectroscopy is a much more sensitive and accurate technique for analyzing for SO_2 in the presence of $SOCl_2$. Quantitative infrared techniques for the analysis of SO_2 in the presence of a large excess of $SOCl_2$ have been discussed in Section 1.2. Although voltammetry has severe limitations in quantitative analysis of $SO_2/SOCl_2$ solutions, it continues to have considerable value as a qualitative technique, especially in combination with IR spectroscopy to identify the number of compounds present in a $SOCl_2$ sample and to qualitatively follow concentration changes with time and temperature. Low temperature analysis of $SOCl_2$ electrolytes is difficult with IR spectroscopy to identify the number of compounds present in a $SOCl_2$ sample and to qualitatively follow concentration changes with time and temperature. Low temperature analysis of $SOCl_2$ electrolytes is difficult with IR spectroscopy but well suited for voltommetry.

Voltammograms of 1.8 M $LiAlCl_4/SOCl_2$ without SO_2 always give an SO_2 reduction peak (cf. Figure 2) and it was not known if this peak was due to traces of SO_2 in the electrolyte or reduction of SO_2 in the region around the working cathode produced during the previous reduction wave for $SOCl_2$ of the cathodic sweep. For Sample No. 6 in Table 1 with 6.38 mM of socl$_2$ but without added SO_2, the SO_2 peak current was 20 μA above the held scan baseline. The 1.8 M $LiAlCl_4/SOCl_2$ electrolyte sample was analyzed for SO_2 by quantitative IR spectrosocopy and the SO_2 concentration was found to be $8.0 \cdot 10^{-4}$M. On addition of approximately 9 mg of the $SOCl_2$ sample to 10 ml of DMF in the voltammetry cell, the concentration of SO_2 present as a background impurity in the $SOCl_2$ electrolyte would be reduced from $8.0 \cdot 10^{-4}$M to $2.5 \cdot 10^{-7}$M. Thus the SO_2 reduction peak found in samples without added SO_2 is clearly due to SO_2 produced during the prior reduction of $SOCl_2$ earlier in the cathodic sweep. This finding is of considerable value in interpreting voltammograms and in explaining the choice of Pt rather than glassy carbon as the working electrode for most of the LSV analyses carried out during the present study. It also shows that residual SO_2 in the electrolyte is not a factor in the low sensitivity of LSV analysis for SO_2 in samples with excess $SOCl_2$.

A second approach to the held scan technique has been discussed by Bard (pgs 233, 263; ref. 32) which could be useful in principle to increase the sensitivity of LSV analysis for both SO_2 and any compounds which give reduction peaks between $SOCl_2$ and SO_2. Using this second held scan technique, the scan is held for a long period of time (e.g. 60 to 150 sec) using a disc working electrode shielded from electrolyte convection and convection free electrolyte conditions (i.e., quiet, vibration free solution). If the convection free conditions can be maintained for a long enough period then the current will decay to zero and when the scan is continued the zero current line can be used as a baseline for the new wave. A shielded Pt disc working electrode similar to the shielded electrode described by Bard (34) was constructed and numerous analyses carried out in DMF electrolyte containing approximately 6 mM $SOCl_2$. In all the SLV analyses the working electrode current did not fall below 7 μA and no new reduction peaks were observed between the $SOCl_2$ and SO_2 peaks. It is thought that the current did not decline to a negligible value because the design of the electrode shield was not properly optimized for the DMF electrolyte. Since the optimization of such a shield would be time consuming and due to the proven effectiveness of IR techniques for the analysis of SO_2, further work with the convection free held scan technique was discontinued.

1.1.6 Voltammetry of Neutral $SOCl_2$ Electrolyte with Added Sulfur

Voltammetry of Sulfur in DMF Electrolyte. - The analysis of sulfur in $SOCl_2$ electrolytes by voltammetry is of interest because sulfur is a discharge product of $Li/SOCl_2$ cells. Although *sulfur and sulfur-SO_2 mixtures* have been investigated earlier in DMF by voltammetry (10), further studies were undertaken to obtain voltammetric data for $SOCl_2$-sulfur solutions which were unavailable yet required to interpret LSV results for electrolyte from discharge $SOCl_2$ cells.

The voltammogram obtained for 15.6 mM of sulfur dissolved in DMF supporting electrolyte is shown in Figure 19. Similar voltammograms were obtained after the solution was stored in the cell for 16.7 and 90.5 hrs at 23°C which indicates that sulfur is stable towards both the DMF electrolyte and the Ag/AgCl reference electrode.

The voltammogram shown in Figure 19 for sulfur is very similar to the results obtained by Dey and Bowden (10) in DMF and by Sawyer and coworkers (35) in DMSO. The first reduction peak in Figure 17 occurred at − 0.725 V and the second at − 1.435 V vs Ag/AgCl compared with peaks at − 0.6 V and − 1.15 V respectively reported by Dey and Bowden.

Following a thorough study of the electrochemistry of sulfur reduction in DMSO solutions Sawyer (35) concluded that the first reduction at − 0.725 V is due to the two electron reduction of elemental sulfur.

$$S_8 + 2e^- \rightarrow S_8^{2-} \quad Ep = -0.725\ V$$

The S_8^{2-} polysulfide product is a linear chain which stabilizes the double negative charge whereas the elemental sulfur has a cyclic structure. The reduction is irreversible probably due to the change from a ring to a liner structure.

The second reduction wave of sulfur at − 1.435 V was assigned by Sawyer to the two electron reduction of the polysulfide S_8^{2-}.

$$S_8^{2-} + 2e^- \quad S_8^{4-} \quad Ep = 1.435\ V$$

The anion S_8^{4-} is unstable and slowly dissociates to the S^{4-} species.

$$S_8^{4-} \rightarrow 2\ S_4^{2-}$$

The observation that elemental sulfur can be reduced at − 0.725 V vs Ag/AgCl or 2.695 V vs Li has some interesting implications in commercial $Li/SOCl_2$ cells. Under similar voltammetric conditions, SO_2 reduces at 2.47 V vs Li. Thus in an electrolyte starved $Li/SOCl_2$ cell in which all the $SOCL_2$ was consumer leaving only SO_2 and S, it would be expected that sulfur would be reduced before SO_2. The preferential reduction of sulfur before SO_2 requires that sulfur be soluble in $LiAlCl_4/SOCl_2$. A search of several review articles (36) on solubilities in SO_2 has failed to reveal any information about the solubility of sulfur in SO_2. Thus to further explore such reactions solubility measurements for sulfur in SO_2 and $LiAlCl_4/SOCl_2$ may have to be carried out.

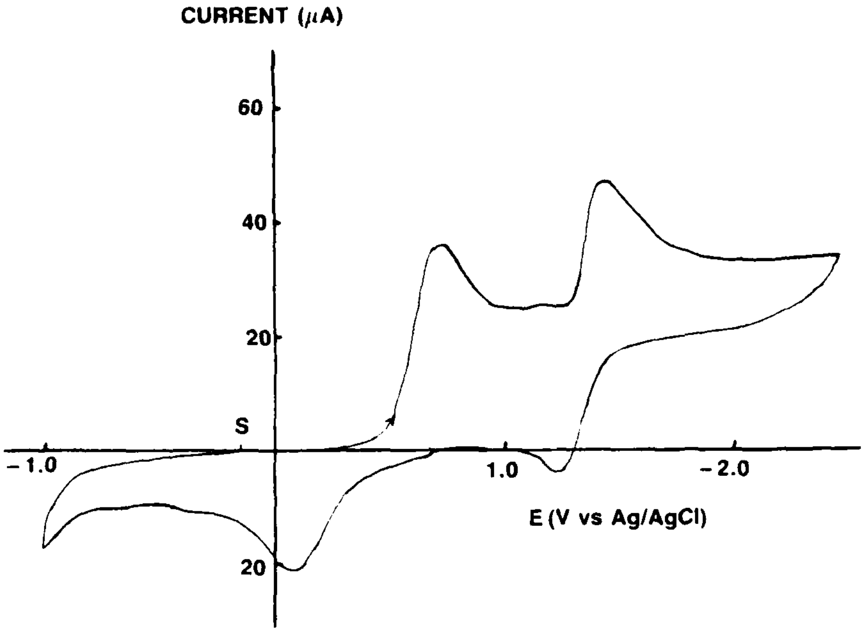

Figure 19: Voltammogram for 15.6 mM sulfur in 0.1M TBAPF$_6$/DMF at 23°C, scan rate 200 mV/sec. (s) indicates the start of the scan at 0.122 V, the OCP.

Voltammetry of Neutral $SOCl_2$ Electrolyte with Sulfur. - Seven voltammograms are shown in Figure 20 for 0.55 mM sulfur with concentrations of $SOCl_2$ ranging from 0.00 to 3.9 mM in DMF. For the analysis without $SOCl_2$ only one small broad peak for sulfur appeared at – 1.175 V and the peak observed at – 0.725 V with 15.6 mM sulfur in Figure 19 was absent. However, with 1.3 to 3.9 mM $SOCl_2$ the first sulfur reduction peak at – 0.825 V could possibly be SO_2 but its constant peak height as the $SOCl_2$ peak increase as more $SOCl_2$ was added suggests that it is more likely sulfur. The second sulfur peak at – 1.175 V observed without added $SOCl_2$ increased significantly when 0.26 and 0.52 mM $SOCl_2$ was added out of proportion to the contribution of the – 1.62 V peak of $SOCl_2$. Thus it appears that low concentrations of $SOCl_2$ somehow increase the response of the Pt working electrode to dissolved sulfur.

To interpret voltammograms of $SOCL_2$ electrolyte from discharged cells which could be saturated with sulfur, a DMF solution containing 31 mM sulfur and 7 mM $SOCl_2$ was analyzed by LSV analysis. The voltammogram which is presented in Figure 21 shows a very sharp sulfur peak at – 1.31 V. It thus appears that at high concentrations of S in $SOCl_2$ the – 0.725 V peak seen with 15.6 mM of pure sulfur in DMF shifts to – 1.31 V and perhaps the – 1.435 V peak combines with the – 1.62 V peak of $SOCl_2$. These findings raise the possibility that the – 1.62 V peak seen with $LiAlCl_4/SOCl_2$ (cf. Figure 2) may in fact be the second sulfur peak which could be from sulfur produced from the reduction of $SOCL_2$ during the first reduction peak of the sweep. To obtain sufficient information to make reliable assignments for the – 1.31 V sulfur and the – 1.62 V $SOCl_2$ peaks it is clear that additional LSV measurements of S and S-$SOCl_2$ mixtures over a wide range of concentrations in DMF are required.

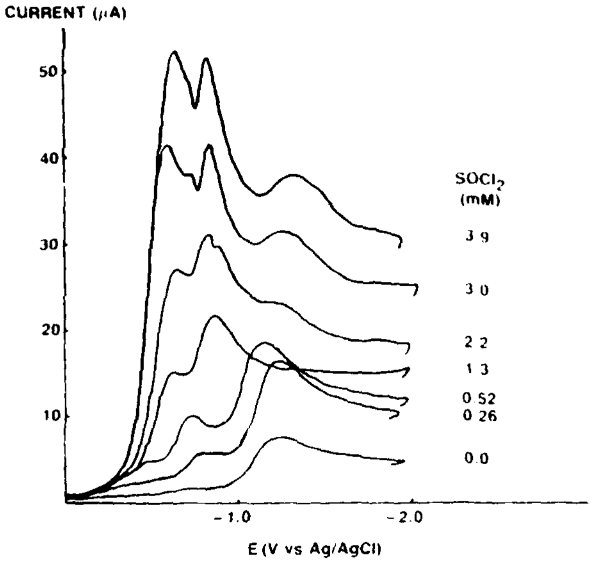

Figure 20: Voltammograms for 0.55 mM sulfur in 0.1M TBAPF$_6$/DMF with from 0.26 to 3.9 mM SOCl$_2$ at 23°C, scan rate 200 MV/sec.

The potential was first scanned in the cathodic direction in all cases and the anodic portion of the scan is not shown to simplify the presentation.

1.1.7 Constant Current Coulometry of SOCl$_2$ Neutral Electrolyte on Glassy Carbon Cathodes at 25°C

Introduction - The reduction mechanism of 1.8 M LiAlCl$_4$/SOCl$_2$ neutral electrolyte at a glassy carbon cathode was investigated using constant current electrolysis combined with LSV analysis to follow the concentration of the discharge products. The apparatus and the general procedure used for the constant current electrolysis experiments is described in Section 1.1.2. The voltammograms obtained after the constant current electrolysis of LiAlCl$_4$/SOCl$_2$ at a 4 cm^2 glassy carbon cathode to n = 1.12 and n = 1.95 equivalents of charge passed per mole of SOCl$_2$ are shown in Figures 22 and 23 respectively. The most remarkable feature of the voltammograms at both n = 1.12 and 1.95 is the absence of the SO$_2$ peak at approximately − 0.95 V which should increase greatly by n = 1.12 since SO$_2$ is one of the main products of SOCl$_2$ reduction. By comparison, electrolysis in the SO$_2$ concentration as shown in Figure 29 and discussed in Section 1.1.9. The very low SO$_2$ concentration could indicate that an intermediate other than SO$_2$ is formed with SOCl$_2$ is reduced at glassy carbon and a number of additional experiments were carried out in an attempt to obtain direct evidence for the existence of such an intermediate. These experiments will be discussed later in this section.

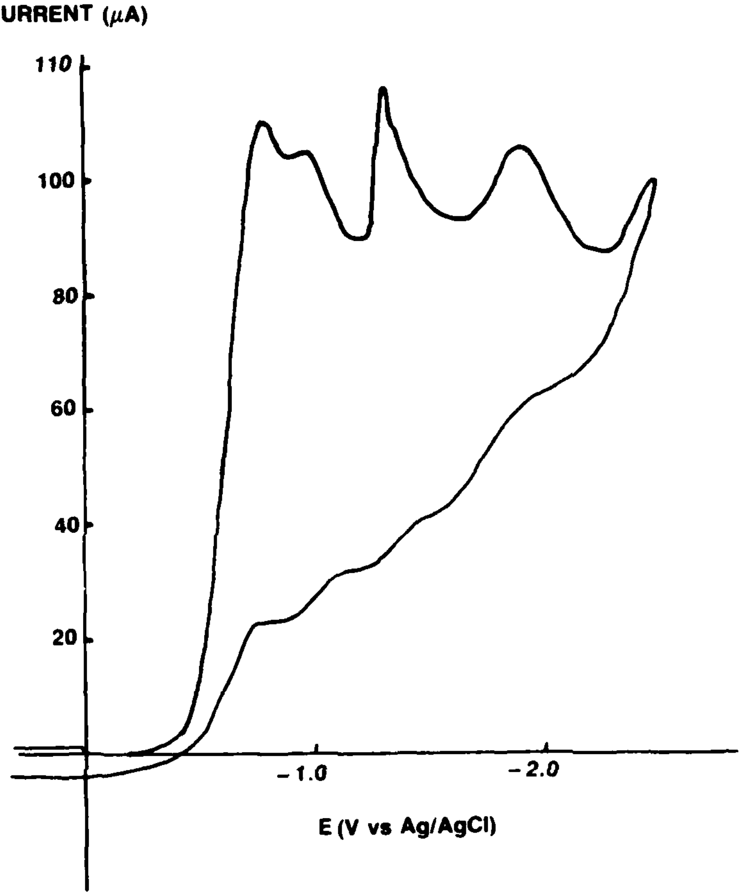

Figure 21: Voltammogram for 31 mM sulfur and $LiAlCl_4/SOCl_2$ after dissolution in 10 ml of 0.1 M $TBAPF_6$/DMF at 23°C, scan rate 200 mV/sec.

Approximately 6 μl of 1.8 M $LiAlCl_4/SOCl_2$ was added to the DMF to prepare the sample.

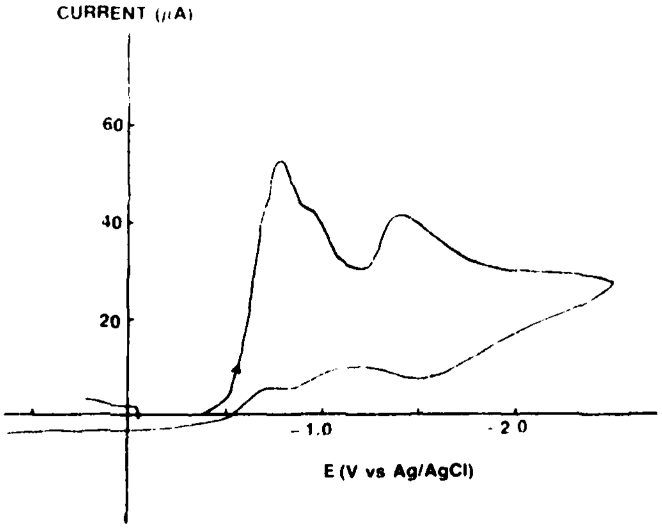

Figure 22: Voltammogram of 6.1 μl of 1.8M $LiAlCl_4/SOCl_2$ in $TBAPF_6$/DMF after electrolysis on a 4 cm² glassy carbon cathode at 0.50 mA/cm² to n = 1.12 at 25°C scan rate 200 mV/sec.

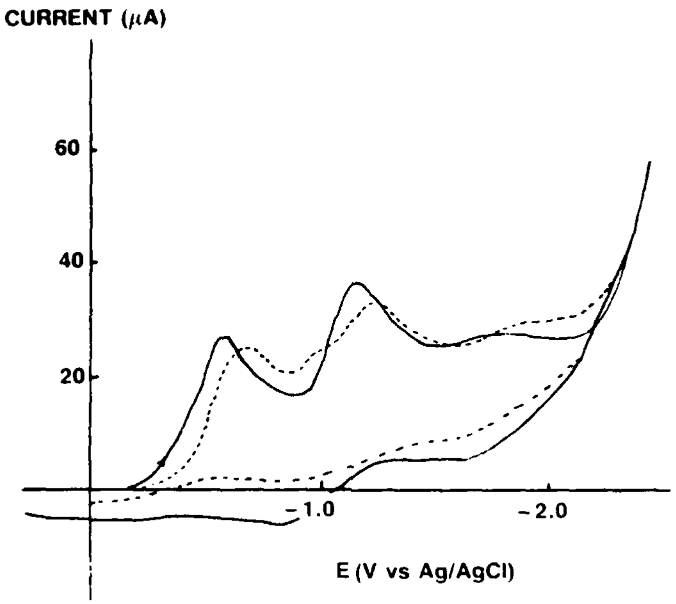

Figure 23: Voltammogram of 6.1 μl of 1.8 M $LiAlCl_4/SOCl_2$ in $TBAPF_6$/DMF after electrolysis on a 4 cm^2 glassy carbon cathode at 0.50 mA/cm^2 to n = 1.95, scan rate 200 mV/sec.

(------------), scan after 26 hours storage, OCP = 0.170V
(. . . . .), scan immediately after electrolysis, OCP = 0.025V

Colometry Results - The cell potential during constant current electrolysis of $LiAlCl_4/SOCl_2$ plotted versus n the equivalents of charge passed/mole of $SOCl_2$ is shown in Figure 24. The potential of the cathode during electrolysis was recorded with a Ag/AgCl reference electrode but converted to a Li reference standard to make the data clearer to those more familiar with Li reference potentials. The sharp cutoff between n = 1.8 and 2.0 is consistent with the generally accepted (2, 11) reaction for the two electron reduction of $SOCl_2$.

$$SOCl_2 + 2e^- \rightarrow 1/2\ SO_2 + 2Cl^- + 1/2\ S \qquad [1]$$

The decline of the potential slightly before n = 2.00 agrees with what one would expect from the Nernst Law since the solution is very dilute and the electrolysis is occurring at an appreciable current density (i.e. 0.5 mA/cm^2) at a smooth electrode.

The finding that the cell potential during electrolysis at 0.5 mC/cm^2 to n = 1.8 holds relatively constant without any plateaus adds further support that the reduction of $SOCl_2$ occurs as in Equation [1] above without any long lived intermediates. This conclusion is limited of course to dilute $SOCl_2$ solutions in DMF supporting electrolyte which may either destabilize or stabilize intermediates possibly present in $LiAlCl_4/SOCl_2$ electrolyte. To increase the sensitivity of the constant current electrolysis to possible intermediates, an electrolysis was carried out at 0.05 mA/cm^2 (cf. Figure 25) instead of the 0.05 mA/cm^2 used for the test described in Figure 24. At 0.05 mA/cm^2 the cell potential rose almost 1.0 V and again no distinct plateaus in the potential were observed until approximately n = 2.5 when the test was voluntarily terminated. The electrolysis at 0.05 mA/cm^2 required 19.5 hrs to complete. Thus, constant current electrolysis experiments at lower rates were considered impractical because of the inaccuracies due to interdiffusion through the cell frit connecting the working and counter electrode compartments would be excessively large for electrolyses carried out for periods over 200 hrs.

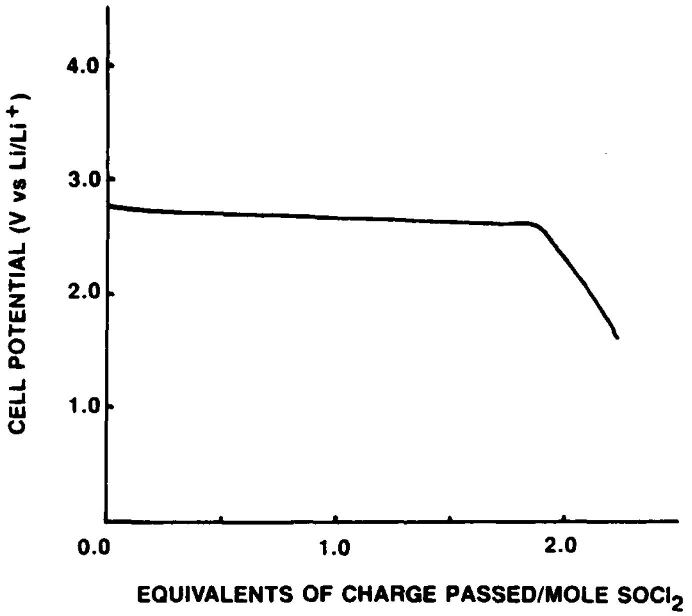

Figure 24: Cell potential during 0.50 mA/cm² constant current electroylsis of 6.0 mM $SOCl_2$ in 0.1M $TBAPF_6$/DMF at a 4 cm² glassy carbon cathode at 25°C.

The sample of 8.78 mg of 1.8M $LiAlCl_4/SOCl_2$ electrolyte was added to 10.0 ml of DMF. Cell potential was monitored with a Ag/AgCl ref. electrode and the potentials converted to a Li/Li+ ref. electrode scale on the basis of Ag/AgCl 3.42V vs Li/Li+.

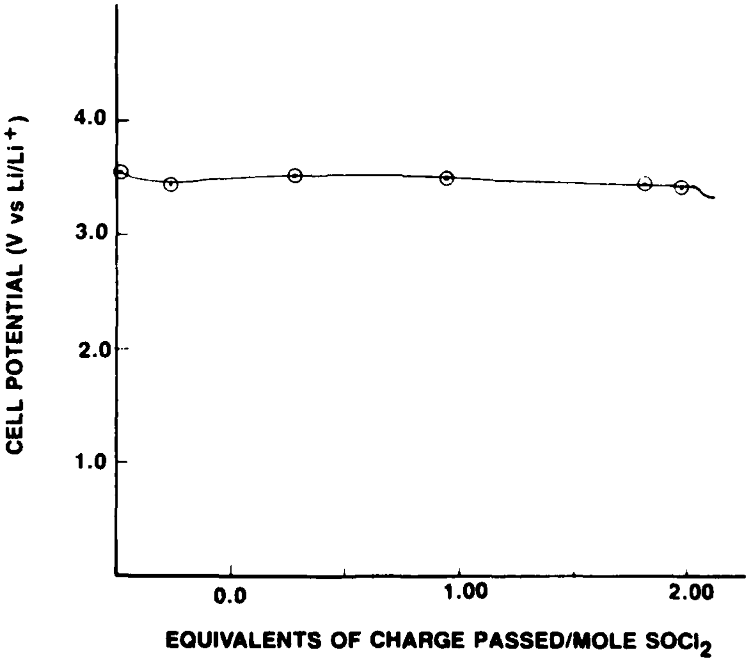

Figure 25: Cell potential during 0.05 mA/cm² constant current electrolysis of 5.6 mM $SOCl_2$ in 0.1M $TBAPF_6$/DMF at a 4 cm² glassy carbon cathode at 25°C.

The sample of 8.18 mg of 1.8 M $LiAlCl_4/SOCl_2$ was added to 10 ml of the DMF supporting electrolyte. The cell potential was monitored with a Ag/AgCl ref electrode and the potentials converted to a Li/Li+ ref electrode scale on the basis of Ag/AgCl 3.55V vs Li/Li+.

Interrupting the constant current electrolysis for 15 minute intervals during the electrolysis to exchange the electrolysis cathode for a platinum wire LSV working electrode causes fluctuations in the potential as shown in Figure 26. These fluctuations are caused by the absence of mass transfer polarization when the electrolysis is resumed. Although it would be desirable to have all three electrodes in the working electrode compartment from the start of the experiments, the small space available makes such an arrangement difficult. However, a design has been developed which is under construction for use in the low temperature coulometry experiments.

The cell potentials during many of the colometry experiments showed plateaus and minima similar to those shown for the uninterrupted electrolysis in Figure 26. These large fluctuations in the potentials during electrolysis were not reproducible and showed no pattern. It is thought that they are due to changes in the stirring rate and position of the small magnetic stir bar in the electrolysis cell (see Figure 1). The stirring rate was found to have a maximum effect of 21 mV on the reference electrode as discussed in Appendix A but the effect on mass transfer to the cathode is apparently much larger.

Voltammetry Results After Coulometry. - Voltammograms taken during the electrolysis of $LiAlCl_4/SOCl_2$ at a glassy carbon electrode show that the $SOCl_2$ concentration decreases during the electrolysis as indicated by the decrease in the $SOCl_2$ peak current. However, the decrease in the $SOCl_2$ peak current is not as great as expected as shown in Figure 27 where the experimental and theoretical values are compared. The theoretical $SOCl_2$ peak current remains at 5 μA beyond $n = 2.0$ in Figure 27 because the electrolyte background current was 5 μA.

The voltammograms obtained after electrolysis to $n = 1.12$ and 1.95 (i.e. Figures 22 and 23) showed a negligible SO_2 peak consequently the missing SO_2 required by the stoichiometry of the $SOCl_2$ reduction reaction must be accounted for in terms of some alternative new product, intermediate or reduction pathway. If an intermediate was formed, it is likely that it would be reduced at a potential slightly cathodic to the reduction potential of $SOCl_2$ and is therefore hidden under the $SOCl_2$ peak. The large $SOCl_2$ peak currents seen in Figure 27 compared to the theoretical peak currents, could be due to the reduction of $SOCl_2$ and somel unknown product or intermediate reduced near the $SOCl_2$ peak potential.

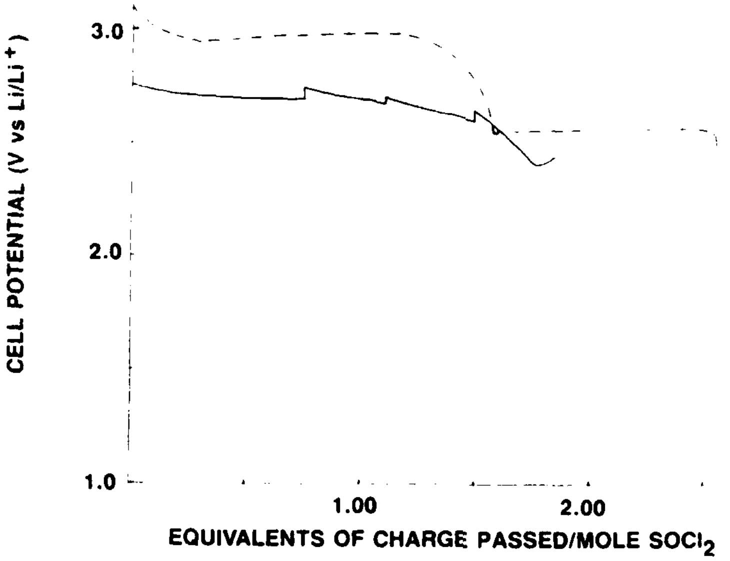

Figure 26: Cell potentials during 0.50 mA/cm² constant current electrolysis of approximately 9 mg samples of 1.8 M $LiAlCl_4/SOCl_2$ in 10 ml $TBAPF_6/DMF$ at a glassy carbon cathode

(-----------------), electrolysis of sample with 6.67 mM $SOCl_2$ with ~ 15 min interruptions at $n = 0.74$, 1.12, 1.49 and 1.86 for LSV analysis

(— —), continuous uninterrupted electrolysis of sample with 6.38 mM $SOCl_2$ to $n = 2.85$. The plateau from $n = 0.0$ to 1.6 is due to a stirring problem.

The cell potential was monitored with a Ag/AgCl ref. electrode and the potentials converted to a Li/Li+ ref. electrode scale on the basis of Ag/AgCl 3.55 vs Li/Li+.

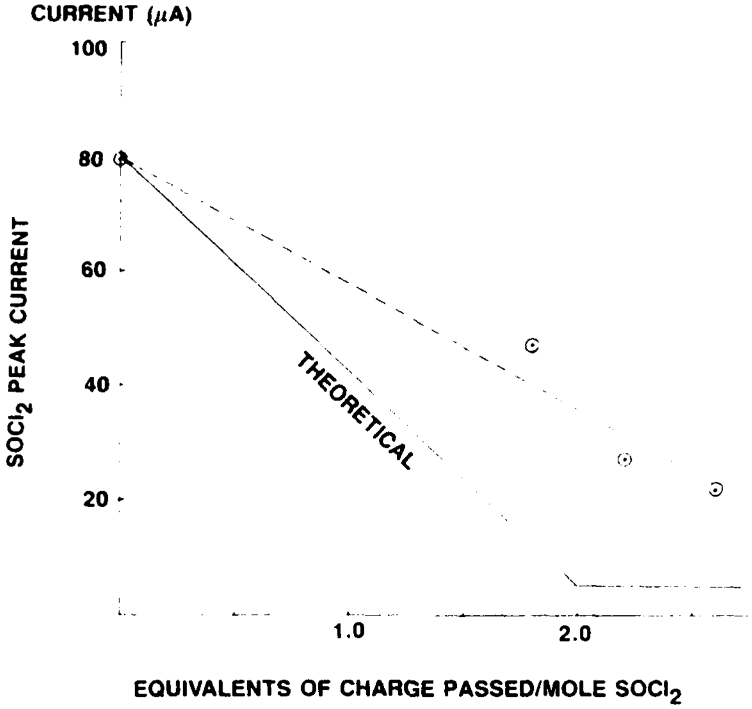

Figure 27: The relationship between the voltammetry current peak for $SOCl_2$ and the equivalents of charge passed/mole of $SOCl_2$ during electrolysis.

For electrolysis of 8.09 mg of 1.8 M $LiAlCl_4/SOCl_2$ in 10 ml $TBAPF_6/DMF$ at 0.5 mA/cm^2 at a 4 cm^{2}5 glassy carbon cathode.

To investigate the possible existence of an intermediate or product hidden under the $SOCl_2$ peak three additional constant current electrolysis experiments were carried out to n = 2.2 and n = 2.6. Two of the electrolyses were carried out at 0.5 mA/cm^2 as before and one at 0.05 mA/cm^2 to determine whether plateaus appeared in the potential-time curves during electrolysis. The electrolyses were extended to n = 2.6 because if an intermediate was present hidden under the $SOCl_2$ peak then the $SOCl_2$ peak current would be sizeable, past n = 2.0.

The LSV results after electrolyses of neutral electrolyte at a glassy carbon electrode showed that the $SOCl_2$ peak current was only reduced by 50% at n = 1.0 and 75% by n = 2.6. The SO_2 peak declined during electrolysis from n = 0 to n = 1.12 and was not detected at n = 1.8, 2.2 and 2.6 which was very surprising. The peak at approximately 2.2V vs the Li/Li+ reference which is thought to be due to sulfur greatly increased as the electrolysis proceeded from n = 1.12 to 1.80 then declined at n = 2.2 and disappeared by n = 2.6.

From these findings, it was concluded that both $SOCl_2$ and SO_2 were probably being reduced concurrently during the constant current electrolysis at 0.5 mA/cm^2 as follows:

$$SOCl_2 + 2e \rightarrow 1/2S + SO_2 + 2Cl^- \quad [1]$$
$$SO_2 + e \rightarrow SO_2^- \quad [3]$$
$$2SO_2^- \rightarrow S_2O_4^= \quad (4)$$

Normally in a battery since $SOCl_2$ reduces at 3.65V vs Li/Li+ and SO_2 at 2.95V, all the $SOCl_2$ would have to be reduced before SO_2 reduction could occur. However, for electroanalysis in DMF with only 7.10^{-3} moles of $SOCl_2$ in the DMF supporting electrolyte, the $SOCl_2$ near the glassy carbon electrolysis electrode is depleted during electrolysis and reduced at a lower potential vs. Li/Li – in accordance with the Nernst equation. The SO_2 product is probably absorbed on the glassy carbon and is present at a high concentration which allows it to be reduced concurrently with the $SOCl_2$. Thus, the postulated reduction mechanism of $SOCl_2$ to $S_2O_4^=$ if it occurs may be entirely due to the use of a very dilute solution of $SOCl_2$ in DMF sup porting electrolyte. To minimize this reduction and other effects which make it difficult to apply the results to commercial Li/$SOCl_2$ cells, we intend to carry out electrolysis experiments during the second half of the present study using $SOCl_2$ electrolytes without an organic supporting electrolyte.

A new large and sharp peak at 1.96 vs Li/Li+ appears during LSV after electrolysis on glassy carbon to n = 2.6 which is not evident at n = 1.8. This peak decays approximately 35% after 2 hours and 90% after 66 hours at 25°C and it is the first intermediate species which has been unequivocally identified. However, this intermediate is of minor significance because it is thought to be some unstable product of sulfur or SO_2 reduction which may be decomposing or reacting with DMF.

Voltammetry after electrolysis to n = 1.12 and n = 1.95 followed by storage periods up to 117 hrs were carried out to determine if new peaks appeared or existing peaks disappeared indicating the existence of long lived $SOCl_2$ reduction intermediates. Voltammetry after electrolysis to n = 1.12 and 88 hours storage and electrolysis to n = 2.2 and 1.0 hour storage showed no significant drop in the $SOCl_2$ peak, or increases in any existing or new peaks. Electrolysis of 1.8M $LiAlCl_4$/$SOCl_2$ to n = 1.95 with LSV analysis after 0, 1, 2, 4, 20, 26 and 117 hrs of storage was carried out to gain information concerning the possible existence of long lived intermediates formed near the end of discharge.

As illustrated in Figure 28 a new reduction peak began to appear after 4 hrs. of storage at 1.84 V vs Li/Li+ and grew in height by 20 hrs. then declined after 26 hrs. (cf Figure 23). This peak is probably due to the same intermediate observed at 1.96 V vs Li/Li+ after electrolysis to n = 2.6 discussed earlier. This intermediate is thought to be some unstable product of sulfur or SO_2 reduction which may be decomposing or reacting with DMF and is considered of minor importance to understanding practical Li/$SOCl_2$ cells. Thus no further work is planned to identify the chemical composition of this intermediate.

1.1.8 Constant Current Coulometry of Neutral and Acid $SOCl_2$ Electrolyte on Platinum Cathodes at 25°C

Electrolysis of $SOCl_2$ Neutral Electrolyte at Platinum. - The reduction mechanism of 1.8M $LiAlCl_4$/$SOCl_2$ neutral electrolyte at 1.0 x 2.0 cm platinum cathode was investigated using constant current electrolysis combined with LSV analysis to follow the concentration of the discharge products. The voltammograms obtained after the constant current electrolysis of $LiAlCl_4$/$SOCl_2$ at a 4 cm^2 platinum cathode to n = 0.94 and n = 1.41 equivalents of charge passed per mole of $SOCl_2$ are shown in Figure 29. As would be expected, the $SOCl_2$ peak current decreases linearly with the amount of charge passed (see Figure 30) and the SO_2 peak current increases significantly. This contrasts sharply with the electrolysis of $SOCl_2$ neutral electrolyte at a glassy carbon cathode (cf. Figures 22 and 23) where a slight decrease rather than an increase in the SO_2 peak current was observed as the electrolysis progressed.

It is well known (17) that platinum supported on carbon acts as a catalyst for $SOCl_2$ reduction in Li/$SOCl_2$ batteries. Thus one could prematurely conclude that the greater increase in the SO_2 peak current obtained by LSV during electrolysis at Pt compared to carbon confirms the catalytic properties of platinum. However, if the amounts of $SOCl_2$ consumed by n = 1.5 as indicated by the reduction in the LSV peak current for $SOCl_2$ is compared for Pt and glassy carbon using the results in Figures 27 and 29 it is found that 45 and 61.6% of the $SOCl_2$ is consumed for the Pt and glassy carbon electrodes respectively. Thus if the most effective catalytic cathode for $SOCl_2$ reduction is defined as the cathode which reduces the most $SOCl_2$ for a given amount of current passed then glassy carbon is clearly the better catalyst in DMF supporting electrolyte. In a commercial battery however, cathode catalysts are evaluated in terms of their effectiveness in stimulating all reduction reactions at the cathode at the highest possible potentials. Since SO_2 appears to be reduced more effectively at glassy carbon than at Pt one is led to conclude from the available data that at least in DMF, glassy carbon is the better catalyst by either definition of catalyses. In commercial batteries, Pt is the better catalyst which may be due to a combination of factors such as the thousand times greater $SOCl_2$ concentration, the absence of DMF and the very high surface area of the supported Pt. To determine the importance of surface area and the nature of the carbon surface on catalytic activity, additional constant current electrolysis experiments were undertaken using Shawinigan carbon cathodes which are discussed in Section 1.1.10.

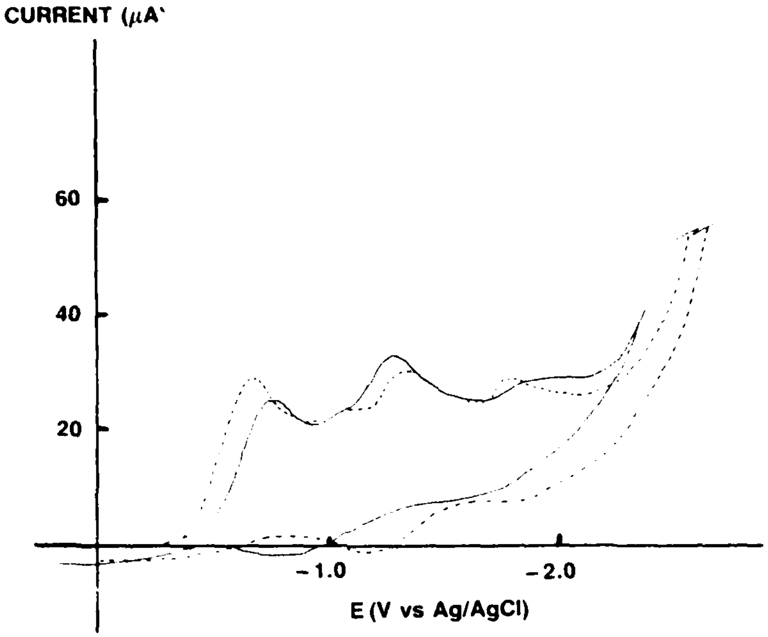

Figure 28: Voltammogram of 6.1 μl of 1.8M $LiAlCl_4/SOCl_2$ in 10 ml of $TBAPF_6/DMF$ after electrolysis on a 4 cm^2 glassy carbon electrode at 0.50 mA/cm^2 to $n = 1.95$ scan rate 200 mV/sec.

(·················), scan after 4 hours storage, OCP = 0.025V

(. _ . _ .), scan after 20 hours storage, OCP = 0.315, due to the change in the OCP the scan has been shifted in this figure 275 mV cathodic (i.e. toward the right side) compared to the experimental scan to facilitate comparison.

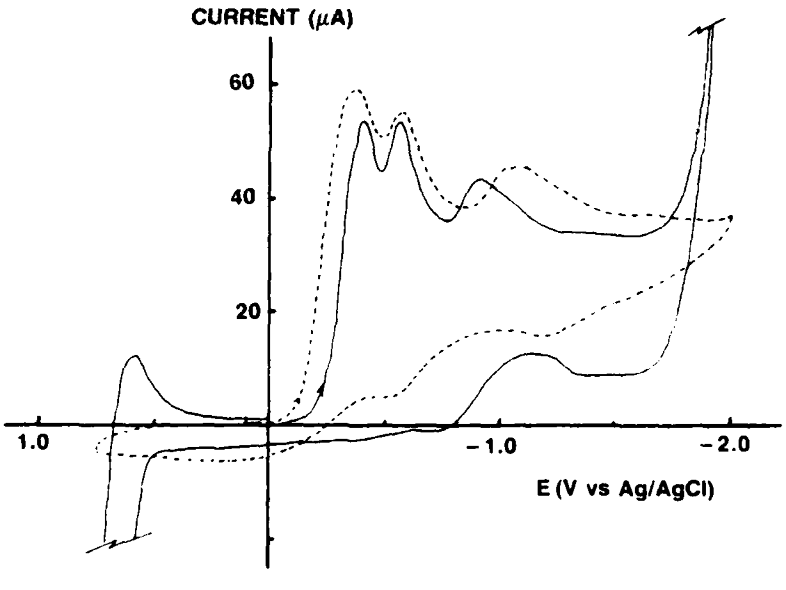

Figure 29: Voltammogram of 4.7 μl of 1.8M $LiAlCl_4/SOCl_2$ in 10 ml of $TBAPF_6/DMF$ after electrolysis on a 4 cm^2 platinum cathode at 0.50 mA/cm^2, 25°C to $n = 0.94$ scan rate 200 mV/sec.

(·················), scan at $n = 0.94$, OCP = 0.100 V

(. _ . _ .), scan at $n = 1.41$, OCP = 0.00 V. The 4.7 μl sample of $LiAlCl_4/SOCl_2$ yielded a DMF solution 5.51 mM in $SOCl_2$.

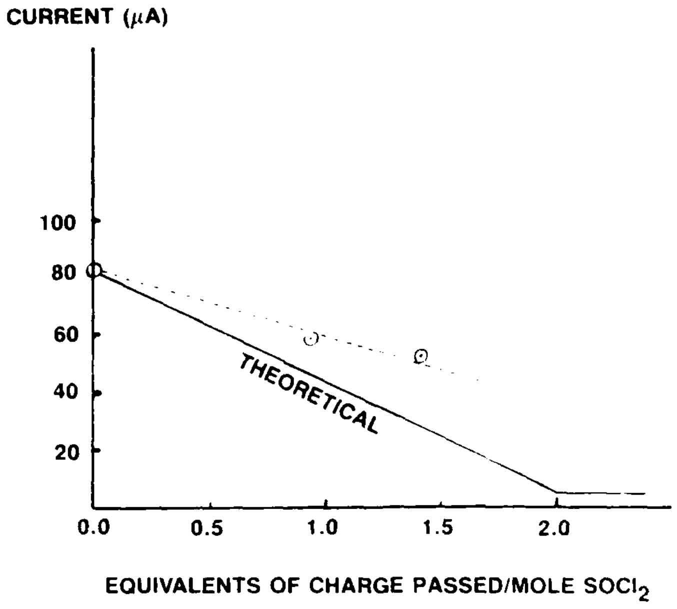

Figure 30: The relationship between the voltammetry current peak for $SOCl_2$ and the equivalents of charge passed per mole of $SOCl_2$ during electrolysis of $LiAlCl_4/SOCl_2$ at a platinum cathode.

For details of the electrolysis conditions see the caption for Figure 28.

Figure 31 shows the voltammograms obtained 60 minutes and 42 hours after electrolysis of $LiAlCl_4/SOCl_2$ electrolyte to n = 1.41. Minimal decay of the SO_2 peak was seen after 60 minutes but after 42 hrs both the $SOCl_2$ and the SO_2 peak declined about equally with much less separation of the two peaks. although the SO_2 peak remains a distinct peak, it is clear that the SO_2 concentration has declined far more than the $SOCl_2$ concentration. As discussed in Section 1.1.5 and illustrated in Figures 13 and 14, SO_2 slowly reacts with $LiAlCl_4/SOCl_2$ in DMF electrolyte causing the merging of the SO_2 and $SOCl_2$ peaks and the formation of a new peak at approximately − 1.2 V. The peak at approximately − 1.2 V became sharper and moved in the anodic direction from the start of the electrolysis to n = 0.94 (cf. Figure 29) which required 51 minutes but the peak at approximately − 1.2 V only increased slightly during the 42 hrs of storage. This lack of any change in the peak height for the − 1.2 V peak is peculiar and may be due to some catalytic effect of the 4 cm^2 Pt electrode surface.

The main conclusion from the voltammograms after storage for the electrolysis of neutral electrolyte at a platinum cathode is that the decline of the SO_2 peak can be explained by a normal reaction of SO_2 with the electrolyte and the decline is not due to the decomposition of an intermediate. Thus the LSV peak assigned to the $SO{\bullet}SOCl_2$ intermediate in the literature (10) is clearly SO_2. The decline in the SO_2 peak reported in the above paper (10) when the electrolyte was warmed after electrolysis was not due to the decomposition of the $SO{\bullet}SOCl_2$ reduction intermediate but was probably caused in part by a lowering of the solubility of SO_2 in the DMF electrolyte at elevated temperatures.

Electrolysis of $SOCl_2$ acid electrolyte at platinum. - The voltammograms obtained before and after the constant current electrolysis of 2.0M $AlCl_3$ - 0.10M $LiAlCl_4/SOCl_2$ acid electrolyte at a 4 cm^2 platinum cathode to n = 1.12 equivalents of charge passed per mole of $SOCl_2$ are shown in Figure 32. The $SOCl_2$ peak current at the start of the electrolysis was 66.5 μA and 38.9 by n = 1.12 thus with a 5 μA background current 45% of the $SOCl_2$ was consumed by n = 1.12 compared with 56% expected. Earlier for electrolysis of neutral $SOCl_2$ electrolyte with a 4 cm^2 Pt cathode it was found that only 45% of the $SOCl_2$ was consumed by n = 1.5 when 75% consumption of the $SOCl_2$ was expected theoretically. Because the coulombic efficiency of $SOCl_2$ reduction is greatly improved by using acid instead of neutral electrolyte it appears that $SOCl_2$ acid electrolyte may function as a homegeneous catalyst in DMF.

Figure 33 shows the voltammograms obtained 0.0 and 16 hrs after the end of the electrolyses of acid electrolyte to n = 1.12 at a 4 cm^2 platinum cathode. After 16 hrs of storage, two unusual changes were evident in the voltammogram (i) a very small peak at − 0.875 V (ii) a large increase in the size of the SO_2 peak current compared to the $SOCl_2$ peak current. An additional voltammogram was taken after 19 hrs storage and again the small peak at − 0.875 was observed, thus it is real and not an instrumental artifact. It is possible that the − 0.875 peak is due to the decomposition of a very small amount of some $SOCl_2$ discharge intermediate.

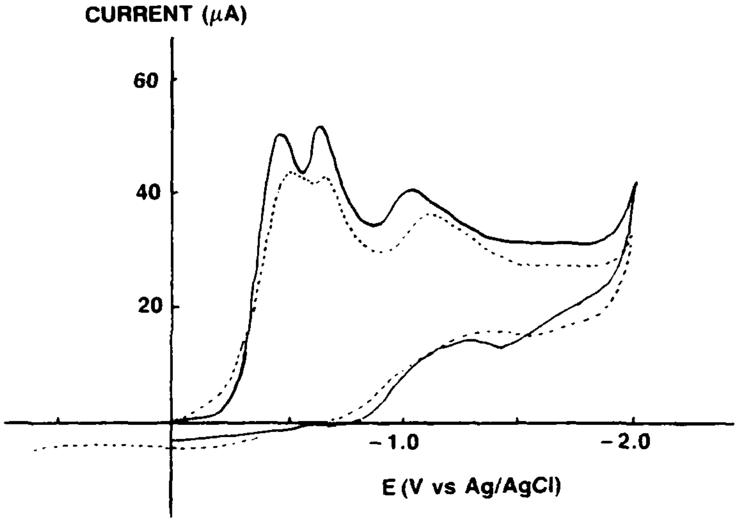

Figure 31: Voltammograms of 4.7 μl of 1.8M $LiAlCl_4/SOCl_2$ in $TBAPF_6$/DMF, 60 minutes and 42 hours after electrolysis on a 4 cm² platinum cathode at 0.50 mA/cm² 25 °C for 1.41 equivalents of charge passed/mole of $SOCl_2$, scan rate 200 mV/sec.

(-----------------), scan after 60 minutes stand
(__________), scan after 42 hours

The 4.7 μl sample of $LiAlCl_4/SOCl_2$ yielded a DMF solution 5.51 mM in $SOCl_2$.

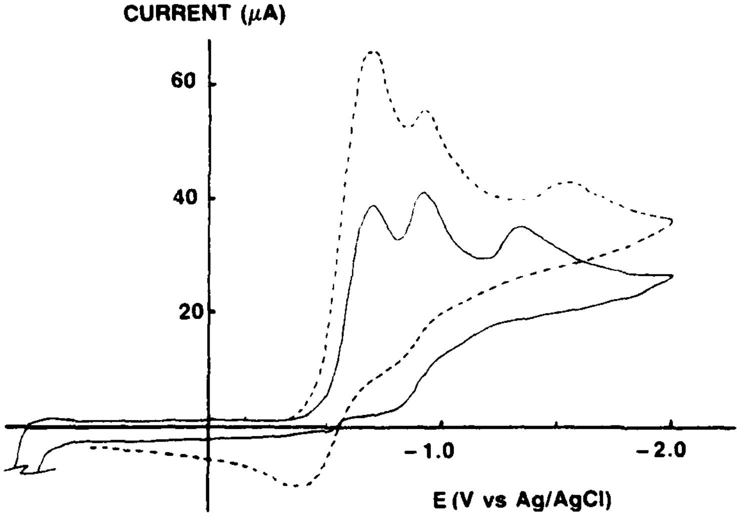

Figure 32: Voltammograms of 8.0 mg of 2.0M $AlCl_3$ − 0.10M $LiCl/SOCl_2$ in 10 ml $TBAPF_6$/DMF after electrolysis on a 4 cm² Pt cathode at 0.50 mA/cm², 25 °C to n = 0.0 and n = 1.12 scan rate 200 mV/sec.

(-----------------), scan at n = 0.00, OCP = 0.217
(__________), scan at n = 1.12, OCP = 0.150

The 8.0 mg of $SOCl_2$ acid electrolyte contained 5.67 mM $SOCl_2$.

---

[1] These values were obtained using the best fit lines shown in the Figures correcting for the background current

The decrease of the $SOCl_2$ peak and the increase in the 1.36 V peak after 16 hrs storage may be caused by some reaction between SO_2 and $SOCl_2$ acid electrolyte in DMF similar to the reactions seen earlier for SO_2 in neutral electrolyte (see Figures 13 and 14). To better understand these changes in the SO_2 and $SOCl_2$ peak currents during extended storage, it will be necessary to carry out voltammetric investigations of acid $SOCl_2$ electrolyte solutions containing known concentrations of SO_2 with various storage periods similar to the investigation described in Section 1.1.5 for SO_2 in neutral electrolyte

1.1.9 Constant current coulometry of acid $SOCl_2$ electrolyte on glassy carbon cathodes at 25°C

The voltammograms obtained before and after the constant current electrolysis of 2.0M $AlCl_3$ - 0.10 M $LiCl/SOCl_2$ acid electrolyte at a 4 cm^2 glassy carbon cathode to n = 1.12 equivalents of charge passed per mole of $SOCl_2$ are shown in Figure 34. The $SOCl_2$ peak current at the start of the electrolysis was 59.0 μA and 27.5 μA by n = 1.12 thus with a 5 μA background current 58% of the $SOCl_2$ was consumed by n = 1.12 compared with 56% expected. Previously for electrolysis of acid $SOCl_2$ electrolyte at a platinum cathode to n = 1.12 only 45% of the $SOCl_2$ was consumed. Thus glassy carbon is a more efficient cathode substrate for $SOCl_2$ reduction than platinum in both acid and neutral $SOCl_2$ electrolyte Figure 35 shows the voltammograms obtained 4 and 23 hrs after the electrolysis of $SOCl_2$ acid electrolyte on glassy carbon to n = 1.12. After 4 hrs of storage the SO_2 peak broadened, then during the next 19 hrs of storage the SO_2 peak became sharper and larger than the $SOCl_2$ peak. The decomposition of large amounts of long lived $SOCl_2$ reduction intermediates can probably be ruled out because none of the existing peaks decreased by a large amount accompanied by the appearance of any large new peaks The sharpening of the broad SO_2 peak during the period from 4 to 23 hrs after electrolysis is peculiar and is possibly due to some reactin between SO_2 and $SOCl_2$ acid electrolyte in DMF similar to the reactions seen earlier for SO_2 in neutral electrolyte. As recommended earlier in Section 1.1.8, it is clear that it will be necessary to carry out additional voltammetric studies of acid electrolyte solutions with known concentrations of SO_2 to be able to understand the charges in the SO_2 and $SOCl_2$ peak currents during storage after electrolysis.

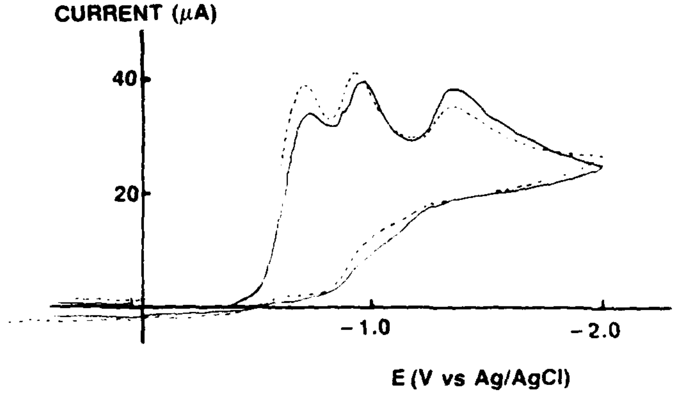

Figure 33: Voltammogram of 8.0 mg of 1.0M $AlCl_3$ – 0.10M $LiCl/SOCl_2$ in 10 ml $TBAPF_6$/DMF after electrolysis on a 4 cm^2 Pt cathode to n = 1.12 after 0.0 and 16 hrs storage.

(-----------------), *immediately after electrolysis*

(___________), *after 16 hrs storage*

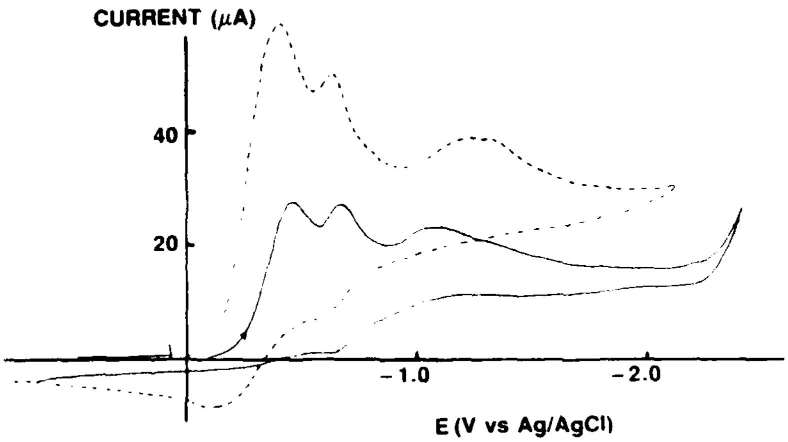

Figure 34: Voltammograms of 8.0 mg of 2.0M $AlCl_3$ – 0.10M $LiCl/SOCl_2$ in 10 ml $TBAPF_6/DMF$ after electrolysis on a 4 cm^2 glassy carbon cathode at 0.50 mA/cm^2 to n = 0.0 and n = 1.12 at 25°C scan rate 200 mV/sec.[1]

(-------------), scan at n = 0.0, OCP = 0.140V
(____________), scan at n = 1.12, OCP = 0.081

The 8.0 mg of $SOCl_2$ acid electrolyte contained 5.67 mM $SOCl_2$

1.1.10 Constant current coulometry of neutral and acid electrolytes on Shawinigan carbon cathodes at 25°C

Electrolysis of neutral electrolyte - Constant current electrolysis investigations were undertaken using Teflon bonded Shawinigan acetylene black carbon cathodes to determine whether the same $SOCl_2$ reduction pathways occur at commercial type porous cathodes as for smooth glassy carbon electrodes. The porous Shawinigan carbon cathodes that were used measured 1.0 x 2.0 cm, were 1.0 mm thick and contained a 5 Ni/0-2/0 Exmet grid with a 0.9 mm dia Ni lead. The 1.0 x 2.0 cm Teflon bonded Shawinigan cathodes each contained about 70 mg of the carbon-Teflon mix which was known to have a surface area of 36 m^2/g. Thus the porous Shawinigan carbon cathodes had a surface area of 2.5 m^2 compared to 4 cm^2 for the smooth Pt and glassy carbon electrodes. To determine the effect of surface area on the $SOCl_2$ reduction reactions at Shawinigan carbon cathodes, some of the porous cathodes were compressed at a pressure of 2400 lb/in^2 using a hydraulic press. The porous Shawinigan cathodes used for electrolysis experiments that were compressed are designated "pressed" and the standard cathodes that were not compressed are designated "porous" in this report.

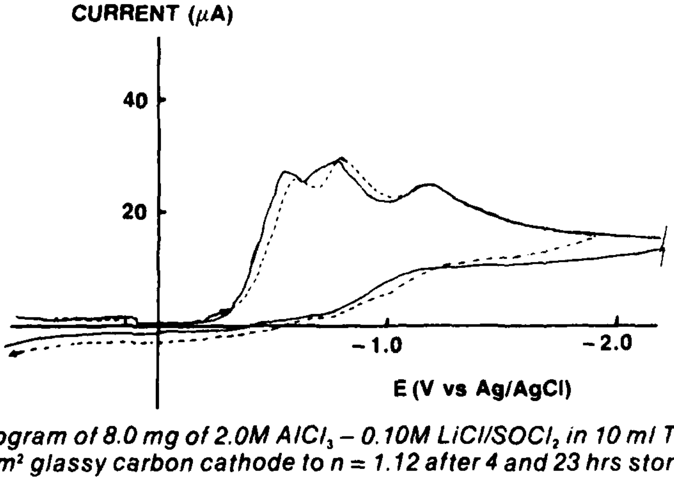

Figure 35: Voltammogram of 8.0 mg of 2.0M $AlCl_3$ – 0.10M $LiCl/SOCl_2$ in 10 ml $TBAPF_6/DMF$ after electrolysis on a 4 cm^2 glassy carbon cathode to n = 1.12 after 4 and 23 hrs storage scan rate 200 mV/sec.

(-------------), after 4 hrs storage, OCP = 0.083 V.
(____________), after 23 hrs storage, OCP = 0.157 V.

The voltammograms obtained after constant current electrolysis of $LiAlCl_4/SOCl_2$ at 1.0 x 2.0 cm "porous" and "pressed" Shawinigan carbon cathodes at 0.50 mA/cm² to n = 0.0 and n = 1.12 are shown in Figures 36 and 38. In both cases substantial amounts of SO_2 were detected by voltammetry but more SO_2 was observed for the pressed Shawinigan carbon cathode. It is thought that less SO_2 was observed with the porous Shawinigan carbon electrode because the porous electrode absorbed more SO_2.

The finding that SO_2 is produced during $SOCl_2$ reduction on Shawinigan black but not at glassy carbon is consistent with the explanation offered earlier for the concurrent reduction of $SOCl_2$ and SO_2 at a glassy carbon electrode. In DMF supporting electrolyte, the small amount of $SOCl_2$ in solution is probably completely absorbed by the high surface area Shawinigan black but only a trace is absorbed by the low surface area, low permeability glassy carbon electrode. Thus during electrolysis, the Shawinigan carbon electrode would have sufficient absorbed $SOCl_2$ so that it would not polarize permitting concurrent SO_2 reduction. It has frequently been assumed in the literature (11) that SO_2 absorption by Shawinigan carbon from $SOCl_2$ electrolytes is negligible but infrared results which will be presented in Section 1.2 indicate that substantial absorption of SO_2 occurs.

The voltammograms obtained for "porous" and "pressed" Shawinigan carbon cathodes after electrolysis to n = 1.12 followed by storage periods up to 88 hrs are presented in Figures 37 and 39

For the porous Shawinigan cathode, the SO_2 peak current rises noticeably during the first two hours of storage then broadens during the following 40 hrs of storage. If the increase in the SO_2 peak current during storage was due to the decomposition of some intermediate then one would expect the $SOCl_2$ peak to decline during storage since the $SOCl_2$ peak would very likely contain a hidden peak for the intermediate. However, since the $SOCl_2$ peak current hold relatively constant during the 43.7 hr storage period, the rise in the SO_2 peak may be due to diffusion of SO_2 out of the Shawinigan cathode as the electrolyte inside and outside the cathode reaches equilibrium with the SO_2 absorbed on the carbon surface.

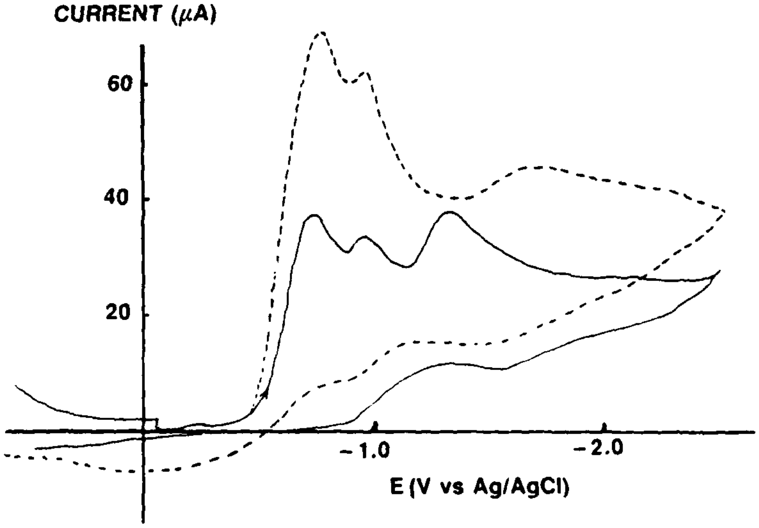

Figure 36: Voltammograms of 8.3 mg of 1.8M $LiAlCl_4/SOCl_2$ in 10 ml $TBAPF_6/DMF$ after electrolysis on a 4 cm² porous Shawinigan carbon cathode at 0.50 mA/cm², 25°C to n = 0.0 and n = 1.12, scan rate 200 mV/sec.

(-------------------), scan at n = 0.0
(____________), scan at n = 1.12

The 8.34 g of $SOCl_2$ neutral electrolyte contained 5.71 mM $SOCl_2$

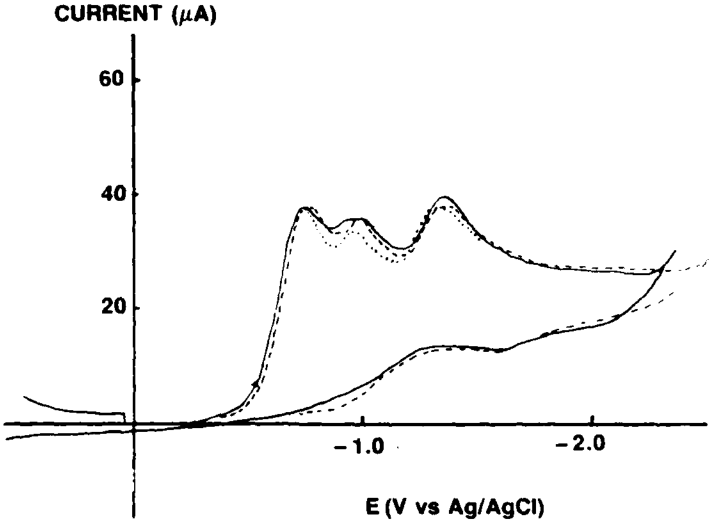

Figure 37: Voltammograms of 8.3 mg of 1.8M $LiAlCl_4/SOCl_2$ in 10 ml $TBAPF_6/DMF$ after electrolysis on a 4 cm^2 porous Shawinigan carbon cathode at 0.50 mA/cm^2, 25°C to n = 1.12 after 0, 2 and 43.7 hrs storage, scan rate 200 mV/sec.

(. . . . .) 0.0 hrs storage
(-----------------) 2.0 hrs storage
(____________) 43.7 hrs storage

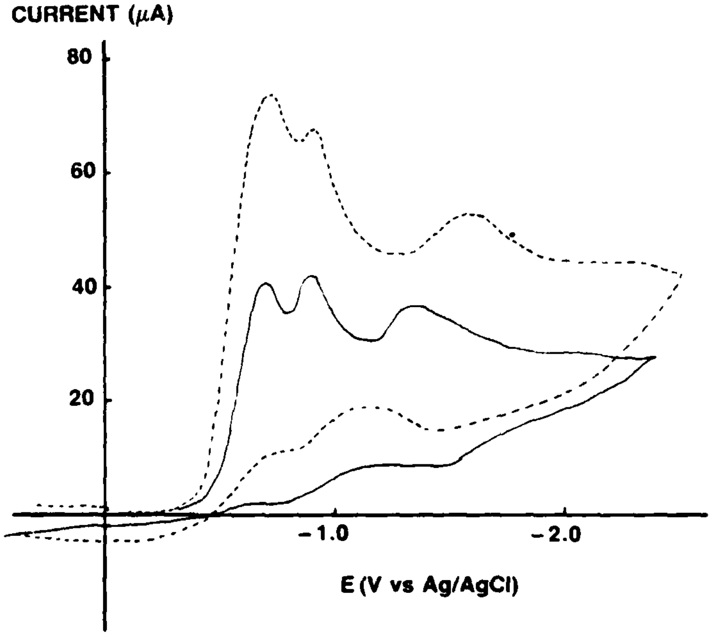

Figure 38: Voltammograms of 8.3 mg of 1.8M $LiAlCl_4/SOCl_2$ in 10 ml $TBAPF_6/DMF$ after electrolysis on a 4 cm^2 pressed Shawinigan carbon cathode at 0.50 mA/cm^2, 25°C to n = 0.0 and n = 1.12, scan rate 200 mV/sec.

(-----------------), scan after 26 hours storage, OCP = 0.170V
(____________), scan immediately after electrolysis, OCP = 0.025V

The 8.34 g of $SOCl_2$ neutral electrolyte contained 5.71 mM $SOCl_2$.

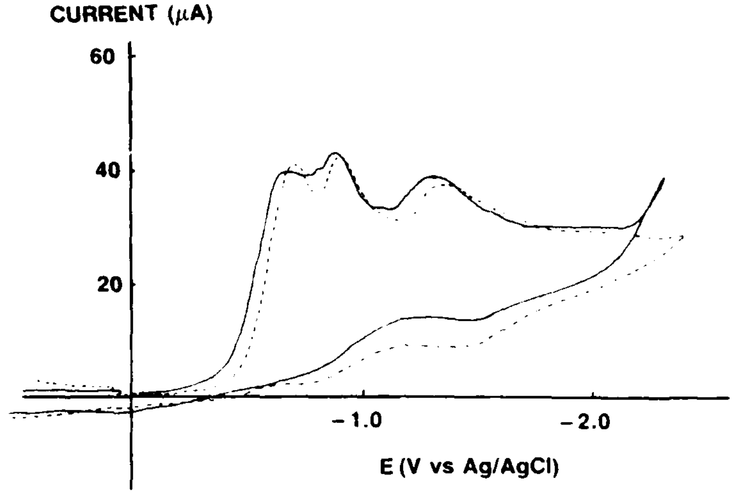

Figure 39: Voltammograms of 8.3 mg of 1.8M $LiAlCl_4/SOCl_2$ in 10 ml $TBAPF_6$/DMF after electrolysis on a 4 cm^2 pressed Shawinigan carbon cathode at 0.50 mA/cm^2, 25° to n = 1.12 after 0 and 88 hs storage, scan rate 200 mV/sec.

(-----------------) 0.0 hrs storage, OCP = 0.075 V.
(__ ______) 88 hrs storage, OCP = 0.080 V.

Increases in the SO_2 peak currents for stored, electrolyzed solutions were not observed during similar earlier measurements for neutral electrolyte reduced at glassy carbon and Pt cathodes (cf. Figures 23, 28, 31). For the electrolysis of acid electrolyte at a Pt cathode the SO_2 peak current rose during storage after electrolysis similar to porous Shawinigan carbon but the $SOCl_2$ peak current decreased. Thus the changes in the voltammograms during storage are probably primarily due to the slow diffusion of SO_2 and other reactants out of the porous cathode rather than reactions between SO_2, DMF and the $LiAlCl_4/SOCl_2$ electrolyte. The latter reactions do occur to some extent since the peak at − 1.35 V increases somewhat during storage. The peak at − 2.35 V is clearly the − 1.21 peak identified in Figures 13 and 14 as the product of the slow reaction of SO_2 with $LiAlCl_4/SOCl_2$ in DMF.

The voltammogram for the "pressed" Shawinigan carbon cathode 88 hrs after electrolysis shows several very small but distinct peaks about halfway between the $SOCl_2$ and SO_2 peaks. These small peaks could be products from the decomposition of very small amounts of long lived $SOCl_2$ reduction intermediates. The broadening of the SO_2 peak after 43.7 hrs for the "porous" Shawinigan carbon cathode also seems to be due to the appearance of several small new peaks between the $SOCl_2$ and SO_2 peaks. A very small peak in this region was also observed 16 hrs after electrolysis of acid electrolyte at a 4 cm^2 Pt cathode (cf. Figure 33). Although all of these small peaks may be due to the decomposition of $SOCL_2$ reduction intermediates the amount of intermediate present is probably very small and therefore it is of minor interest in understanding thermal runaway. However, very reactive intermediates are usually present at very small concentrations and would be of considerable interest to understand $SOCl_2$ reduction catalysts. Such reactive intermediates could be stabilized or react with the DMF supporting electrolyte and probably should be investigated using all inorganic electrolyte electrolysis cells and infrared and electron spin spectroscopy.

Electrolysis of Acid Electrolyte. - The voltammograms obtained before and after the constant current electrolysis of 2.0M $AlCl_3$ − 0.10M $LiCl/SOCl_2$ acid electrolyte at a 1.0 x 2.0 cm "porous" Shawinigan carbon cathode to n = 1.12 are shown in Figure 40. A comparison with Figure 36 shows that "porous" Shawinigan carbon cathodes produce more SO_2 to n = 1.12 in acid than in neutral electrolyte. This is similar to the case for glassy carbon cathodes (cf. Figures 22 and 34) which operate more efficiently and produce more SO_2 in acid than in neutral $SOCl_2$ electrolyte.

Previously it was thought that acid electrolytes improved high rate $SOCl_2$ battery performance primarily by dissolving LiCl out of the cathode and reducing passivation. In the $TBAPF_6$/DMF electrolyte there is very little Li+ present to passivate the cathode for both acid and neutral electrolytes therefore the present *results indicate for the first time that $SOCl_2$ reduction is catalyzed by $AlCl_3$* which apparently is functioning as a soluble homogeneous catalyst.

The $SOCl_2$ peak current at the start of the electrolysis of the acid electrolyte was 67 μA and decreased to 45.4 μA by n = 1.12, thus with a 5 μA background current only 33.8% of the $SOCl_2$ was consumed by n = 1.12 compared with 56% theoretically expected. The electrolysis of acid electrolyte at a glassy carbon electrode was found to occur with a utilization of 58% (see Section 1.1.9) thus the 33.8% utilization found for the porous Shawinigan carbon cathode appears to be rather low and inconsistent with the high SO_2 concentration detected. However, if the voltammograms for the electrolyses of acid electrolyte at the Shawinigan carbon electrode after 4 and 93 hrs of storage in Figure 41 are examined, it will be noted that the $SOCl_2$ peak has increased from 45.4 μA immediately after the electrolysis to 51.8 μA after 4 hrs to 51.0 μA after 93 hrs. Thus the $SOCl_2$ peak increased and the SO_2 peak decreased during storage which is very peculiar since it is doubtful whether $SOCl_2$ can reform after it has been electrochemically reduced in DMF electrolyte. It is therefore possible that the increase of the $SOCl_2$ peak current during storage is caused by the decomposition of substantial amounts of long lived $SOCl_2$ reduction intermediates to form unusual new products that reduce near the $SOCl_2$ potential. The composition of the intermediates and the products are presently unknown. The above conclusions are tentative and based on limited LSV data. Thus additional experiments at various n values and storage periods will be required to firmly establish the existence of substantial quantities of $SOCl_2$ reduction intermediates.

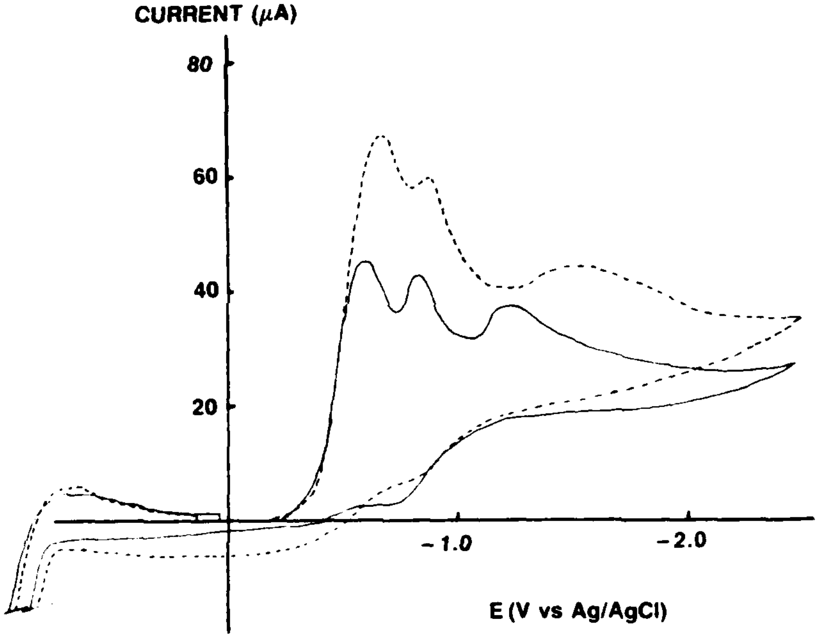

Figure 40: Voltammograms of 8.0 mg of 2.0M $AlCl_3$ – 0.10M $LiAlCl_4/SOCl_2$ in 10 ml $TBAPF_6$/DMF after electrolysis on a 4 cm² porous Shawinigan carbon electrode at 0.50 mA/cm² to n = 0.0 and n = 1.12 at 25°C, scan rate 200 mV/sec.

(··················) scan at n = 0.0, OCP = 0.128 V
(__________) scan at n = 1.12, OCP = 0.030 V

The 8.0 mg of $SOCl_2$ acid electrolyte contained 5.65 mM $SOCl_2$.

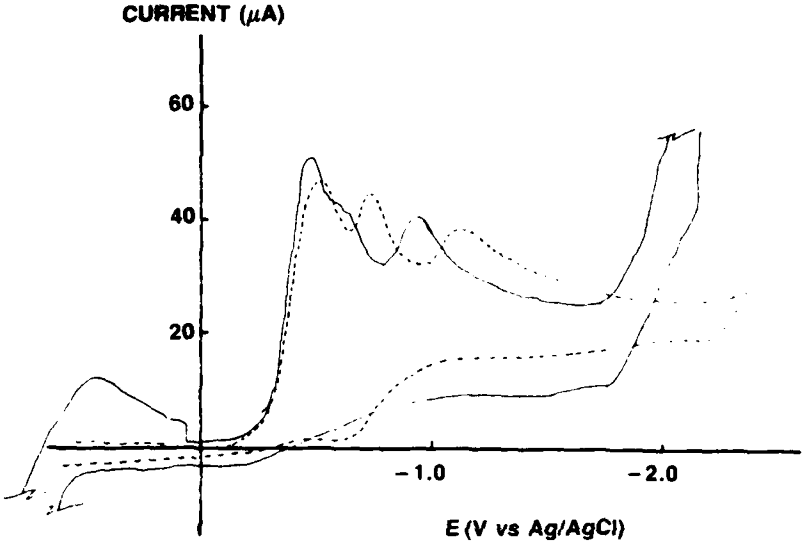

Figure 41: Voltammograms of 8.0 mg of 2.0 $AlCl_3$ – 0.1M $LiAlCl_4/SOCl_2$ in 10 ml $TBAPF_6$/DMF after electrolysis on a 4 cm^2 porous Shawinigan carbon electrode at 0.50 mA/cm^2 to n = 1.12 after 1.0 and 93 hrs storage, scan rate 200 mV/sec.

(---------------), 1 hr storage, OCP = 0.150 V
(______________), 93 hrs storage, OCP = 0.072 V

1.2 INVESTIGATIONS OF REACTIONS OCCURRING IN HERMETICALLY SEALED 0.6 AH LITHIUM-THIONYL CELLS

1.2.1 Introduction

The information generated from the electrochemical investigation of $SOCl_2$ reduction pathways discussed in the previous section of this report is somewhat limited in its relevance to commercial $Li/SOCl_2$ batteries. First, the constant current electrolyses were carried out in a DMF supporting electrolyte which could react with or destabilized certain discharge intermediates which would be stable in $SOCl_2$ battery electrolytes. Second, the $SOCl_2$ is present in millimolar concentrations which can lead to side reactions such as those discussed in Section 1.1.7 for glassy carbon cathodes. Third, commercial cells contain lithium which could possibly react with $SOCl_2$ reduction intermediates. Finally, commercial $Li/SOCl_2$ cells are electrolyte limited which would increase concentration of all $SOCl_2$ reduction products in the electrolyte and thereby stimulate possible side reactions such as those discussed in Section 1.1.7 for glassy carbon cathodes. Third, commercial cells contain lithium which could possibly react with $SOCl_2$ reduction intermediates. Finally, commercial $Li/SOCl_2$ cells are electrolyte limited which would increase the concentration of all $SOCl_2$ reduction products in the electrolyte and thereby stimulate possible side reactions between products.

In view of the above restrictions on the applicability of the electrolysis results for $SOCl_2$ in DMF electrolytes, a test program was undertaken in which 0.60 Ah $Li/SOCl_2$ cells were discharged at various conditions and electrolyte samples withdrawn at various points during discharge and analyzed by voltammetry The 0.60 Ahr $Li/SOCl_2$ test cells contained the same low ratios of electrolyte to electrode volume used in commercial cells. The cells were discharged at rates from 1 to 40 mA/cm^2 at 25 and − 20°C and utilized both acid and neutral $SOCl_2$ electrolytes.

1.2.2 Experimental

The design of the 0.6 Ahr $Li/SOCl_2$ restricted volume hermetically sealed test cell. is shown in Figure 42 The two cathodes measured 2.0 x 3.0 cm, were 1.0 mm thick and consisted of standard Shawinigan carbon − 4% Teflon cathode mix on a 5 Ni 10-2/0 nickel Exmet grid. The three lithium electrodes in the cell package measured 4.0 x 2.2 cm and also contained a 5 Ni 10-2/0 nickel Exmet grid. The two cathodes were each wrapped with three layers of 0.005 in thick Mead glass fiber separator paper before the electrode package was assembled. The electrolyte volume inside the 1 in. I.D. thick walled Pyrex glass tube used to contain the cell was restricted using two Teflon half cylinders and Teflon shims machained to fit the rounded contour of the cell bottom.

The acid and neutral $SOCl_2$ electrolytes were prepared as described in Section 1.1.2. The cells were evacuated to less than 100 μ when vacuum filled. All discharges except where noted otherwise were at constant load with a resistor.

Cell pressure during discharge was monitored with an electronic pressure transducer (Data Instruments Inc., Model AB) connected to the side tube with appropriate 316 stainless steel pipe fittings.

1.2.3 Results for Cells Discharged at 25°C

The discharge conditions, linear sweep voltammetry results and the calculated values for sulfur dioxide found by voltammetry are given in Tables 2, 3 and 4 respectively for the $Li/SOCl_2$ cells discharged at 25°C. From the electrolyte volume, current densities and $SOCl_2$ utilizations in Table 2, it can be seen that it is very difficult to achieve high $SOCl_2$ utilizations at rates above 1 mA/cm^2. Considerable effort was made to shape and fit the Teflon spacers in the 0.6 Ahr cells so that during the series of experiments the electrolyte volume was reduced from 8.2 to 3.43 ml. High $SOCl_2$ utilizations are required in the present investigations to generate enough SO_2 and other products to facilitate accurate chemical analysis for the products by voltammetry. Low utilizations cause the products to be excessively diluted by $SOCl_2$ electrolyte. The difficulty of accurately determining low concentrations of SO_2 in the presence of excess $SOCl_2$ has been discussed in detail earlier in Section 1.1.5 (cf. Figure 18). Although SO_2 could be determined by quantitative infrared spectroscopy, voltammetry was required because it was the preferred analytical method for the detection of $SOCl_2$ reduction intermediates. The LSV results obtained for electrolyte samples from the discharge 0.6 Ahr $Li/SOCl_2$ cells are briefly summarized in Table 3. Figure 43 shows the unusual voltammogram obtained for an electrolyte sample from Cell No. 1 after 60% discharge. The voltammogram shows four peaks and it somewhat resembles the voltammograms (cf. Figures 13 and 14) for $LiAlCl_4/SOCl$ solutions which have aged four hours or longer in DMF. Six additional cells were discharged under similar

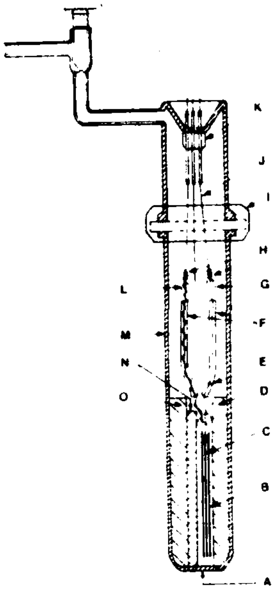

Figure 42: 0.6 Ah Restricted Volume Li/SOCl$_2$ Test Cell

A, lithium anodes; B, carbon cathodes; C, glass fiber separator; D, O, half-cylinder Teflon spacer; E, 7 cm mark on cathode lead; F, Teflon tubing insulator; G, 0.020 inn Ni cathode lead; H, tungsten-nickel resistance welds; I, metal coupler with Teflon flat gasket; J, tungston leads; K, glass to metal seals; L, anode leads; M, 1.0 in. I.D. heavy wall pyrex glass tube; N, Teflon shim.

TABLE 2

Discharge Conditions and SOCl$_2$ Utilizations for Li/SOCl$_2$ Cells Discharged at 25°

Cell Number	Electrolyte**	Current Density (mA/cm^2)	Electrolyte Volume (ml)	Cutoff Potential (V)	Discharge Time (Hrs)	SOCl$_2$ Utilization to Cutoff (%)
1	N	5	6.43	0.48	5.0	6.3
2	N	5	8.20	0.50	4.5	4.4
3	N	10	5.17	0.50	2.0	12.9
4	N	10	4.80	0.50	1.5	4.4
5	N	1	4.32	0.53	23.7	21.0
6	N	1	3.72	2.00	26.3	27.3
9	A	1	4.14	2.00	30.0	28.1
10	A	10	4.36	2.0	2.0	18.0
11	A	5	4.64	2.0	5.18	20.0
14	N	5	3.43	0.91	4.62	14.1
15	N	5	4.00	2.00	4.75	21.6
16	N	5	4.30	1.87	3.37	7.76
17	N	5	4.76	2.00	4.72	9.85

---

* Cells 1 and 2 had only a single 2.0 x 3.0 cathode

** N, designates 1.8M LiAlCl$_4$/SOCl$_2$ and A, designates 2.0M AlCl$_3$, 0.1M LiAlCl$_4$/SOCl$_2$ acid electrolyte

† The SOCl$_2$ utilization to cutoff is the percentage of SOCl$_2$ in the electrolyte which should have been reduced based on the number of equivalents of charge passed during the discharge. The calculation assumes 2.0 equivalents of charge are required per mole SOCl$_2$ reduced.

conditions, then analyzed by LSV in an attempt to duplicate the interesting results shown in Figure 43. It was found that most of the duplicate cells gave voltammograms similar to undischarged 1.8 M $LiAlCl_4/SOCl_2$. Since other peculiar voltammograms similar to Figure 43 were obtained from time to time with electrolyte samples from 0.6 Ahr cells it was concluded that some type of absorption or distillation process is occurring which yields samples which are unusually concentrated in reactants. All cells were shaken and inverted several times before sampling thus the process causing the concentrated samples is complex and difficult to control.

The moles of SO_2 found per mole of $SOCl_2$ reduced that were calculated from the voltammetry results are listed in Table 4. The generally accepted two electron reduction of $SOCl_2$ (Equation [1], Section 1.1.7) requires 0.5 moles of SO_2/mole $SOCl_2$ reduced. The SO_2 values in Table 4 have such large errors that no conclusions concerning the $SOCl_2$ reduction reaction are possible. Negative values for the SO_2 concentrations were calculated when the ratio of the SO_2 and $SOCl_2$ peak currents was less than the ratio for neutral electrolyte without added SO_2.

The SO_2 concentrations for the electrolyte samples in Table 3 could have been calculated using the held scan baseline technique described in Section 1.1.5 instead of the simple ratio of the SO_2 and $SOCl_2$ peak currents used in Table 4. However, it was concluded that the determination of SO_2 in electrolyte from discharged cells by voltammetry is intrinsically inaccurate and complicated by severe sampling problems. Because of these analytical problems, it was decided not to analyse the LSV results using the time consuming held scan baseline method but instead to investigate ways to improve the cell design and eliminate the sampling problem. To investigate the sampling problem, measurements of SO_2 absorption by Shawinigan carbon from 1.8M $LiAlCl_4/SOCl_2$ electrolyte containing known amounts of SO_2 were carried out which are described in Section 1.2.5.

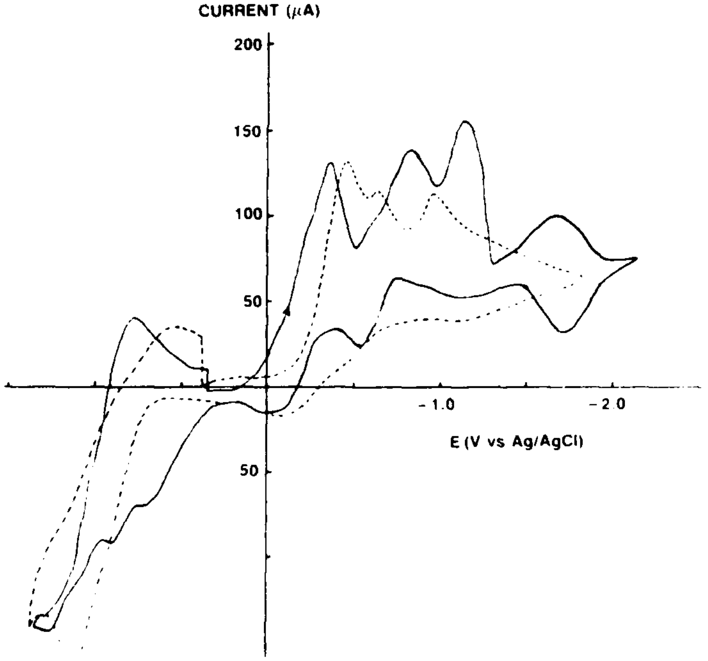

*Figure 43: Voltammograms of 20 mg of 1.8M $LiAlCl_4/SOCl_2$ from 0.3 Ah $Li/SOCl_2$ cells before and after discharge at 5 mA/cm$_2$, scan rate 200 mV/sec.**

(-----------------), After 60% discharge, for cell 1 in Table 2, for 100% defined as 0.48 V cutoff.
(   ), before discharge

**Both samples were added to 10 ml of 0.1M $TBAPF_6/DMF$ supporting electrolyte.*

TABLE 3

Linear Sweep Voltammetry Results for Electrolyte Samples from Li/$SOCl_2$ Cells Discharged at 25°

Cell Number	Sample Size (mg)	$SOCl_2$ Peak Current (μA)	$SOCl_2$ Peak Potential (V)	SO_2 Peak Current (μA)	SO_2 Peak Potential (V)	OCP (V)
1	20	138	−0.605	138	−0.775	0.220
2	20	157	−0.695	130	−0.895	0.135
3	20	205	−0.750	176	−0.910	0.070
4	20	169	−0.735	155	−0.888	0.200
5	20	173	−0.60	159	−0.77	0.180
6	20	224	−0.48	188	−0.70	0.180
9	20	206	−0.72	196	−0.82	0.050
10	20	170	−0.77	155	−1.02	0.050
11	20	183	−0.48	164	−0.69	0.100
14	20	201	−0.69	182	−0.77	0.050
15	10	111	−0.65	95	−0.88	0.100
16	10	102	−0.67	90	−0.92	0.265
17	10	84	−0.50	76	−0.75	0.380

---

† The discharge conditions are given in Table 2. The LSV analyses were carried out in $TBAPF_6$/DMF supporting electrolyte using a platinum working electrode and a Ag/AgCl reference electrode as described in Sections 1.1.2 and 1.1.3.

The pressures during the discharge of Cells 5 and 10 which utilized neutral and acid electrolytes are plotted versus capacity in Figures 44 and 45 respectively. The finding that the total cell pressure during discharge is substantially below the pressure calculated from the amount of SO_2 expected based on the number of equivalents of charge passed is similar to the findings of several previous investigators (11, 37-39). The gas pressure above the $SOCl_2$ electrolyte is lower than expected because SO_2 is soluble in $SOCl_2$ electrolytes [e.g. 3.9M at 24°C in neutral electrolyte (33)] and is absorbed in large amounts on the carbon electrode [see Section 1.2.5]. Thus before deviations from the theoretical pressure behavior can be interpreted in terms of $SOCl_2$ reduction pathways, it is clear that more accurate data for the absorption of SO_2 on carbon will be required. It is likely that the sharp increase in electrolyte SO_2 concentration observed by Schlaikjer and co-workers (11) towards the end of discharge may have been due to a drop in SO_2 absorption by the carbon cathode near the end of discharge as it became filled with solid LiCl. Because the SO_2 absorption capacity of the carbon cathode probably changes with the depth and rate of discharge, predicting the theoretical SO_2 pressure is expected to be difficult even with a large amount of SO_2 absorption data. Thus deviations of the SO_2 pressure behavior is probably of little value for the investigation of $SOCl_2$ reduction pathways.

1.2.4 Results for Cells Discharged at Low Temperatures

The discharge conditions, linear sweep voltammetry results and the calculated values for sulfur dioxide found by voltammetry are given in Tables 5, 6 and 4 respectively for the Li/$SOCl_2$ cells discharged at low temperature. As discussed in the previous section the low accuracies obtained using voltammetric analysis for SO_2 in the presence of a large excess of $SOCl_2$ prevents one from reaching any conclusions concerning $SOCl_2$ reduction pathways.

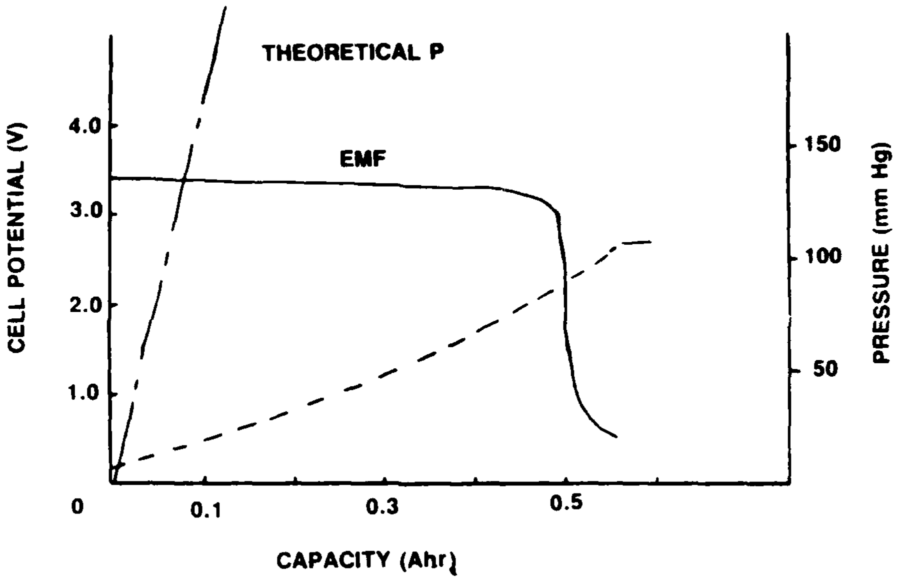

*Figure 44: Total Pressure and Cell Potential During Discharge of Cell 5 at 1 mA/cm², 25°C, 1.8M LiAlCl₄/SOCl₂ electrolyte.**

**Additional information is given in Table 2.*

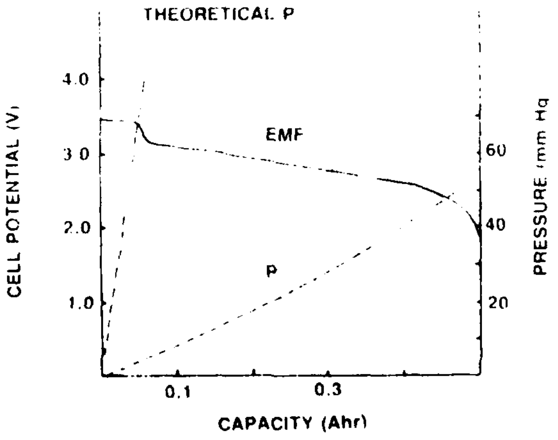

*Figure 45: Total Pressure and Cell Potential During Discharge of Cell 10 at 10 mA/cm², 25°C, 2.0M AlCl₃, 0.1M LiCl/SOCl₂ electrolyte.**

**Additional information is given in Table 2.*

TABLE 4

Calculated Values for Sulfur Dioxide Found by LSV Analysis of the Electrolyte from Li/$SOCl_2$ Cells Discharged at 25 and − 20 °C

Cell Number	Temp (°)	Current (mA/cm^2)	Depth of Discharge (%)	Moles of SO_2 found per mole $SOCl_2$ reduced*
1	25	5	60	4.8 ± 1.3
1	25	5	100	4.3 ± 0.8
2	25	5	60	2.4 ± 1.9
2	25	5	100	− 0.9 ± 1.1
3	25	10	100	− 9.7 ± 0.4
4	25	10	100	1.0 ± 1.1
5	25	1	100	− 0.23 ± 0.24
6	25	1	100	− 0.12 ± 0.18
7	− 20	8	100	0.94 ± 0.50
8	− 20	8	100	

---

*The moles of SO_2 were computed using the ratios of the SO_2 and $SOCl_2$ peak current instead of the held scan technique described in Section 1.1.5.

TABLE 5

Discharge Conditions and $SOCl_2$ Utilizations for Li/$SOCl_2$ Cells Discharged at 20°

Cell Number	Electrolyte**	Current Density (mA/cm^2)	Electrolyte Volume (ml)	Cutoff Potential (V)	Discharge Time (Hrs)	$SOCl_2$ Utilization to Cutoff (%)
7	N	8	4.49	1.98	1.4	9.8
8	N	8	4.39	2.00	1.4	10.2
12	A	40	4.69	1.40	0.21	6.7
13	A	20	5.43	2.00	0.50	6.9
18	N	8	3.95	2.0	14.8	14.8
19	N	8	4.85	2.0	2.63	15.5
20	N	1	4.08	2.0	18.5	27.5

---

* N. designated 1.8M $LiAlCl_4/SOCl_2$ and A. designates 2.0M $AlCl_3$ o.1M $LiCl/SOCl_2$ acid electrolyte
+see footnote to Table 2

TABLE 6

Linear Sweep Voltammetry Results for Electrolyte Samples from Li/$SOCl_2$ Cells Discharged at 25°

Cell Number	Sample Size (mg)	$SOCl_2$ Peak Current (μA)	$SOCl_2$ Peak Potential (V)	SO_2 Peak Current (μA)	SO_2 Peak Potential (V)	OCP (V)
7	20	191	−0.605	184	−0.77	0.140
8	20	173	−0.48	163	−0.60	0.160
12	20	158	−0.64	144	−0.85	0.050
13	20	188	−0.75	165	−0.97	0.100
18	11	88	−0.62	79	−0.87	0.410
19	11	106	−0.80	91	−1.07	−0.124
20	11	77	−0.64	70	−0.93	0.325

+ The discharge conditions are given in Table 5.

The LSV analyses were carried out in $TBAPF_6$/DMF supporting electrolyte using a platinum working electrode and a Ag/AgCl reference electrode as described in Sections 1.1.2 and 1.1.3.

The LSV results, did not however show any unusual new large peaks at low temperatures which could indicate the presence of large amounts of reduction intermediates or unexpected reduction products. Thus the LSV analyses of electrolyte samples discharged over the whole range of rates and conditions listed in Table 5 are −20 °C are consistent with earlier findings at 25 °C and show no sign of a major change in the reduction mechanism. Minor changes in the reduction mechanism and even substantial side reactions are probably beyond the detection limits of the electroanalytical techniques employed.

Because of the very high solubility of SO_2 in $LiAlCl_4/SOCl_2$ at low temperatures [e.g. 8.65M at 0 °C. ref 33] the pressures were not monitored for the cells discharge at −20 °C.

1.2.5 Results for Sulfur Dioxide Absorption by Carbon from $SOCl_2$ Neutral Electrolyte

The large variations in the voltammetry results obtained when samples from six 0.6 Ahr cells were analyzed after similar discharge conditions (cf. Section 1.2.3) strongly suggested a sampling problem involving SO_2 absorption by the carbon cathode. A search of the literature revealed only the measurements by Schlaikjer and coworkers (11) which provide indirect information concerning the change in SO_2 absorption as a function of temperature but no values for the amount of SO_2 absorbed on carbon cathode materials from $LiAlCl_4/SOCl_2 - SO_2$ solutions.

To determine whether SO_2 absorption on carbon from $SOCl_2 - SO_2$ solutions is great enough to cause the sampling problems discussed above, SO_2 absorption measurements were carried out using the following procedure. From 0.002 to 0.250 g of vacuum dried Shawinigan acetylene carbon were placed in a 15 ml screw cap vial with either 2.0 or 5.0 g of 1.8 M $LiAlCl_4/SOCl_2$ containing a known amount of SO_2 in the concentration range 0.273 to 2.73 M. The carbon and the solution were then placed in an untrasonic mixer for 5 minutes after which they were allowed to stand for 16 hrs to reach equilibrium. Next, the slurry was centrifuged, a small aliquot of solution was withdrawn, diluted 1:10 and analyzed for SO_2 by measuring the infrared absorbance at 1333 cm^{-1} using a Perkin-Elmer Model 621 infrared spectrophotometer. The quantitative infrared analytical procedure was calibrated at several concentrations from 0.035 to 0.29M SO_2 and the results used to prepare a Beer's law plot which was accurate to within ±7%.

The SO_2 concentrations of the $SOCl_2$ solutions that were measured before and after (i.e. at equilibrium) the solutions were in contact with the carbon are listed in Table 7 together with the weight of carbon and electrolyte used for each sample. The ratio of the mass of SO_2 absorbed over the mass of carbon is plotted versus the SO_2 concentration in Figure 46. The absorption of SO_2 on carbon from $SOCl_2 - SO_2$ solutions is clearly a classical equilibrium process since it was found as shown in Figure 47 to closely obey the empirical Freundlich absorption equation (40) for the absorption of a solute from a solution onto a solid surface. The results in Table 7 show two aspects of the SO_2 absorption process that are of particular interest in understanding the distribution of SO_2 in Li/$SOCl_2$ cells. First of all, as the total amount of SO_2 at equilibrium

TABLE 7

Sulfur Dioxide Absorption by Shawinigan Carbon at 23°C from 1.8M $LiAlCl_4/SOCl_2$ - $SOCl_2$ Solutions

Carbon Weight (g)	Electrolyte Volume Start	SO_2 Concent. Equilib. (m/1)	SO_2 Concent. Absorbed (m/1)	Weight SO_2 Y* (mg)	
0.050	2.0	2.73	1.60	145	2.90
0.050	2.0	1.73	0.65	92	1.84
0.250	5.0	0.273	0.065	66.6	0.266
0.125	5.0	0.273	0.105	53.8	0.430
0.050	5.0	0.273	0.175	31.4	0.628
0.050	5.0	0.273	0.255	5.76	1.153
0.002	2.0	0.293	0.219	9.5	4.74
0.020	2.0	0.293	0.085	26.6	1.33
0.050	2.0	0.293	0.058	30.1	0.602
0.100	2.0	0.293	0.024	34.5	0.345

---

*Y = mass SO_2 absorbed/mass carbon

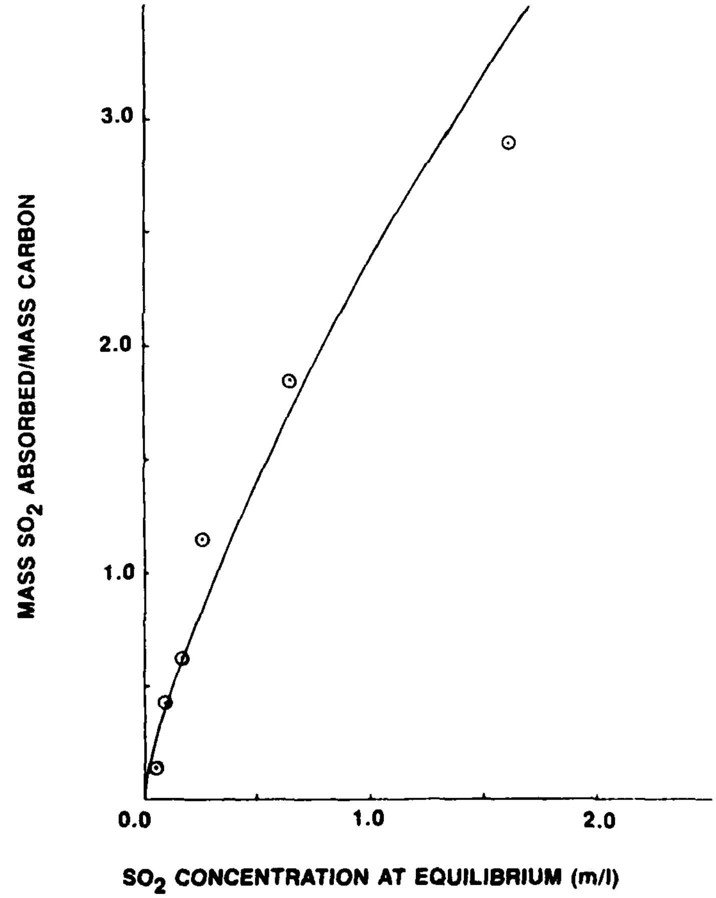

*Figure 46: Sulfur Dioxide Absorption by Shawinigan Carbon at 23°C from 1.8M $LiAlCl_4/SOCl_2$ – SO_2 Solutions**

*The data was selected from Table 7. The solid line is a replot of the linear least squares fit of Log Y vs Log C from Figure 47 increases, the weight of SO_2 absorbed per unit weight of carbon increases. However, as the SO_2 concentration at equilibrium increases the proportion of the SO_2 absorbed decreases. For example from Table 7 as the SO_2 concentration was increased from 1.37M to 2.73M the proportion of SO_2 absorbed decreased from 52.6 to 40.4%. These later two measurements were carried out at a ratio of 0.0147 g carbon/g of electrolyte compared to a ratio of 0.098 g carbon/g electrolyte found in cells. On the basis of the higher ratio of carbon to electrolyte found in practical cells, it would be expected than an ever larger portion of the SO_2 would be absorbed on the cathode during cell discharge.

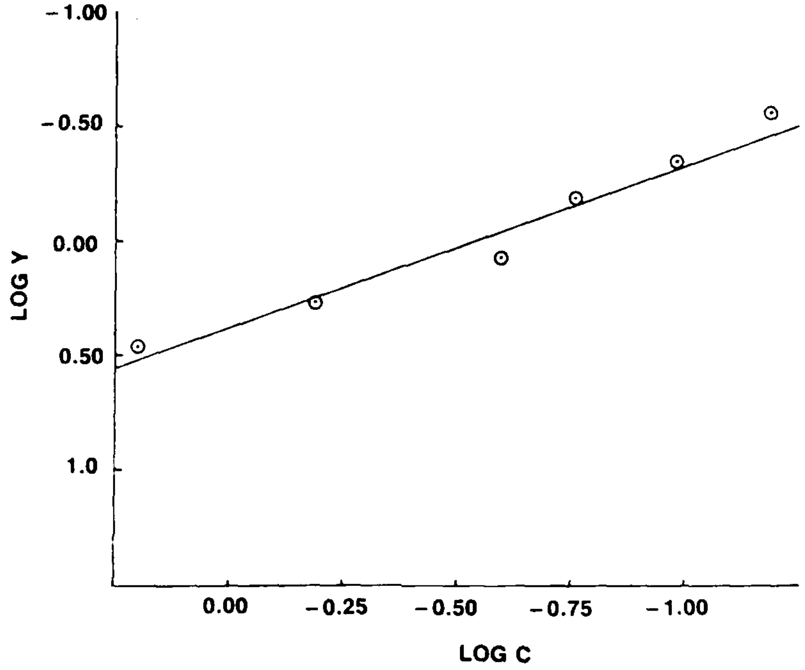

*Figure 47: Application of Freundlich Absorption Equation to Absorption of Sulfur Dioxide on Shawinigan Carbon at 23°C from 1.8M $LiAlCl_4/SOCl_2 - SO_2$ Solutions**

*The data was selected from Table 7 The line is the linear least squares best fit.

Now that it is known that Shawinigan carbon can absorb over 40% of the SO_2 from $SOCl_2$ electrolytes even at high SO_2 concentrations, our understanding of three important areas of Task 1 have been greatly advanced. First, high SO_2 absorption by carbon may explain the low SO_2 concentrations found earlier in electrolyte from discharged cells which was accounted for in the literature by postulating the existence of intermediates. Second, because large quantitites of SO_2 are absorbed by the cathode, it is clear that analyzing electrolyte samples from practical cells would give erroneously low concentrations for SO_2 and for other species and intermediates which would also probably be strongly absorbed. Finally, the finding that large quantities of SO_2 or $SO_2 \bullet SOCl_2$ adduct are absorbed on the carbon cathode have important implications concerning the function of catalysts which improve high rate performance. Such electrocatalysts may function to prevent SO_2 absorption in microscopic areas of the surface so that charge transfer may occur. Thus the limiting factor of catalysis may be the provision of an SO_2 free surface rather than charge transfer.

It is known from BET surface area measurements that the surface area of Shawinigan carbon 4% Teflon mix used in commercial cells is approximately 36 m^2/g which is considerbly less than Shawinigan carbon which has a surface area of 60 m^2/g. Thus the carbon-Teflon cathode mix would be expected to absorb only about 60% of the amount of SO_2 as absorbed by Shawinigan carbon. To determine whether the SO_2 absorption is lower for the carbon-Teflon mix on additional series of SO_2 absorption measurements over a full range of SO_2 concentrations are planned to be completed during the second half of the present contract. Additional SO_2 absorption measurements at higher carbon to electrolyte weight ratios are also planned.

A number of new techniques to allow a more accurate analysis of the electrolyte from $SOCl_2$ cells during discharge have been conceived which would decrease the errors caused by the absorption of SO_2 and other species on the carbon cathode. Work has been carried out with a two compartment all inorganic electrolyte electrolysis cell but various experimental problems remain to be solved before it will be known if this new cell will permit a more accurate analysis of the products of $SOCl_2$ reduction. The new two compartment all inorganic electrolyte electrolysis cell utilizes a 0.4M $(CH_3)_4N\ AlCl_4/SOCl_2$ electrolyte. The elimination of DMF from the electrolyte avoids the possibility that the organic solvent could stabilize or react with $SOCl_2$ reduction intermediates. The use of $(CH_2)_4N\ AlCl_4$ instead of $LiAlCl_4$ prevents the passivation of the carbon cathode with LiCl and in principle allows the electrolysis of a large volume of $SOCl_2$ by a small cathode with less carbon to absorb reduction products. Considerable work with this new cell at high rates is planned during the second half of the present study.

1.3 CONCLUSIONS FOR PART I

The present investigation of reactions occurring in the $Li/SOCl_2$ cell using electroanalytical methods has yielded a number of results which have increased our understanding of cell hazards and which could lead to improvements in performance. Voltammetric analyses for the products of $SOCl_2$ reduction on platinum and glassy carbon cathodes in organic electrolytes with DMF have shown no signs of significant quantities of unstable intermediates with lifetimes from 0.1 to 48 hrs. The electroanalyses were carried out in both 1.8M $LiAlCl_4/SOCl_2$ neutral electrolyte and 2.0M $AlCl_3$ – 0.1M $LiCl/SOCl_2$ acid electrolyte at 25 °C after from 50 to 100% of the $SOCl_2$ has been reduced. Unusual compounds or intermediates that were detected as very small voltammetry current peaks were clearly at such low concentrations ($\geq 5\%$) that even if the intermediates spontaneously decomposed with a large heat of reaction the total heat produced would not lead to a hazard in practical cells.

The large voltammetry current peaks attributed to large concentrations of $SOCl_2$ reduction intermediates in preliminary studies reported in the literature were found during the present investigation to be caused by SO_2, an expected product of the reduction of $SOCl_2$. Furthermore, the decline of the SO_2 current peak and the development of new current peaks seen by voltammetry after approximately 12 hrs storage were determined as being caused by a slow reaction between SO_2, DMF, $SOCl_2$ and possibly $LiAlCl_4$. Earlier it had been postulated in the literature that these changes were due to the slow decomposition of short lived $SOCl_2$ reduction intermediates.

Exhaustive electrolysis of 1.8M $LiAlCl_4/SOCl_2$ electrolyte in DMF supporting electrolyte at a glassy carbon cathode showed that the reduction of $SOCl_2$ involves two equivalents of charge per mole of $SOCl_2$ at 25 °C. The electroanalytical results obtained during the present investigation, taking into account the limitations of the experimental techniques, support the following generally accepted reaction for the reduction of $SOCl_2$ in both acid and neutral $SOCl_2$ electrolyte:

$$SOCl_2 + 2e^- \ , 1/250_2 + 2Cl^- + 1/2S \quad [1]$$

The electrochemical reduction of $SOCl_2$ is not yet fully understood. Thus, the conclusions stated earlier must be interpreted considering the limitations of the analytical techniques and various complications which arise due to the absorption of reaction products on the carbon cathode. The voltammetry analyses for $SOCl_2$ reaction products were all carried out in the presence of a large excess of DMF supporting electrolyte. The DMF could in principle react with or destabilize $SOCl_2$ reduction intermediates which could be present in $SOCl_2$ battery electrolytes which do not contain organic solvents. However, the chemical stability of DMF is well characterized and there is a high probability that DMF doesn't significantly effect the reduction mechanism of $SOCl_2$. But because unequivocal experimental results are required to establish with certainty the products and mechanism for $SOCl_2$ reduction, further experimental investigations will be carried out during the second half of the contract. These further investigations will involve two compartment electrolysis cells with thionyl chloride electrolytes without organic cosolvents. The investigations will also be extended to low temperatures and rates over 10 mA/cm^2.

Results have been obtained using quantitative infrared spectroscopy which have demonstrated that substantial amounts of SO_2 are absorbed on Shawinigan carbon from 1.8M $LiAlCl_4/SOCl_2$ – SO_2 solutions. For example 41.4 wt% of the SO_2 was absorbed by the carbon from a neutral electrolyte solution originally containing 2.73M SO_2. Practical cells contain carbon to electrolyte ratios 6.6 times greater than those used for the SO_2 absorption measurements and would be expected to absorb a much greater proportion of the SO_2 present in solution.

It was not previously known that SO_2 was absorbed by carbon from $SOCl_2$ electrolytes. Therefore, this new information has important applications in understanding cell hazards and in improving $Li/SOCl_2$ cell performance. In the area of cell hazards, it is clear that analyzing electrolyte samples from practical cells will give erroneously low concentrations for SO_2 and other species and intermediates which would also probably be strongly absorbed. Thus to understand the $SOCl_2$ reduction mechanism and thereby evaluate cell hazards, new experimental methods will have to be developed to avoid or correct for absorption of reduction products by the carbon cathode. In the area of improving high rate discharge performance, the finding that large quantities of SO_2 are absorbed on the carbon cathode has important applications concerning the function and selection of catalysts to improve high rate performance. Such electrocatalysts may function to prevent SO_2 absorption in microscopic areas of the cathode surface so that charge transfer may occur. To further evaluate the importance of SO_2 absorption in $Li/SOCl_2$ cells, additional absorption measurements are planned using the Shawinigan carbon – 4% Teflon mix used in commercial cells.

PART II ANALYSIS OF THE IMPACT OF IMPURITIES ON PERFORMANCE AND SAFETY

2.1 INTRODUCTION

The objective of Part II of the project were to perform detailed analyses for impurities that may be present in each reagent and component used in cell construction. The analyses were to qualitatively and quantitatively identify impurities that are present or likely to be present within the components and cell. The specific reagents and components that were to be analyzed included but were not limited to: a) lithium, b) thionyl chloride, c) lithium chloride, d) aluminum chloride, e) carbon black, f) separator material, g) current collector and/or structural materials used for the electrodes, and h) other cell components necessary for cell operation. The objectives of Part II also encompass experimental investigations to provide a detailed parametric assessment of the impact of each impurity upon cell safety and performance. As a result of work performed during Part II of the contract, recommended concentration limits were to be set for the key detrimental impurities.

Work on Part II was begun in the context of over ten years' experience concerning the effect of impurities on the operation of Li/$SOCl_2$ batteries. The generation of the hydrolysis products HC1 and $AlCl_3OH^-$ by the reaction of traces of water present in cell components with $LiAlCl_4/SOCl_2$ electrolyte has been extensively studied using infrared spectroscopy (11, 24, 41, 47). In addition, the effect of hydrolysis products in $SOCl_2$ electrolytes on voltage delay and other aspects of cell performance has been investigated by many laboratories (2, 37, 42, 43). However, a precise relationship between the level of water contamination and performance parameters such as voltage delay and anode corrosion had not been established and was selected for investigation.

Iron dissolved in the electrolyte has long been known to aggravate the voltage delay problem in Li/$SOCl_2$ cells (37). Estimation of the problem is difficult, since the lithium was found to remove iron from the electrolyte. The severity of the delay problem would therefore be affected both by the concentration of iron in the electrolyte and the surface area of the anode. These factors were taken into account during the matrix of cell tests which were undertaken to ascertain the recommended concentration limits for iron impurities.

Previous to the present investigation, very little work had been reported concerning the composition, amounts and effects of organic impurities in Li/$SOCl_2$ cells. This lack of information was partially due to the difficulty of quantitative analysis for traces of organic compounds in materials such as $SOCl_2$, carbon and $AlCl_3$. Certain commercial glass fiber separators widely used in Li/$SOCl_2$ cells are known to contain over 7 wt % of organic binder materials such as polyvinyl alcohol, which reacts with the electrolyte to generate hydrolysis products, which are likely to contribute to anode corrosion, voltage delay and excessive head space gas pressure. Aluminum chloride, particularly as obtained from commercial U.S. sources, contains unidentified materials which often contribute an amber or a dark brown color to the electrolyte. The best known commercial source (Fluka) also contains significant amounts of these materials, the amount varying from lot to lot. Highly purified aluminum chloride is available, but expensive. The nature and level of organic impurities in $AlCl_3$, LiCl, $SOCl_2$, and the carbon cathode were initially unknown but were determined, during the present contract by extracting these materials with ether, concentrating the extract by evaporation then analyzing the extract. The organic analyses were carried out using Fourier Transform Infrared Spectroscopy (FTIR) and gas chromatography-mass spectroscopy (GC/MS).

The polymers used to bind separators are not soluble in low boiling solvents suitable for extraction but they were present in large enough quantities to be determined by the weight change after pyrolysis and air oxidation. The slow reaction between organic separator binders and $SOCl_2$ electrolyte at 25°C was followed for over 30 days by monitoring the pressure increase in hermetically-sealed glass vessels fitted with sensitive pressure sensors.

2.2 EXPERIMENTAL

Construction of Cells - The standard design case negative AA size Li/$SOCl_2$ cells used to study the effects of water, hydrolysis products and iron impurities on performance were constructed as shown in Figure 48. The cylindrical Li anode was 1.375 inches in circumference, 1.50 inches high and 0.030 inches thick, and contained 0.50 g Li. The Shawinigan carbon – 4% Teflon cylindrical bobbin-type cathode was 1.41 inches high, 0.406 inches in diameter and weighed 0.80 g. The cell was vacuum-filled with 4.0M of $SOCl_2$ electrolyte prepared as described in Section 1.1.2. The design and performance of the AA cell has been described in detail in several publications (44-46).

The reverse polarity AA cells were constructed using a 3.81 cm high, 1.11 cm diameter, cylindrical Li anode of 0.56 mm thick Li attached to the glass-to-metal feed thru pin. The Shawinigan carbon – 4% Teflon cathode was 4.44 inches high, 0.86mm thick with a Ni Exmet screen and a 4.4 cm circumference. Nickel tabs on the Exmet screen of the cathode were electric resistance welded to the stainless steel case.

Extraction and Analysis of Cell Components for Organic Impurities - The battery components selected for analysis for organic impurities were standard materials used in the manufacture of large prismatic $Li/SOCl_2$ cells except for the glass fiber separators. The $AlCl_3$ (Fluka, Puriss.) and LiCl (Baker) were from freshly opened bottles of the same grade normally used to prepare $SOCl_2$ electrolyte. The 1.8M $LiAlCl_4/SOCl_2$ electrolyte was standard production quality electrolyte obtained from GTE Communications Products Corporation in Waltham, MA. The Teflon-bonded cathode material was also obtained from the above source and weighed 4.58g without the usual Exmet grid.

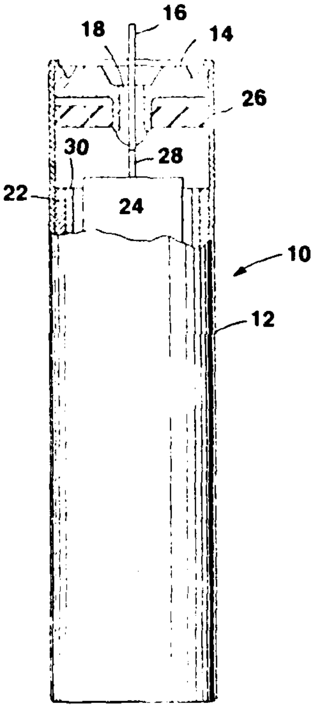

Figure 48: Standard Case Negative AA Size $Li/SOCl_2$ Cell.

12, 304 Stainless Steel Case; 14, Stainless Steel Cover; 16 Cathode Terminal; 18, Glass-to-Metal Seal; 26, Plastic Washer; 22, Lithium Anode: 24, Carbon Cathode Current Collector; 28, Cathode Contact; 30, Glass Fiber Separator.[1]

The diethyl ether used for the extractions (Fisher Scientific, E138, Reagent ACS) was listed by the manufacturer as having the following maximum limits of impurities: alcohol (C_2H_5OH). 0.01%; residue after evaporation, 5 ppm, acid-The LiCl, carbon cathode material, Crane glass separator and Lydell "binderless" glass separator were extracted with 500 ml of either diethyl ether or methylene chloride, using standard Soxhlet extraction techniques. The extraction thimble had a volume of 30 ml and was refilled several times to extract 141g of LiCl. After the sample was extracted with boiling solvent for at least two days, the 500 ml of extract solution was concentrated by evaporation to ≈ 2 ml. The infrared and GC/MS analysis was then carried out using these concentrates or solutions diluted by a factor of 2 with diethyl ether. Because $AlCl_3$ dissolves in diethyl ether and other organic solvents suitable for Soxhlet extractions of a powdered solid, a two phase liquid-liquid extraction technique was used for the extraction of $AlCl_3$ and 1.8M $LiAlCl_4/SOCl_2$ electrolyte. The $AlCl_3$ or $SOCl_2$ electrolyte was first hydrolyzed with a large quantity of distilled water, the pH adjusted with HCl until all the $Al(OH)_3$ dissolved, then a portion of the water solution was shaken with about 200 ml of ether in a large separatory funnel. The ether layers were combined and concentrated by evaporation for IR and GC/MS analysis.

The concentrated extract solution of the battery components were analyzed using a Fourier Transform Infrared Spectrometer (Nicolet Model MS-1). The samples for the IR analysis were contained ina NaCl cell with a 0.1 mm path length. To permit the detection of impurities in the unknown samples, the IR spectra of a concentrated diethyl ether blank was subtracted from the sample's spectra using the microcomputer in the data reduction system of the spectrometer. The ether blank was intended to simulate the concentration of impurities present in the ether and was prepared by evaporating 450 ml of pure ether down to $\approx$ 2 ml.

The gas chromatography/mass spectroscopy (GC/MS) was carried out using a Hewlett Packard GC/MS (5982A) interfaced to a Hewlett Packard Data System (5934A). Using a glass syringe, 5 μl of each sample was injected into the instrument. The column used was 10′ x 4 mm. I.D. stainless steel packed with 3% SP2100 (i.e. methyl silicone fluid, Supelco, Inc.) on 80/100 mesh acid washed, DMCS treated diatomite (supelcoport, Supelco, Inc.). The oven was programmed from 40 to 230 °C at a rate of 16 °C/minutes. Helium was used as the carrier gas at a flow rate of 30 ml/min. The mass spectrometer was operated in the continuous scan mode from 35 a.m.u. at a rate of 1.2 sec/scan.

The amount of volatile and combustible impurities in the glass fiber separators was determined by first weighing a sample of the separator, then heating the separator in a ceramic crucible with a nickel cover in a natural gas flame to approximately 800 °C for 10 minutes. The crucible was then cooled for an hour and weighed. The procedure was then repeated with subsequent heating periods of first 15 minutes, then 20 minutes.

Gas Evolution Measurements for Separators in $SOCl_2$ Electrolytes. - The main features of the hermetically sealed glass apparatus used to measure gas evolution for separators immersed in $SOCl_2$ electrolyte are shown in Figure 49. The apparatus consisted of an approximately 23 cm long thick walled glass tube (I.D. 1.1. cm) into which a roll of separator material was hermetically sealed with a small closed end Hg manometer and 4.0 ml of 1.8M $LiAlCl_4/SOCl_2$ electrolyte. The apparatus was cooled and sealed under anhydrous conditions using a glass blowing torch. The height of the Hg in the 8 cm long closed end manometer was measured to four significant figures, using a cathetometer fitted with a long focus microscope.

The hermetically sealed glass apparatus was used instead of an apparatus using pipe fittings because the use of a sealed glass apparatus avoids seal leakage and corrosion problems and losses of hydrogen and other gasses caused by diffusion through plastic gasket materials. Since the sealed glass tubes can be weighed before and after long term tests to within 0.1 mg, even the smallest of leaks can be detected. Several liquids including $SOCl_2$ electrolyte were evaluated as fluids for the closed end manometer and Hg was found to give the best results. Mercury does react slowly with $SOCl_2$ vapor at room temperature to produce Hg_2Cl_2, S and SO_2 but a Hg_2Cl_2 layer forms on the Hg surface inhibiting the reaction. To obtain information to correct the pressure results for the slow reaction of Hg and $SOCl_2$ control tests were carried out with 1.8M $LiAlCl_4/SOCl_2$ and the Hg manometer alone. After 895 hours the pressure in the tube was only 0.009 atmospheres indicating negligible gas evolution.

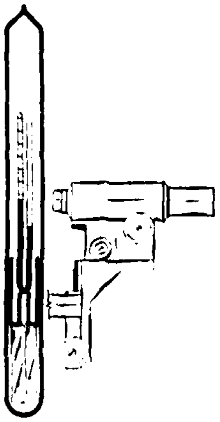

Figure 49: Sealed Glass Tube With Manometer for $SOCl_2$ Gas Evolution Measurements.

Prior to the gasing tests, the separator papers were cut, coiled and weighed then stored in the dry room for 14 days at a humidity of 1.9% R.H. (– 28 °C dewpoint).

2.3 THE EFFECT OF WATER AND HYDROLYSIS PRODUCTS ON PERFORMANCE

To determine the effect of water on discharge performance 60 AA size $Li/SOCl_2$ cells were constructed, thirty using the standard polarity and thirty using the reverse polarity. Three levels of water were used in the electrolyte 0 PPM H_2O (or the driest we could attain), 20 PPM and 100 PPM. Schematically, the storage breakdown looked as follows:

STANDARD POLARITY

0 PPM H_2O
- 5 cells *Room* Temp.
- 5 cells 55 °C

20 PPM H_3O
- 5 cells *Room* Temp.
- 5 cells 55 °C

100 PPM H_2O
- 5 cells *Room* Temp.
- 5 cells 55 °C

REVERSE POLARITY

0 PPM H_2O
- 5 cells Room Temp.
- 5 cells 55 °

20 PPM H_2O
- 5 cells Room Temp.
- 5 cells 55 °C

100 PPM H_2O
- 5 cells Room Temp.
- 5 cells 55 °

The cells were stored one month, then delay tested at 3 mA/cm^2. They were later discharged with a load of 150Λ.

The voltage delay results for the AA size Li/$SOCl_2$ cells with the three levels of water are presented in Figures 50 to 53, and the discharge performance at 25 °C in Figures 54 to 57. At 55 °C storage for one month, the reverse polarity cells (cf. Figure 50) show the worst delay performance as expected, since there is no self-discharge against the can, the passivating film is more stable and probably thicker. Although all three H_2O levels show poor start-up characteristics, the 100 PPM did start slightly higher, 0.90V vs 0.80V for the others, and recovered to its operating voltage much more quickly.

A comparison of the reverse polarity cells stored at room temperature and 55 °C reveals that all the cells showed similar start-up behavior, with the cells containing 100 PPM added H_2O showing a slightly higher start-up potential. The start-up potentials are shown in Figures 50 and 51.

The standard polarity cells (anode on can) show similar trends. At room temperature, the 100 PPM cells have better startup and attain the running potential quicker. AT 55 °C storage the 100 PPM cells show a poorer startup than the 20 PPM cells, but their potential rises above the 20 PPM cells starting potential in 12 seconds and attains its running potential faster as in the other cases. These curves are shown in Figures 52 and 53.

In terms of delay performance, it would appear that up to 100 PPM H_2O has no detrimental effect. In fact, the data indicates that 100 PPM may decrease delay and help the cell attain its running potential faster. There are two possible explanations for this observance. When water is added to the electrolyte, HCl and SO_2 are formed:

$$SOCl_2 + H_2O \, . \, SO_2 + HC1$$

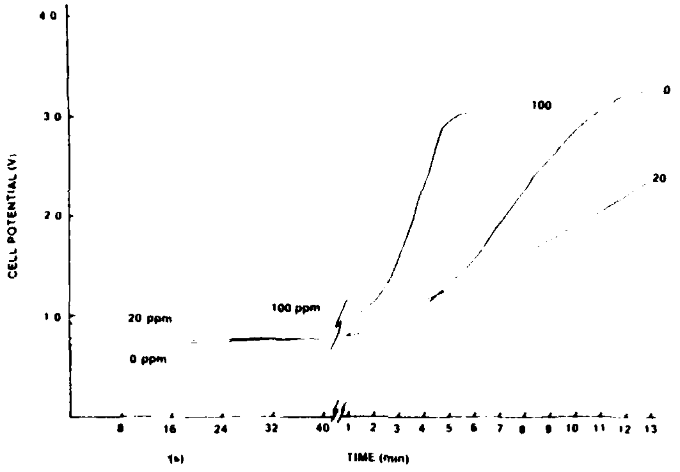

Figure 50: Voltage Delay for Reverse Polarity AA Size Li/$SOCl_2$ Cells with 0, 20 and 100 PPM Water added to the Electrolyte.*

*Cells were discharged at 23 °C after one month storage at 55 °C. Each curve represents the average performance of five cells Discharge was with a 216 ohm load (~ 3 mA/cm²).

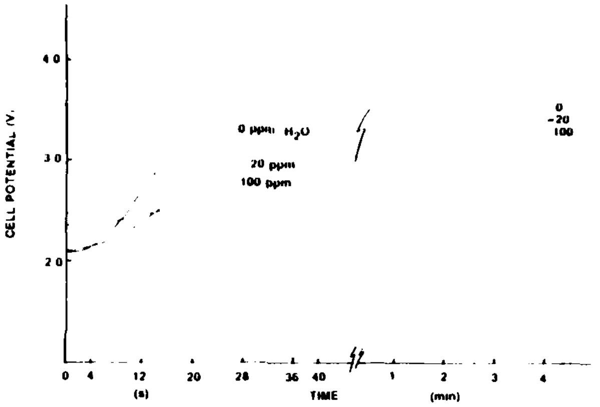

*Figure 51: Voltage Delay for Reverse Polarity AA Size Li/SOCl$_2$ Cells with 0, 20 and 100 PPM water added to the Electrolyte.**

*Cells were discharged at 23°C after one month storage at 23°C. Each curve is the data from a single cell chosen to present the average performance of a group of four or five cells of similar H_2O concentration. Discharge was with a 216 ohm load (≈ 3mA/cm²).

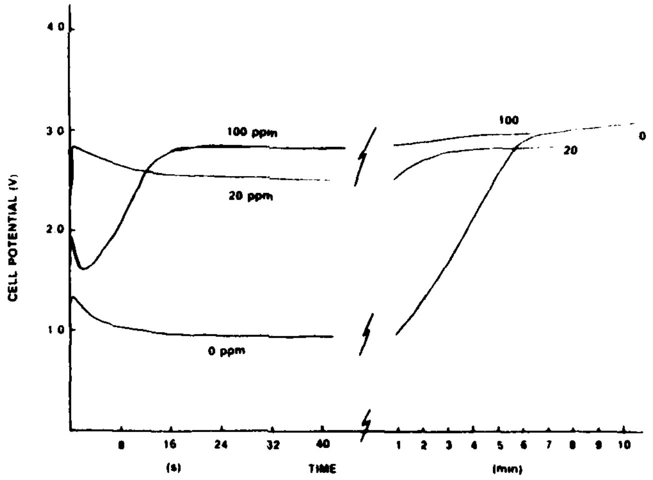

*Figure 52: Voltage Delay for Regular Polarity AA Size Li/SOCl$_2$ Cells with 0, 20 and 100 PPM water added to the Electrolyte.**

*The cells were discharged at 23°C after one month storage at 55°C. Each curve in the data from a single cell chosen to represent the average performance of a group of three to five cells of similar H_2O concentration. Discharge was with an 80 ohm load (≈ 3mA/cm²)

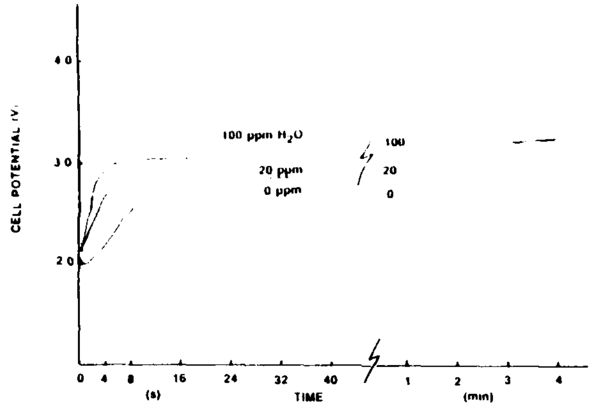

*Figure 53: Voltage Delay for Regular Polarity AA Size $Li/SOCl_2$ Cells with 0, 30 and 100 PPM water added to the Electrolyte.**

*The cells were discharged at 23 °C after one month storage at 23 °C. Each curve in the data from a single cell chosen to represent the average performance of a group of four to five cells of similar H_2O concentration. Discharge was with an 80 ohm load (≈ mA/cm^2).

It has been reported by Chua, Mertz and Bishop (47) that the presence of SO_2 in electrolyte have aided delay performance. So, in fact, SO_2 is added to the electrolyte indirectly.

The other possible explanation is the formation of a solid with the addition of water that incorporates itself in the passivating film and results in a somewhat more amorphous film easier to break down. The reaction for the formation of such a film could be as follows:

$$AlCl_3 + H_2O \rightarrow AlCl_2OH + HCl$$

With regard to capacity, the reverse polarity cells stored at room temperature showed a dramatic difference in capacities as shown in Figure 54. There is over a 50% difference in capacity between the 0 PPM and 100 PPM water level cells with the 20 PPM cells between these two extremes in capacity.

The standard polarity in cells stored at room temperature showed a much closer grouping, apparently the self-discharge against the can eliminates a lot of subtle effects that might otherwise be seen. These results are shown in Figure 55.

High temperature storage seems to have the same leveling effect as employing an anode on the can construction. As Figure 56 and 57 show, there is virtually no difference in capacity, or operating voltage between the reverse polarity and standard polarity after four weeks storage at 55 °C.

The conclusion drawn from these results regarding the presence of traces of water in $Li/SOCl_2$ cells are as follows:

1. At up to 100 PPM H_2O no detrimental effects were observed in terms of capacity or voltage delay.

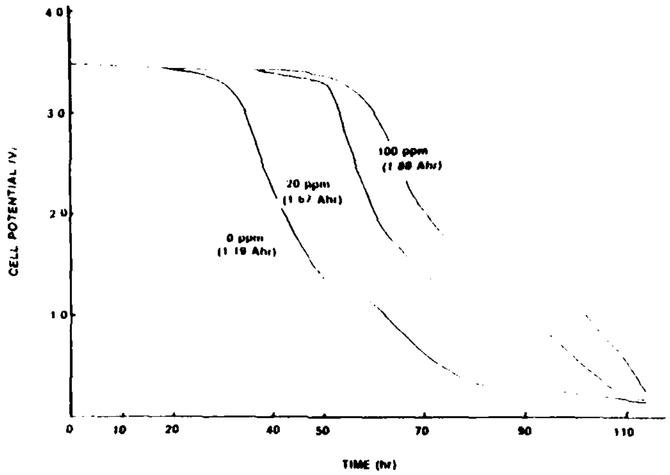

*Figure 54: Discharge Characteristics for Reverse Polarity AA Size Li/SOCl$_2$ Cells with 0, 20 and 100 PPM water added to the Electrolyte.**

*The cells were discharged at 23°C after one month storage at room temperature. Discharge was with a 150 ohm load.

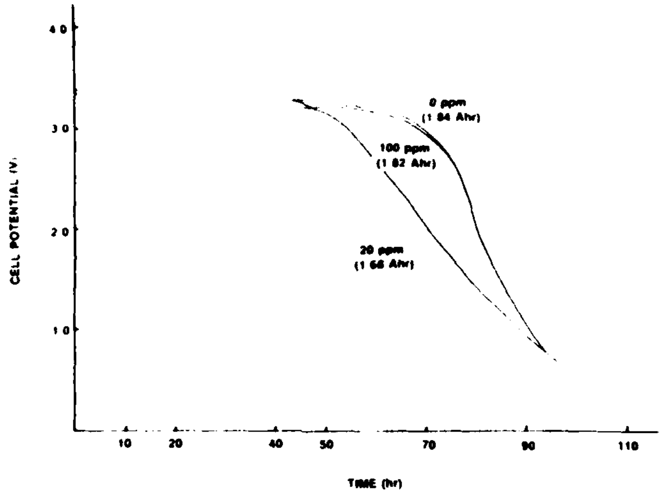

*Figure 55: Discharge Characteristics for Regular Polarity AA Size Li/SOCl$_2$ Cells with 0, 20 and 100 PPM water added to the Electrolyte.**

*The cells were discharged at 23°C after one month storage at room temperature. Discharge was with a 150 ohm load

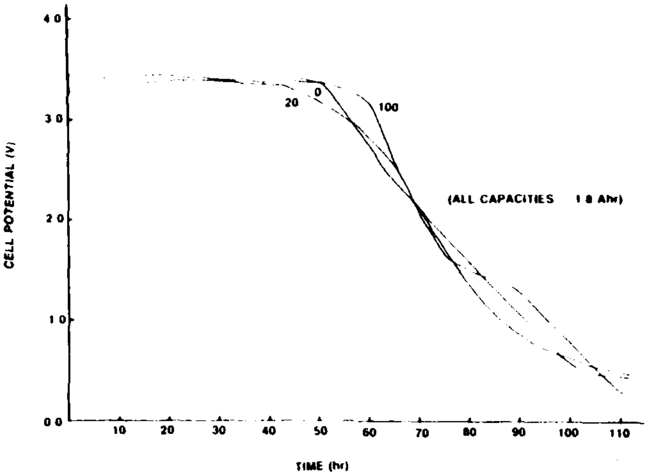

*Figure 56: Discharge Characteristics for Reverse Polarity AA Size Li/SOCl$_2$ with 0, 20 and 100 PPM Water Added to the Electrolyte.**

*The cells were discharged at 23°C after one month storage at 55°C. Discharge was with a 150 ohm load.

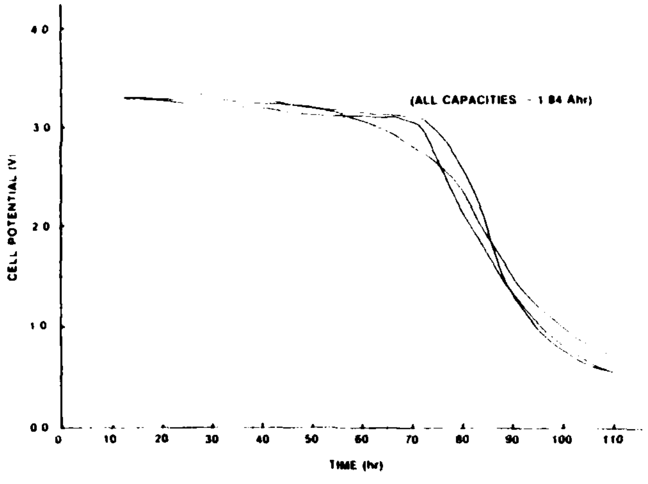

*Figure 57: Discharge Characteristics for Regular Polarity AA Size Li/SOCl$_2$ Cells with 0, 20 and 100 PPM water added to the Electrolyte.**

*The cells were discharged at 34°C after one month storage at 55°C. Discharge was with a 150 ohm load.

2. Reversing polarity has a much more dramatic effect on voltage delay than the addition of water up to 100 PPM.

3. High temperature storage has a much more overwhelming effect on capacity than whatever subtle effects water may have.

4. Generally, up to 100 PPM H_2O appears to alleviate some of the voltage delay and, in most cases, cells attain operating potential more quickly.

5. Lastly, water in the system ultimately generates hydrogen (H_2). There is evidence suggesting it is a danger and undesirable, but at low levels, it may be soluble and pose no danger. This aspect of the problem should be investigated more thoroughly.

2.4 THE EFFECT OF IRON ON PERFORMANCE

To determine the effect of iron contamination on discharge performance, 30 AA size cells were constructed and divided into three groups of ten cells each. The first group of ten were spiked with 5 PPM iron as $FeCl_3$, the second group with 20 PPM iron and the third group with 100 PPM iron. Each group of ten were divided into two separate groups of five each. Each group of five from the same iron concentration was stored either at room temperature or 55 °C. Schematically, the storage breakdown looked as follows:

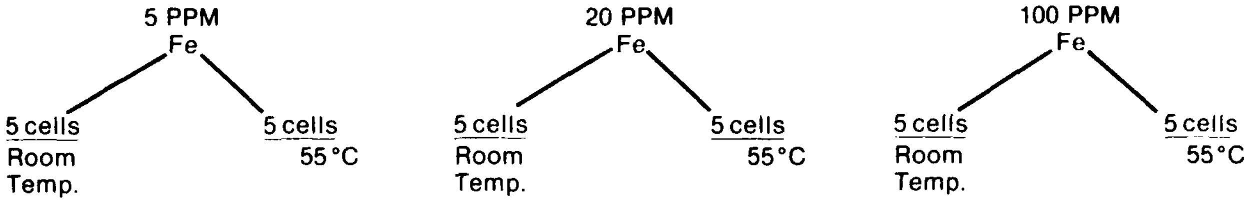

The cells were stored one month then delay tested with an 89 ohm load (≈ 3 mA/cm²) Figures 58 and 59 show the resultant curves.

After one month storage at 55 °C the cells with 5 and 20 PPM added iron recovered to an acceptable operating potential in two to three minutes but the cells with 100 PPM iron did not recover even after five minutes. From these results it is recommended that the iron concentration in the electrolyte in $Li/SOCl_2$ cells should be held to a concentration 5 PPM or lower.

In regular polarity $Li/SOCl_2$ cells, the 304 L stainless steel cell case is electrically connected to the Li anode and is, therefore, cathodically protected from $SOCl_2$ corrosion. Careful chemical analysis (48) of electrolyte and cell components from regular polarity AA cells stored up to 4.5 years at room temperature has shown only 1.62 to 2.85 mg of Fe present in the electrolyte or reduced on the Li anode. However, similar information regarding the rate of corrosion of 304 L stainless steel without cathodic protection was not available. Therefore, a series of 18 tests were carried out.

Eighteen AA cans were divided into two groups as shown in the following test matrix:

STORAGE TIME	ROOM TEMPERATURE			55 °C		
1 week	1 cell	1 cell	1 cell	1 cell	1 cell	1 cell
2 weeks	1 cell	1 cell	1 cell	1 cell	1 cell	1 cell
6 weeks	1 cell	1 cell	1 cell	1 cell	1 cell	1 cell

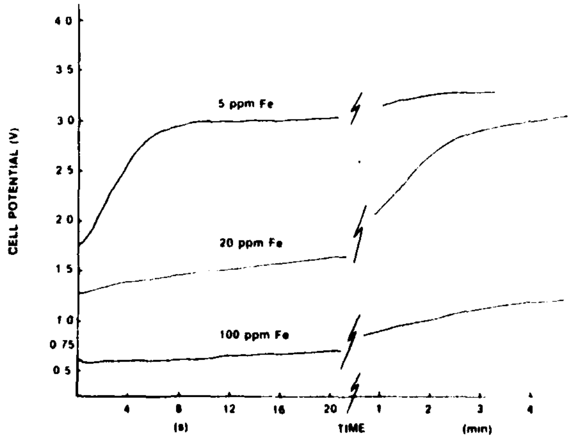

*Figure 58: Voltage Delay for Regular Polarity AA Size $Li/SOCl_2$ with 5, 20 and 100 PPM Iron in the Electrolyte as $FeCl_3$**

*The cells were discharged at 23 °C after one month storage at room temperature with an 80 ohm load (≈ 3 mA/cm²) Each curve is the data from a single cell chosen to represent the average performance of a group of fine cells of similar iron concentration

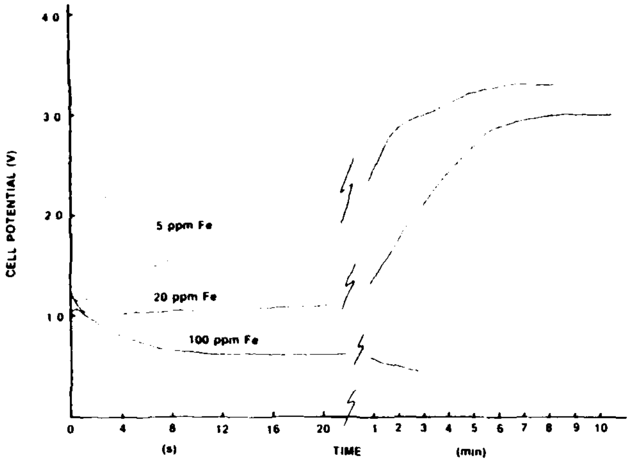

Figure 59: Voltage Delay for Regular Polarity AA Size Li/SOCl$_2$ Cells with 5, 20 and 100 PPM Iron in the Electrolyte as FeCl$_3$

*The cells were discharged at 23 °C after one month storage at 55 °C with an 80 ohm load (~ 3 mA/cm^2). each curve is the data from a single cell chosen to represent the average performance of a group of fine cells of similar iron concentration.

These AA cans contained cathode attached to the can and were filled with electrolyte. After one week, three cans from each group were opened and the electrolyte analyzed for iron. The following averages were obtained for each group.

Fe Content of Stored Cells

STORAGE TIME	ROOM TEMPERATURE	55 °C
1 week	49.4 PPM	52.9 PPM
2 weeks	51.0 PPM	60.0 PPM
6 weeks	53.0 PPM	73

The electrolyte initially had 1.8 PPM iron. It would appear that most of the corrosion takes place in the first week and then the can passivates.

A series of measurements were carried out to determine the rate at which lithium surfaces can scavenge iron from SOCl$_2$ electrolyte. Iron dissolved in SOCl$_2$ electrolyte is lower on the EMF series than metallic lithium and would be spontaneously reduced. However, the reduced iron would form a passivating film on the lithium surface, which would reduce the rate of iron reduction as a function of time.

Two flasks were prepared containing 29 and 137 PPM Fe as FeCl$_3$. Enough Li was put into each flask to approximate the lithium surface area/electrolyte volume ratio of an AA cell. Electrolyte samples from each flask were analyzed for iron after two and six weeks.

The iron concentrations determined by atomic absorption analysis were as follows:

TIME	PPM Fe originally in Flask	
2 weeks	137	29
6 weeks	59.2	26
6 weeks	48.4	22.3

The results indicate that the scavenging ability of the lithium foil diminishes as the initial iron concentration is reduced.

2.5 RESULTS OF ORGANIC IMPURITY ANALYSES

2.5.1 Analytical Results for Organic Solvent Extracts of Cell Components

The size of the samples of the various battery components extracted and the extraction method and solvents are listed in Table 8. The concentrated extracts (see Section 2.2) were analyzed by gas chromatography/mass spectroscopy (GC/MS) and the gas chromatograms are given in Figures 60 to 66. The mass spectograms for each of the major peaks of the gas chromatograms are given in Figures 65 to 77. The infrared spectra for the extracts with and without the spectrum of the processed extraction solvent subtracted are presented in Figures 78 to 84.

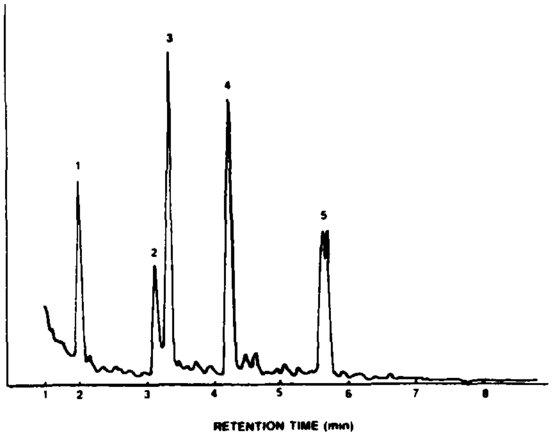

Figure 60: Gas Chromotographic Analysis of $AlCl_3$ Extract

TABLE 8

Extraction Conditions for the Analysis of Battery Components for Organic Impurities

Battery Component	Wt of Sample Extracted (g)	Extraction Method	Extraction Solvent*
Carbon Cathode	4.58	SOXHLET	Et_2O
1.8M $LiAlCl_4SOCl_2$	1700	2 PHASE	H_2O/Et_2O
LiCl	141.5	SOXHLET	Et_2O
$AlCl_3$	320	2 PHASE	H_2O/Et_2O
Crane Separator	0.342	SOXHLET	$SOCl_2$
Lydell Separator	0.736	SOXHLET	MeCl

*Abbreviations: Et_2O, Diethyl Ether; MeCl, Methylene Chloride

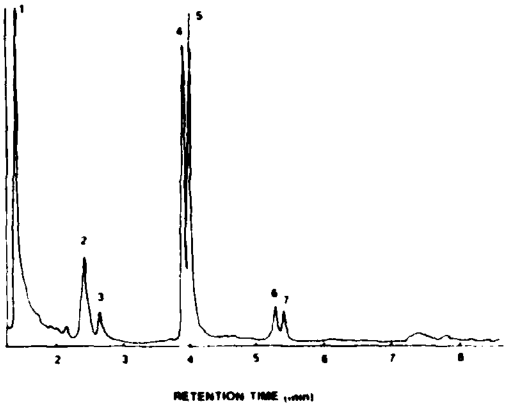

Figure 61: Gas Chromotographic Analysis of LiCl Extract

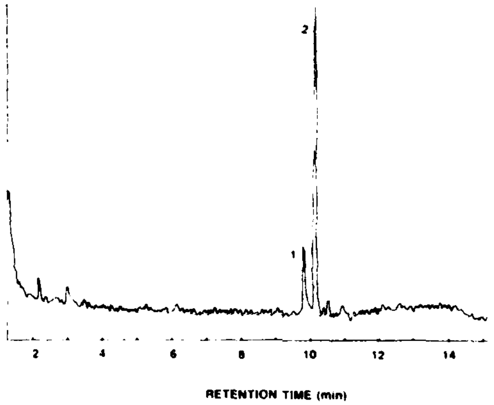

Figure 62: Gas Chromotographic Analysis of 1.8 M $LiAlCl_4/SOCl_2$ Electrolyte Extract

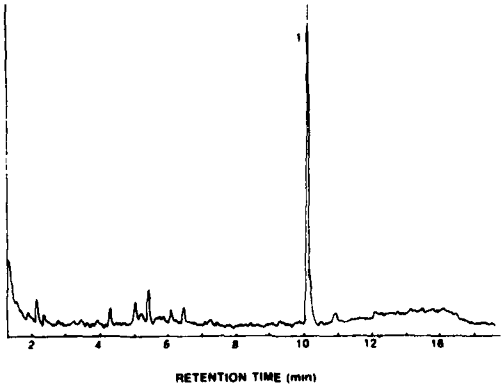

Figure 63: Gas Chromotographic Analysis of Carbon Cathode Extract

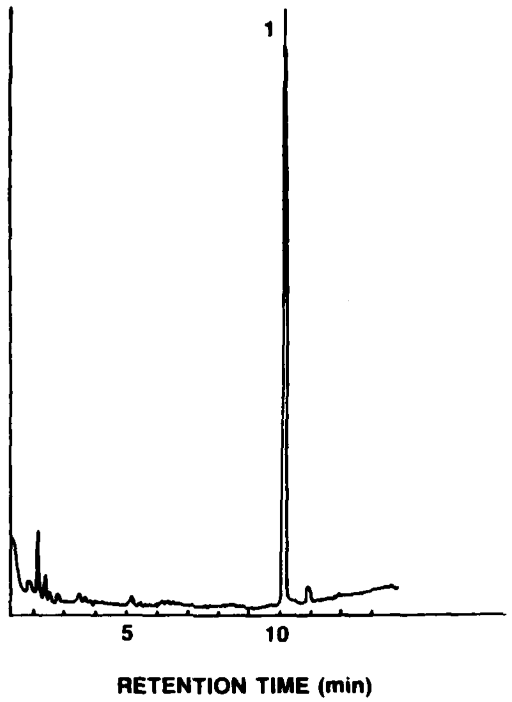

Figure 64: Gas Chromotographic Analysis of Processed Diethyl Ether Blank

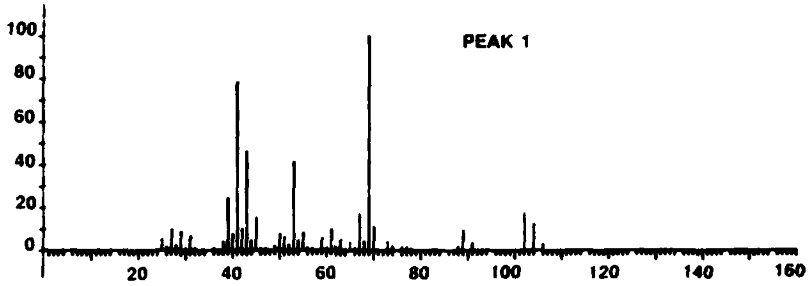

Figure 65: Mass Spectrogram of Peak 1 from Gas Chromotographic Analysis of $AlCl_3$ Extract

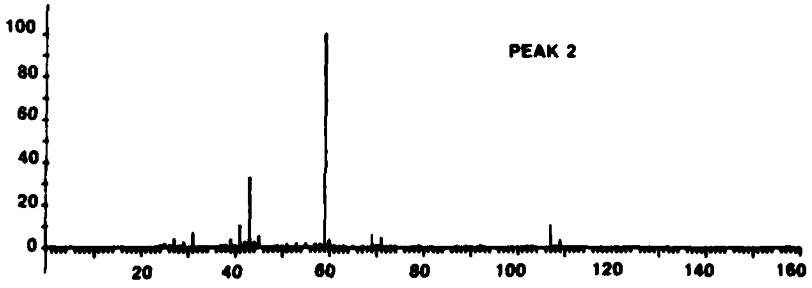

Figure 66: Mass Spectrogram of Peak 1 from Gas Chromatographic Analysis of $AlCl_3$ Extract (cf. Fig 58)

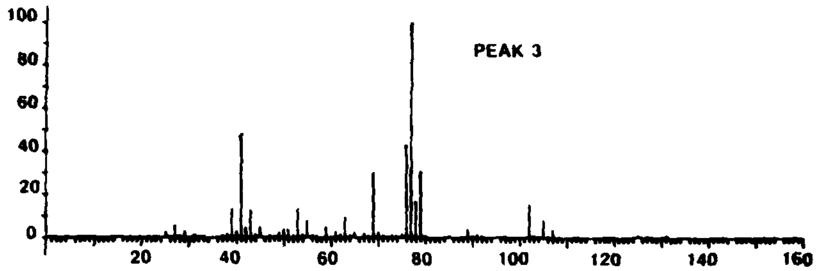

Figure 67: Mass Spectrogram of Peak 3 from Gas Chromatographic Analysis of $AlCl_3$ Extract

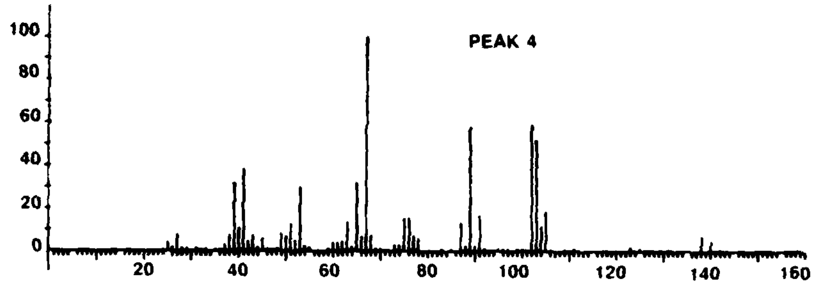

Figure 68: Mass Spectrogram of Peak 4 from Gas Chromatographic Analysis of $AlCl_3$ Extract

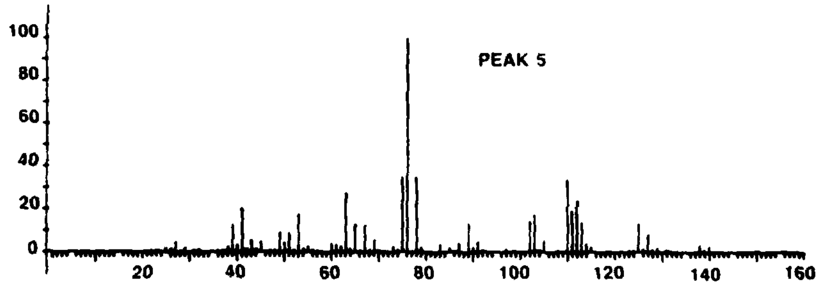

Figure 69: Mass Spectrogram of Peak 5 from Gas Chromatographic Analysis of $AlCl_3$ Extract

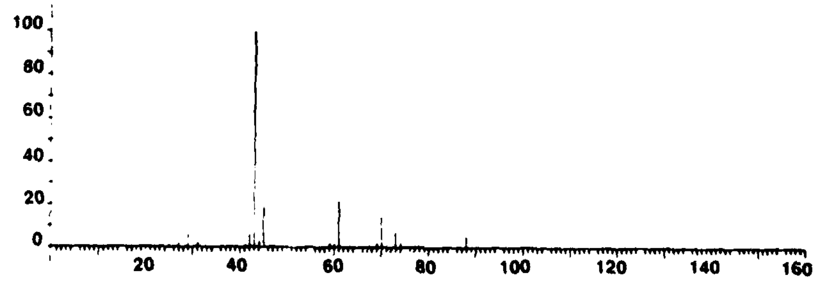

Figure 70: Mass Spectrogram of Peak 1 from Gas Chromatographic Analysis of LiCl Extract

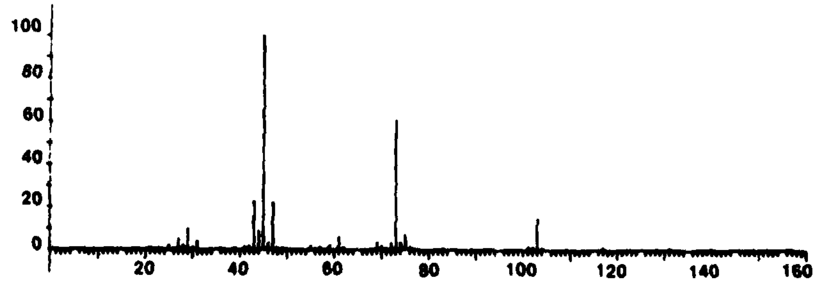

Figure 71: Mass Spectrogram of Peak 2 from Gas Chromatographic Analysis of LiCl Extract

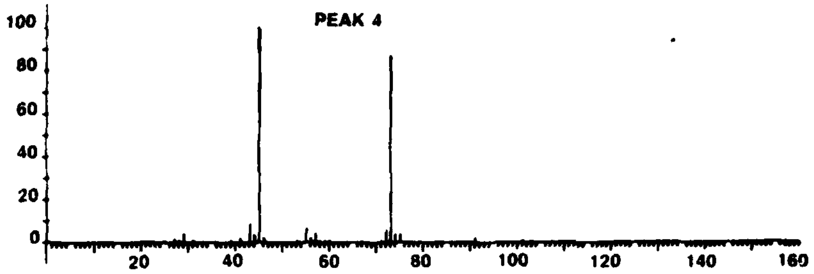

Figure 72: Mass Spectrogram of Peak 4 from Gas Chromatographic Analsysis of LiCl Extract

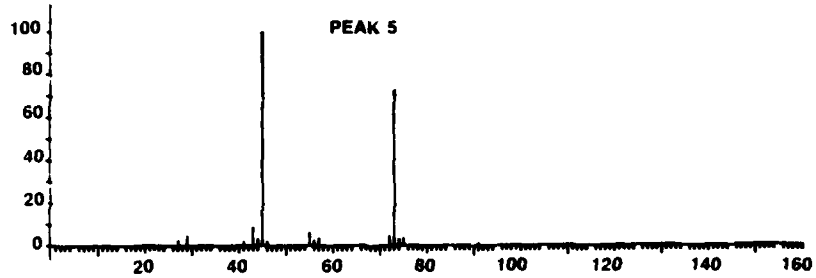

Figure 73: Mass Spectrogram of Peak 5 from Gas Chromatographic Analsysis of LiCl Extract

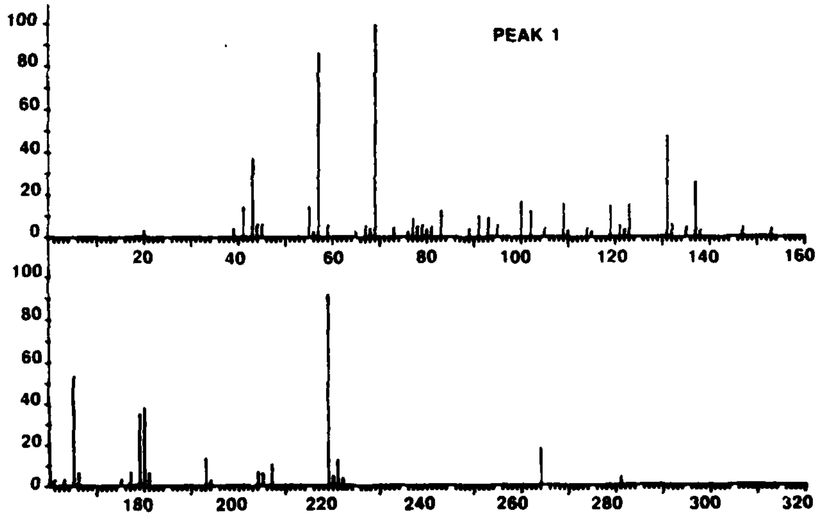

Figure 74: Mass Spectrogram of Peak 1 from Gas Chromatographic Analsysis of 1.8 M $LiAlCl_4$/ $SOCl_2$ Electrolyte Extract

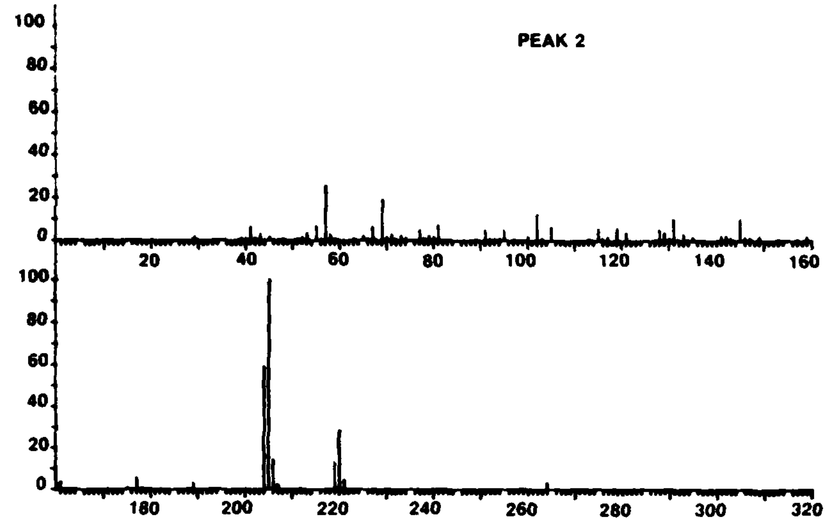

Figure 75: Mass Spectrogram of Peak 2 from Gas Chromatographic Analsysis of 1.7 M $LiAlCl_4$/$SOCl_2$ Electrolyte Extract

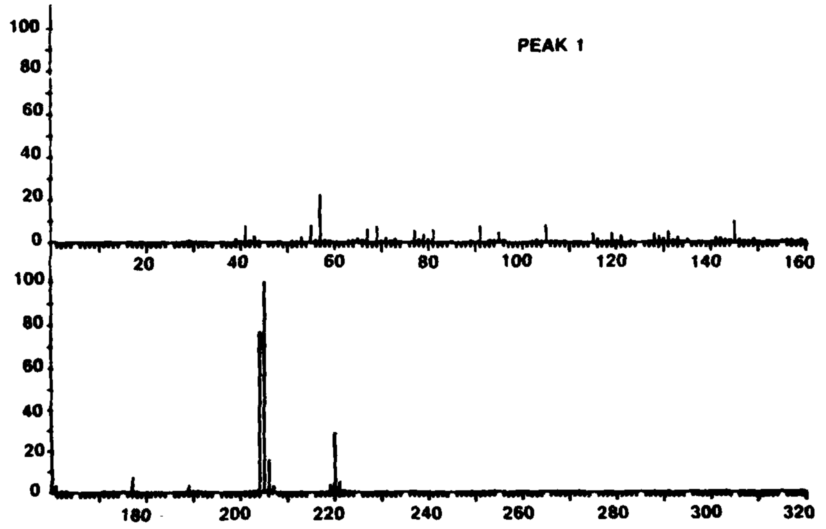

Figure 76: Mass Spectrogram of Peak 1 from Gas Chromatographic Analsysis of Carbon Cathode Extract

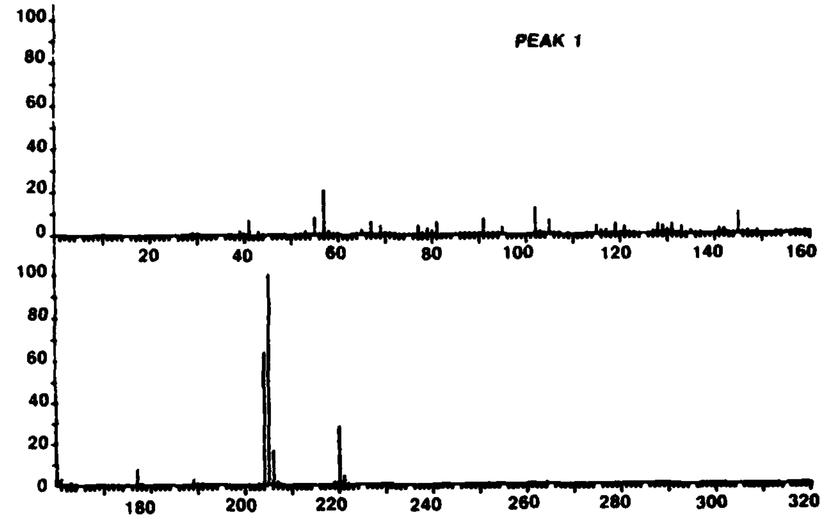

Figure 77: Mass Spectrogram of Peak 1 from Gas Chromatographic Analsysis of Processed Diethyl Ether Blank

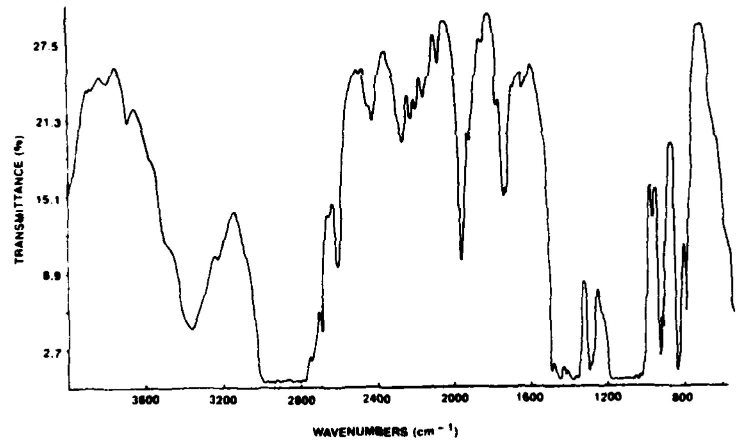

Figure 78: Infrared Spectrum of $AlCl_3$ Extract in Diethyl Ether

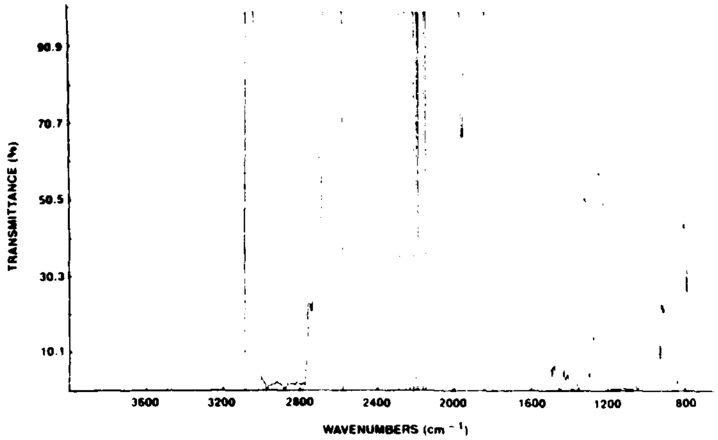

Figure 79: Infrared Spectrum of Processed Diethyl Ether Blank

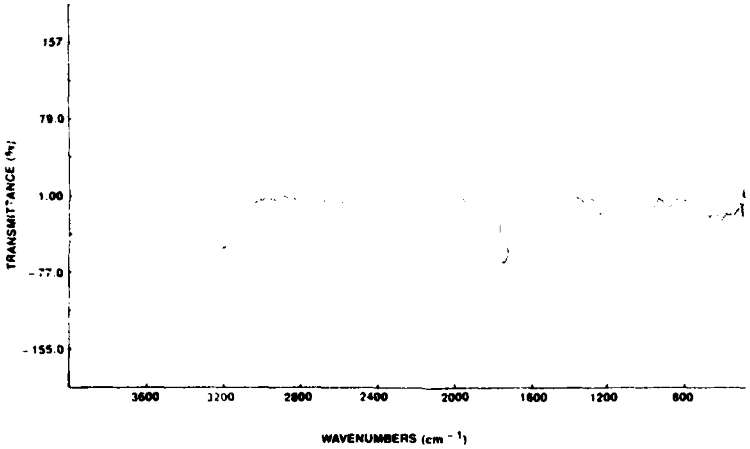

Figure 80: Infrared Spectrum of AlCl$_3$ Extract in Diethyl Ether with the Spectra of the Processed Diethyl Ether Blank Subtracted

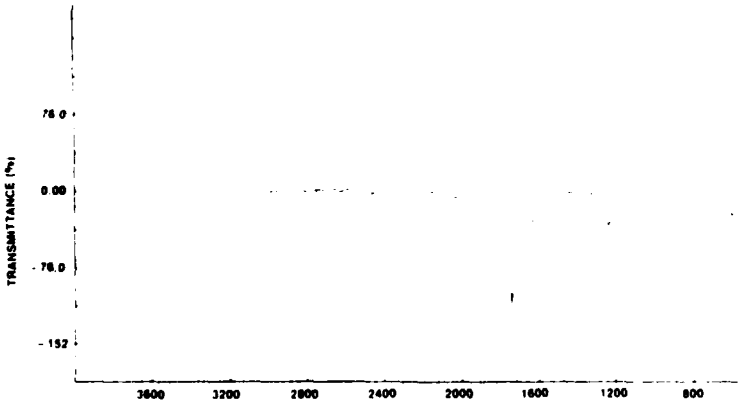

Figure 81: Infrared Spectrum of LiCl Extract in Diethyl Ether with the Spectra of the Processed Diethyl Ether Blank Subtracted

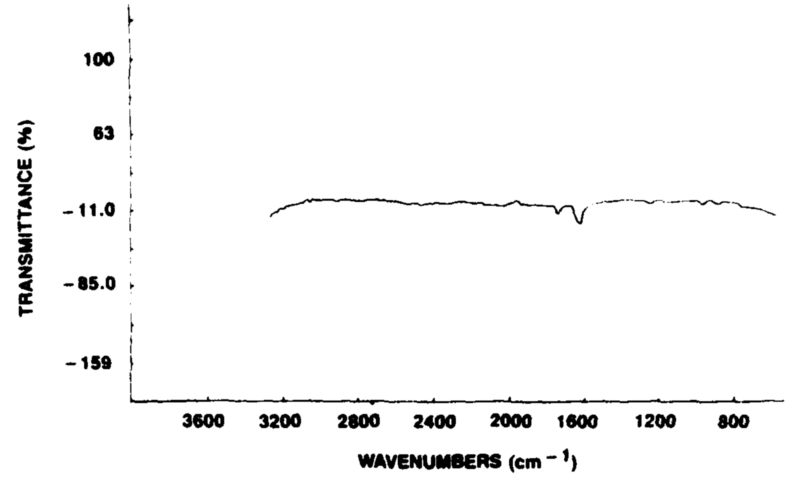

Figure 82: Infrared Spectrum of 1.8M $LiAlCl_4/SOCl_2$ Electrolyte Extract with the Spectra of the Processed Diethyl Ether Blank Subtracted

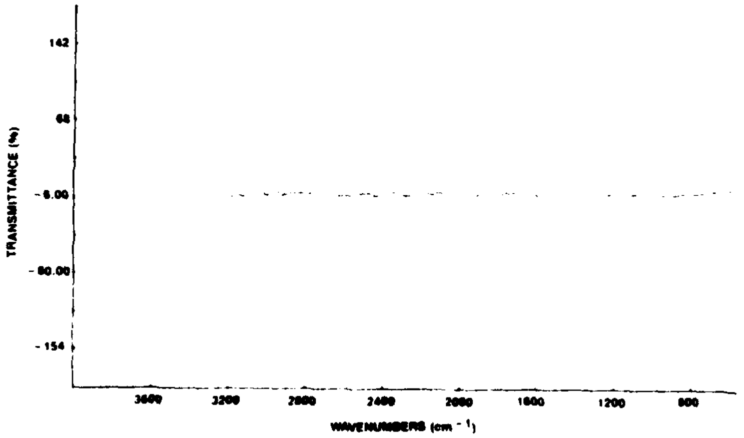

Figure 83: Infrared Spectrum of Carbon Cathode Extract with the Spectra of the Processed Diethyl Ether Blank Subtracted

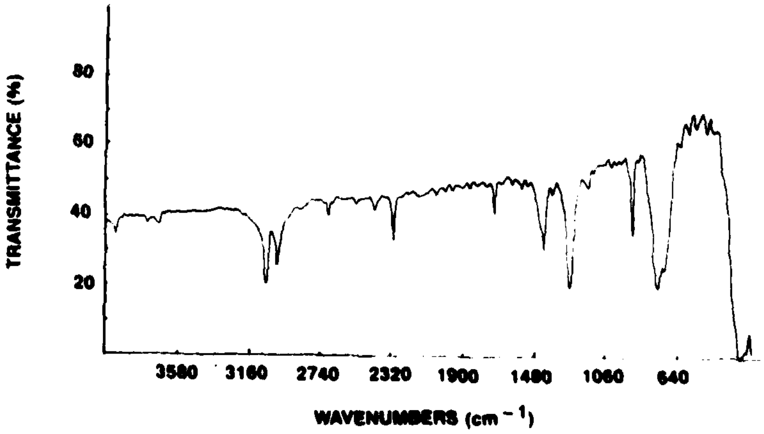

Figure 84: Infrared Spectrum of Lydall Separator Extract in Methylene Chloride

The GC/MS results show five and seven ether soluble impurities in $AlCl_3$ and LiCl respectively and only one in the 1.8M $LiAlCl_4/SOCl_2$ electrolyte extract. The GC/MS results for the carbon cathode extract did not reveal any impurities within the detection limits of the instrument. Peak two in the gas chromatogram for the electrolyte extract (cf. Figure 62) and Peak one for the carbon cathode extract (cf. Figure 63) yielded similar mass spectra (cf. Figures 75, 76, 77) as Peak one (cf. Figure 64) for the processed diethyl ether blank. Thus, all the above peaks are due to an impurity in the diethyl ether used for the extractions.

For our present objective of setting limits for impurities in the components used to manufacture $Li/SOCl_2$ batteries, we are primarily interested in knowing the total amount of ether soluble impurities present in each component rather than the exact composition of each of the organic impurities. From a knowledge of the sensitivity of the GC/MS, the amount of material extracted and the concentration factor due to evaporation of the extract, it is conservatively estimated that the total ether soluble impurities in the $AlCl_3$, LiCl, electrolyte and carbon cathode are less than 30 PPM, 100 PPM, 20 PPM, and 1% respectively. Because of the high sensitivity of the GC/MS it is possible that the ether soluble impurity levels are from one to three orders of magnitude lower than the values given above. The uncertainty in determining the impurity concentractions arises because the sensitivity of GC/MS and IR all depend on the nature of the compound being analyzed which is unknown. In the case of mass spectroscopy, the efficiency in which various organic compounds are ionized by the ionizing electron beam can vary over many orders of magnitude depending on the compound. Furthermore, the MS used for the measurements is sensitive only to positive ions which could cause a loss in sensitivity for halogenated compounds which are ionized preferentially to negative ions by the MS.

The very large samples of LiCl, $AlCl_3$ and electrolyte that were extracted account for the high sensitivities estimated for the analyses of these components. Although five and seven compounds were identified in the GC/MS results for $ALCl_3$ and LiCl respectively, the likelihood that concentrations of any of these compounds do not exceed 30 PPM in $ALCl_3$ and 100 PPM in LICl makes the identification of the exact composition of each of the organic impurities a low priority task. Compared to the 7 to 9 Wt% organic binder known to be present in Crane separator paper and the estimated 1% detection limit for ether soluble impurities in the carbon cathode, it is clear that materials with less than 100 PPM levels of impurities are presently of negligible concern.

In view of these priorities, the GC and IR results for $AlCl_3$, LICl and 1.8M $LiAlCl_4/SOCl_2$ electrolyte will be very briefly discussed. Comparing the mass spectra obtained for $AlCl_3$ with the EPA/NIH Mass Spectral Data Base (49) peaks 1, 2, 3 and 5 in Figure 60 were tentatively assigned to 1 chloro-2-methylbut-2-ene, silane (chloromethyl) dimethyl, 2-chloro-2-methyl butane and 2, 3 dichloromethyl butane. No identification was possible for peak 4. A similar comparison with the MS data base for the results for LiCl indicate that peaks 1, 4 and 5 in Figure 59 are the ether solvent peak and high molecular weight ethers. No identifications were possible for peaks 2, 3, 6 and 7 for LiCl.

The infrared spectra obtained for the $AlCl_3$ extract in diethyl ether with the Fourier transform spectrophotometer has too many large ether peaks (cf. Figure 78) to be able to detect trace organic impurities. However, after the IR spectra of the processed diethyl ether blank (i.e. Figure 79) was subtracted out using the data processing system of the FT-IR, two medium absorption peaks at 1745 cm^{-1} and 1238^{cm-1} remained as well as smaller peaks at 1632, 1322, 955.8 and 878.3 cm^{-1}. Similarly for the LiCl ether extract, medium peaks at 1745, 1632 and 1238 cm $_1$ and smaller peaks at 948 and 871 cm^{1} remained after the spectrum for the ether blank was subtracted out. It is unusual that both LiCl and $AlCl_3$ contained impurities with strong absorptions at 1745, 1632, and 1238 cm $_1$and it was thought that the samples were perhaps contaminated by some substance during processing. Acetone which was used to clean the glassware was suspected since the 1745 cm^{-1} band is characteristic of the C = O stretching vibration. However, acetone was eliminated since it absorbs at 1700 cm^{-1} not 1745 cm^{-1}. Methyl acetate has a C = O stretch at 1742 cm^{-1} and C-O stretches at 1241 and 1048 cm^{-1} but the C-H stretching vibration at 3000 cm^{-1} and the C-H bending at 1434 and 1369 cm^{-} present for methyl acetate are absent in the spectra for the LiCl and $AlCl_3$ extracts. The absence of the various C-H bands is largely due to the subtraction of these bands for the ether blank. From the present IR results it is only possible to tentatively conclude that an acetyl ketone and possibly other compounds such as esters are present in the LiCl and $AlCl_3$ extracts. Although the exact nature of the ether soluble impurities present in the LiCl and $AlCl_3$ extracts were not precisely identified, the GC/MS and IR results are of considerable value as fingerprints to characterize the impurities for quality control purposes.

The GC results from the 1.8M $LiAlCl_4/SOCl_2$ electrolyte extract shows two peaks. The mass spectra results indicate that Peak 1 is an isomer of Peak 2 and that Peak 2 is the same impurity as found in the processed ether blank which is thought to be 2,6 tert-butyl-4-methyl phenol. The FT-IR spectra for the electrolyte extract with the ether blank is given in Figure 82 and shows peaks at 1745, 1632, 1238, 963 and 878 cm^{-1}. The somewhat stronger peaks at 1745 and 1632 cm^{-1} are the same as those found in the LiCl and $AlCl_3$ extracts interpreted earlier but the 1632 cm^{-1} peak is stronger relative to the 1745 cm^{-1} peak. Comparing the GC/MS results obtained for the $SoCl_2$ electrolyte extract with those obtained for the $AlCl_3$ and LiCl extracts, it is clear that the numerous impurities found in the $AlCl_3$ and LiCl are not present in the $SOCl_2$ electrolyte. Thus the standard purification procedure during which the electrolyte is refluxed with Li foil most likely scavenges trace organic compounds from the electrolyte.

The GC results from the carbon cathode extract shows only one peak (cf. Figure 63) which is identified from the mass spectra as the 2,6 tert-butyl-4-methyl phenol from the processed ether blank. The infrared spectra presented in Figure 83 shows essentially a straight line and indicates the absence of impurities after the ether blank is subtracted out. The sensitivity of the measurements is however limited to approximately 1% since only 4.58 g of carbon cathode material was extracted. A relatively small amount of carbon cathode was extracted because the material has a very low density and 4.6 g was all that the Soxhlet extraction thimble would hold. If at some time in the future a more sensitive analysis for organic impurities in the carbon cathode is required, it is recommended that larger quantities of cathode (i.e. 100g) be extracted using a larger Soxhlet extractor and that the extracts from multiple ether extractions be combined and concentrated.

An infrared spectra for the extract from Lydell separator paper extracted with methylene chloride is given in Figure 84. The large absorptions at 1265, 896, 747 and 707 cm^{-1} are characteristic of methylene chloride but the peak at 2305 cm^{-1} appears to be new and may be due to an impurity. The 0.736 g sample size is clearly too small to achieve high sensitivity and to justify GC/MS analysis. Because the separators were known to contain polymeric binders which are not soluble in low boiling organic solvents, it was decided to determine the amount of organic impurities by measuring the weight loss after high temperature pyrolysis. The results of the high temperature pyrolysis tests are discussed in the next section.

2.5.2 Analytical Results for Organic Content of Separators

The amount of organic material present in five separator materials was determined by measuring the weights before and after the separators had been heated to approximately 800°C. The organic content of the separators determined using this technique are listed in Table 9. The high organic content of the Mead and Crane glass fiber separators was expected since it was known that the separators used polyacrylic and polyvinyl alcohol binders respectively. However, the Lydell separator was described as binderless by the manufacturer and therefore the 3.71% weight loss found on heating indicates that the separator may contain other organics such as anti-static agents or surfactants.

TABLE 9

Organic Content of Separators

Separator	Wt Before Heating (g)	Wt After Heating (g)	Percent Organics
Lydall (Test 1)	0.3528	0.3397	3.71
Mead	0.1277	0.1187	7.05
Craneglass 200	0.1119	0.1009	9.83
Craneglass 200*	0.2012	0.1856	7.76
Paulflex E-8.7X	0.3451	0.3409	1.23
Al-2 Alumina	0.6111	0.5982	2.16

Lower temperature heat treatment

All the separators were stored in the 4% R.H. dry room for at least one week so that the weight loss due to simple water loss on heating would be minimal. To investigate whether the water loss was indeed minimal and that the weight loss was due to the pyrolysis of organic materials, a 0.332 g sample of Crane separator was treated at 150, 175, 400 and 500°C and weighed successively. The weights and percentage weight losses after each stage of treatment are listed in Table 10. The weight losses found for the heat treatment of the Crane separator agree well with the thermogravametric measurements of Krischer (50) for polyvinyl alcohol (PVA). Krischer found that the decomposition of PVA begins at approximately 125°C and increases in rate until 200°C, then plateaus between 200 and 325°C then increases in rate between 350 to 425, reaching a plateau of 460°C. Thus, the 0.90% weight loss found for the Crane paper when it was heated at 150°C for 8 hours may be partially due to decomposition of the PVA.

TABLE 10

Weight Loss of Crane Separator Paper After Treatment at Various Temperatures

Treatment Conditions	Wt Before Treatment (g)	Wt After Treatment* (g)	Wt Loss (%)
Initial	0.3320	0.3320	0
8 hrs, Vacuum, 150°C+	0.3320	0.3290	0.90
4 hrs, 275°C, Air	0.3290	0.3158	4.01
4 hrs, 400°C, Air	0.3158	0.3041	3.70
4 hrs, 500°C, Air	0.3041	0.3018	0.75
		Total Wt. Loss	9.35

* All weights were taken after the sample had cooled to 24°C at 4% R.H.

\+ The weights at 150°C were constant after a second 1 hr under vacuum.

The Crane separator turned brown after treatment at 275°C and it could be seen that the brown color was due to individual strands of brown fiber woven into the glass paper. Microphotographs were taken and are on file. It appears that the PVA is utilized in the Crane separator as either fibers of solid PVA woven into the glass fabric or that some of the glass fibers are coated with PVA then woven into the separator during its manufacture. After treatment at 400°C the Crane separator was white, and brown fibers were no longer visible. Also, the Crane separator had a smooth texture and was easier to break apart. The rust color of PVA as the material undergoes pyrolysis at moderate temperatures has been reported in the literature.

2.5.3 Gas Evolution Results for Separators Immersed in $SOCl_2$ Electrolyte

To determine whether the organic polymer binders present in glass fiber separators react with $SOCl_2$ electrolyte at 25°C to evolve gas, tests were carried out in sealed glass pressure tubes containing mercury manometers. The gas pressures measured in the tubes containing the separators in $SOCl_2$ electrolyte over periods greater than 800 hrs are shown in Figures 85-87 and Table 11. Of the four glass fiber separators tested the Lydall No. 991 showed the least amount of gas evolution closely followed by the Mead separator and the Lydall separators with Tefzel[2] and Halar[3] binders.

Comparing the results of the tests with and without Li present in Figure 85 the greater gas evolution with Li present is particularly noticeable. Taking into account that the test with Li used a smaller amount of Crane separator (i.e. 0.2069 vs 0.3926 g) the gas pressure with Li present was 292% greater. Without Li foil in contact with the evolved gas, the polyvinyl alcohol binder of the Crane separator would react with $SOCl_2$ electrolyte as follows:

$$ROH + SOCl_2 \rightarrow RCl + HCl + SO_2$$

However with Li present the HCl would react further to form H_2:

$$HCl + Li \rightarrow LiCl + 1/2\ H_2$$

---

[2] Tefzel is the DuPont trade name for a copolymer of ethylene and tetrafluoroethylene (FTEE) which has undergone certain proprietary modifications.

[3] Halar is a copolymer of ethylene and chlorotrifluoroethylene manufactured by Allied Chemical.

TABLE 11

The Chemical Stability of Mead and Lydall No. 991 Binderless Separator Paper in 1.8M $LiAlCl_4/SOCl_2$ Electrolyte

in Terms of Evolved Gas Pressure at 25°C.

Reaction Time (hours)	Pressure* (atmos.)	Temperature (°C)
I. Lydall No. 991 Separator		
0.0	0.00	25
48	0.00	25
218	0.00	25
243	0.00302	24.2
411	0.0040	25.2
579	0.00118	25.0
891	0.0293	25.6
II. Mead Separator		
0.0	0.0	25
72	0.0	25
408	0.012	25
576	0.020	25
816	0.020	25
III. Control Test without Separator		
0.0	0.00	25
24	0.00	25.4
232.5	0.00	22.8
576	0.0081	25.2
840	0.0097	24.8
1056	0.0097	25.0

*The free gas space of the tubes is ≈ 20 ml. The Lydall separator sample measured 4.0 x 9.48 cm, was 0.71 mm thick and weighed 0.3342 g.

The higher gas pressure with Li is thought to be due not to additional evolved gas but to a much lower solubility of H_2 in $SOCl_2$ electrolyte than HCl. Furthermore the test with Li used only 1 ml of $SOCl_2$ electrolyte compared to 4 ml for the test without Li, therefore there was much less electrolyte to dissolve the evolved gas.

To put the gas evolution results into a more meaningful form in terms of battery design, the results were used to calculate the pressures which would be produced in a 10,000 Ahr MESP (1, 51) prismatic $Li/SOCl_2$ cell. Taking into account the 5.98 liter free gas space of an MESP cell and the $1.2 \cdot 10^5$ cm^2 area of Crane separator used, it is estimated that the pressure build up of 0.28 atmospheres in the small glass pressure tube without Li after 895 hrs would correspond to 0.783 atmospheres or 11.5 psi in a MESP cell. Because of the slow reaction of Hg in the manometer with $SOCl_2$, the 0.289 atmosphere reading for the pressure tube with the Crane separator at 895 hours was reduced by 0.009 atmospheres, the pressure of the control to give a corrected pressure of 0.280 atmospheres.

Repeating the above calculations using the results shown in Figure 85 for Crane glass separator with Li foil, it was estimated that the reaction would produce a pressure buildup of 33.6 psi in a MESP cell after 915 hrs at 25°C. No correction was made for the increase in the gas solubility in the electrolyte of the MESP cell due to the higher gas pressure as a result of Henry's Law because the required solubility pressure data are not yet available.

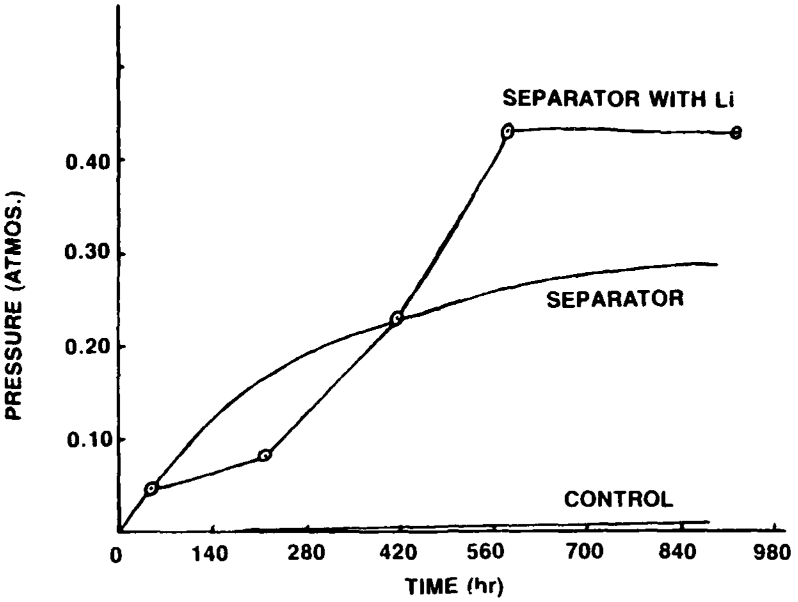

Figure 85: The Chemical Stability of Glass Separator Paper with Binder in 1.8M $LiAlCl_4/SOCl_2$ Electrolyte in Terms of Evolved Gas Pressure at 25°C without and with Lithium Foil. The Crane separator (Spec. 310) sample without Li foil had an area of 191.60 cm ± and a weight of 0.39262 g. The Crane separator with Li foil had an area of 70.8 cm ± and a weight of 0.20692 g and was wound with 0.015 in. thick Li foil of area 70.8 cm ±. The free gas space of the tubes is ~ 20 ml and the samples with and without Li used 1.0 and 4.0 ml of 1.8M $LiAlCl_4/SOCl_2$ electrolyte respectively.

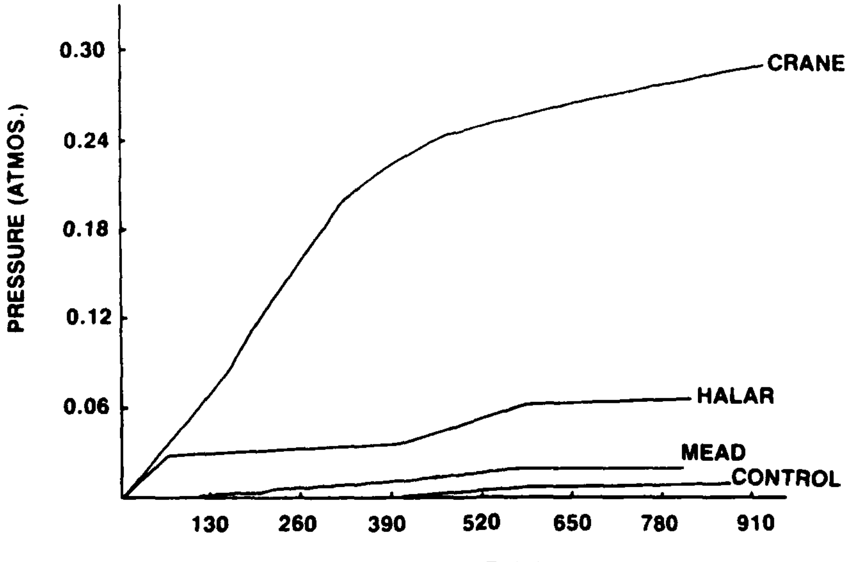

Figure 86: The Chemical Stability of Three Separator Materials in 1.8 $LiAlCl_4/SOCl_2$ Electrolyte in Terms of Evolved Gas Pressure. The sample of Crane, beta glass separator, spec 310 had an area of 141.6 cm ± and a weight of 0.3926 g. The Mead and Lydall separators with 10% Halar each had an area of 100.0 cm ± and weighed 0.2589 gm and 0.7664 gm respectively. The separators were each immersed in 4.0 ml of 1.8M $LiAlCl_4/SOCl_2$. Each tube had a free gas space of ≃ 20 ml.

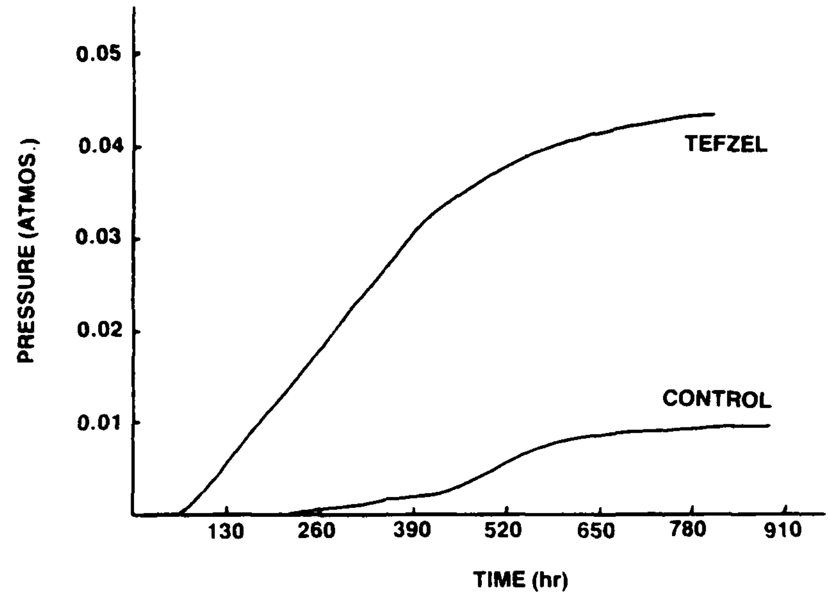

Figure 87: The Chemical Stability of Lydall Separator with 10% Tefzel Binder in 1.8M $LiAlCl_4/SOCl_2$ Electrolyte in Terms of the Evolved Gas Pressure at 25°C. The sample had an area of 100.0 cm ± and a weight of 0.6238g and was saturated with 4.0 ml of 1.8M $LiAlCl_4/SOCl_2$ electrolyte. The free gas space of the tubes was ≃ 20 ml.

For the Lydall separator with 10% Tefzel as binder (cf. Figure 87) the gas pressure in the sealed glass tube with the separator was 0.044 atmos. after 816 hrs at 25°C. It is estimated that the above pressure would correspond to 0.89 psi in a 10 KAhr MESP cell. This would amount to approximately 13 times less gas evolution compared to the Crane glass separator which earlier tests estimated would produce 11.5 psi pressure in an MESP cell after a similar period. Thus, the results of the gas evolution suggest that the Lydall separator with 10% Tefzel as binder would be an excellent replacement for the Crane separator if it can also meet various other mechanical and electrical requirements.

Gas evolution results with Mead glass fiber separator with 5% acrylic binder show a pressure of 0.012 atmos after 336 hrs. at 25°C. This is approximately 1800% less gas than produced by Crane separator after a similar period at 25°C.

Since Mead separator has been used in the past because of its favorable mechanical properties, it is recommended that it be reinvestigated for other applications.

It is also recommended that work should be carried out to characterize the mechanical properties and the cell performance characteristics of Mead, Lydall and other separators from −40 to 70°C. The mechanical properties of interest would include the stretch modulus, the elastic limit and a measure of the puncture resistance. If a separator is selected on the basis of superior cell performance which contains a binder, then additional testing should be carried out to determine whether the binder reacts with or is soluble in $SOCl_2$ electrolytes.

2.6 REACTION OF HYDROGEN WITH SULFUR DIOXIDE

Hydrogen gas will result when organic impurities or water react with $SOCl_2$ to produce HCl which then reacts with Li to produce hydrogen. An extensive literature dealing with the reaction between H_2 and SO_2 was expected because the reaction could occur as a side reaction in the petroleum refining and smelting industries. A literature search was therefore undertaken since it was likely that an abundance of published data would eliminate the need for any new experimental measurements.

A search of Chemical Abstracts and an evaluation of the more suitable references indicated that the papers by Murdock (52) and Lepsoe (53) are the most relevant to reactions in $Li/SOCl_2$ cells. In brief, it is well established that hydrogen and sulfur dioxide do not react at temperature below 500°C in the absence of a catalyst, but the reaction does occur at temperatures as low as 200°C in the presence of molten sulfur which serves as a catalytic agent. The thermodynamics of the reaction of hydrogen and sulfur dioxide have been treated comprehensively by Lepsoe (53). Since the complex kinetics of the reaction between H_2 and SO_2 has been reviewed in detail by Murdock (52), the kinetics will not be summarized here.

2.7 CONCLUSIONS FOR PART II

From the chemical analysis of the reagents and cell components used in $Li/SOCl_2$ cell construction and cell discharge tests with cells containing known amounts of impurities, information was gained pertaining to the impact of several key impurities on cell performance and hazards. In the case of hydrolysis products (i.e. water), iron and organic impurities present in the separator, sufficient information was gained to recommend concentration limits required to achieve maximum performance.

It was concluded from the results of voltage delay and discharge tests with 60 $Li/SOCl_2$ cells that up to 100 PPM water can be added to the electrolyte without detrimental effects in terms of capacity and voltage delay. At water levels above 100 PPM, voltage delay and hydrogen gas generation can become problems depending on the specific application. Up to 100 PPM water added to the electrolyte has no detrimental effect on voltage delay for cells stored one month at 55°C and discharged at 3 mA/cm^2 at 25°C. For more demanding conditions such as longer term storage at temperatures above 55°C or for start up at temperatures below 25°C or rates higher than 3 mA/cm^2, additional testing will be required to determine the upper permissible water concentration.

The results of tests with 30 $Li/SOCl_2$ cells with 5, 20 and 100 PPM of soluble iron added to the electrolyte indicate that serious voltage delay will occur unless the iron concentration is held to a concentration of 5 PPM or lower. The voltage delay conditions, similar to those for water contamination are after one month of 55°C storage for discharge at 3 mA/cm^2 at 25°C. Since 1.8M $LiAlCl_4/SOCl_2$ electrolyte generally contains approximately 1.8 PPM iron, it is recommended that the iron concentration be limited to 1.8 to 3.0 PPM. Because every $Li/SOCl_2$ battery application has different storage and performance requirements, the tradeoffs between the expenses of high purity materials and performance will be different and will have to be calculated on an individual basis.

Analysis of diethyl ether extracts of the $AlCl_3$, LiCl, electrolyte and carbon cathode indicate that total ether soluble organic impurities are less than 30 PPM, 100 PPM, 20 PPM and 1 Wt% respectively. Compared to the 7.8 and 7.0% organic binder present in the Crane and Mead separator papers, it is clear that the organic impurities present at concentrations below 500 PPM are of negligible importance relative to battery performance or hazards. Although impurities were not detected by infrared or gas chromatographic analysis of the extracts from the carbon cathode, it is recommended that larger quantities of cathode (i.e. 100 g instead of 4.6 g) be extracted to increase the sensitivity of the analysis from 1% to 0.05%.

The most serious problem involving organic impurities that was identified involved gas evolution due to a reaction between the organic polymer binder in separators and $LiAlCl_4/SOCl_2$ electrolyte. Crane, spec 310 beta glass separator which is widely used in $Li/SOCl_2$ commercial cells was found to continuously evolve gas for over 500 hrs at 25°C. The pressure of the gas evolved was measured and calculations show that the evolved hydrogen gas could produce a pressure buildup of 33.6 psi in a 10,000 Ahr MESP cell after 915 hrs at 25°C. The calculations neglected solubility of hydrogen in $SOCl_2$ electrolyte since the solubility is unknown but expected to be small.

The organic content of five separators used in $Li/SOCl_2$ cells was determined by measuring the weight loss after pyrolysis in air at approximately 800°C. The Lydall No. 991 binderless glass fiber separator was found to contain 3.71 Wt% combustible material but it was observed to evolve only negligible quantities of gas during immersion in $SOCl_2$ electrolyte for 816 hrs at 25°C. Although it would appear that the Crane separator should be replaced by either the Mead or Lydall No. 991 separator, the mechanical properties of the Crane separator are well characterized and the amounts of gas generated is acceptable in 10,000 Ahr MESP cells with suitably designed pressure release valves.

Before the Mead or another separator can be used to replace the Crane separator, much more information is required concerning the effect of the separator on the high rate discharge performance and the ability of the separator to prevent short circuits resulting from mechanical abuse. It is recommended that such information relative to separator performance be obtained as part of Task III.

REFERENCES

1. F. Goebel, R.C. McDonald and N. Marinic, "Proc. 29th Power Sources Symp.," Atlantic City, N.J., June 1980.
2. A.N. Dey, Thin Solid Films, 43, 131 (1977).
3. J.J. Auborn, K.W. French, S.I. Liberman, V.K. Shah and A. Heller, J. Electrochem. Soc., 120, 1613 (1973)
4. W.K. Behl, J.A. Christopulos, M. Ramirez, and S. Gilman, J. Electrochem. Soc. 120, 1619 (1973) Report ECOM-4101 (April 1973).
5. A.N. Dey, Proc. 27th Power Sources Symp., Atlantic City, N.J. 42 (1976).
6. *A.N. Dey, Contract No. DAAB07-74-C-0109, Final Report,* ERADCOM-74-0109 (July 1978).
7. J.F. McCartney, W.H. Shipman and C.R. Gunderson, Proc. 11th IECEC, 457 (1976)d.
8. L. Marcoux, NASA Goddard Space Flight Center Battery Workshop, NASA Conference Publication 1982.
9. W.P. Kilroy and S.D. James, J. Electrochem Soc. 128, 934 (1981).
10. W.L. Bowden and A.N. Dey, J. Electrochem. Soc. 127, 1419 (1980).
11. C.R. Schlaikjer, F. Goebel, and N. Marinic, J. Electrochem. Soc. 126, 513 (1979).
12. P. Bro, J. Electrochem. Soc. 125, 674 (1978).
13. A.N. Dey, "Proc. 28th Power Sources Symp.," Atlantic City, N.J., June 1978.
14. D.M. Allen and W.S. Bishop, "Proc. 30th Power Sources Symp.," Atlantic City, N.J. (1982).
15. A.M. Dey, W. Bowden, J. Miller and P. Witalis, Contract No. DAAB07-78-C-0563, First Quarterly Report. ERADCOM, DELET-TR-78-0563-1, April (1979).
16. W.C. Merz and C.R. Walk, Contract No. N66001-77-C-0284, Final Report, Naval Ocean Systems Center. AD A 087669, August (1978).
17. K.A. Klinedinst, Abstract No. 7s6, Electrochemic Society, Fall Meeting (1981).
18. N. Doddapaneni, Abstract No. 83, Electrochemical Society, Fall Meeting (1981).
19. W.K. Behl, "Proceedings 27th Power Sources Symposium", Atlantic City, N.J., June 1976.
20. W.K. Behl, J. Electroanal. Chem. 101, 367 (1979).
21. G.E. Blomgren, V.Z. Leger, T. Kalnoki-Kis, M.L. Kronenberg, and R.J. Brodd, in "Proceedings 11th Internat. *Power Sources Symposium," Brighton, England, 583 (1978).*
22. W. Bowden and A.N. Dey, J. Electrochem. Soc. 126, 2035 (1979).
23. L. Friedman and W.P. Wetter, J. Chem. Soc., A 36 (1967).
24. K. French, P. Cukor, C. Persiani, and J. Auborn, J. Electrochem. Soc. 121, 1045 (1974).
25. C.A. Young, J. Electrochem. Soc. 128, 1292 (1981).
26. W.L. Bowden and A.N. Dey, J. Electrochem. Soc. 128, 1292 (1981).
27. A.J. Bard, Anal. Chem. 33, 22 (1961).
28. R.P. Martin and D.T. Sawyer, Inorganic Chem. 11, 2644 (1972).
29. C.L. Gardner, D.T. Fouchard and W.R. Fawcett, J. Electrochem. Soc. 128, 2337 (1981).
30. C.L. Gardner, D.T. Fouchard and W.R. Fawcett, J. Electrochem. Soc. 128, 2345, (1981).
31. Y. Bedfer, J. Corset, M.C. Dhamelincourt, F. Wallart and P. Barbier, J. Power Sources, 9, 267, (1983)
32. A.J. Bard and L.R. Faulkner, 'Electrochemical Methods, Fundamentals and Applications', John Wiley & Sons, New York pg. 232 (1980).

33.K.A. Klinedinst and M.L. McLaughlin, J. Chem. Eng. Data, 24, 203 (1979).

34. A.J. Bard, Anal. Chem. 33, 11 (1961).
35. R.P. Martin, W.H. Doub, J.L. Roberts and D.T. Sawyer, Inorg. Chem. 12, 1921 (1973).
36. D.F. Burow in "The Chemistry of Non-Aqueous Solvents," J.J. Lagowski
37. N. Marincic and A. Lombardi, U.S. Army Final Report, ECOM-74-0108-F (April 1977).
38. A.N. Dey, U.S. Army, ERADCOM, Final Report, DELET-TR-74-0109-F (July 1978).
39. *D.R. Cogley and M.J. Turchan, U.S. Army, Second Quarterly Report, ECOM-0030-2 (Mary 1974).*
40. A.W. Adamson, 'Physical Chemistry of Surfaces', Second Edition, Interscience Publishers, New York (1967).
41. R.J. Staniewicz and R.A. Gary, J. Electrochem. Soc. 126, 981 (1979).
42. J.R. Driscoll, G.L. Holleck, P.G. Gudrais and S.B. Brummer, U.S. Army, Thirteenth Progress Report, ECOM-74-0030-13, (June 1977).
43. A.M. Dey, U.S. Army, ECOM-74-0109-10, (Dec. 1976).
44. J.J. Auborn and N. Marincic, Proc. 9th International Power Sources Symposium, Pg. 683, Academic Press, London 1975.
45. N. Marincic, J. Applied Electrochem. 313 (1975).
46. D. Morley and R.J. Solar, Proc. 28th Power Sources Symposium, Atlantic City, N.J., 232 (1978).
47. D.L. Chua, W.C. Merz and W.S. Bishop, Proc. 27th Power Sources Symposium, Atlantic City, N.J., 33 (1976).

48. M.J. Harney and S. Brown, Abstract No. 72 Electrochemical Society, Fall Meeting (1979).
49. S.R. Heller and G.W.A. Milne, EPA/NIH Mass Spectral Data Base, National Bureau of Standards, NSRDS-NBS 63, U.S. Department of Commerce (1978).
50. B. Kaesche-Krischer, Chem. Ing. Tech. 37, 944 (1965).
51. N. Marincic and F. Goebel, Proc. 28th Power Sources Symposium, Atlantic City, N.J., P. 244 (1978).
52. D.L. Murdock and G.A. Atwood, Ind. Eng. Chem., Process Des. Develop. 13, 254 (1974).
53. R. Lepsoe, Ind. Eng. Chem. 30, 92 (1938).

APPENDIX A

The Silver-Silver Chloride Reference Electrode

A. 1 Preparation of the Ag/AgCl Reference Electrode

The Ag/AgCl reference electrodes were prepared by first electrolytically depositing 36 coulombs of Ag on a 5 cm, 1 mm dia. Ag wire (m3N) froma 3M KCN-0.5M $AGNO_3$ aqueous solution. Next, the electrodes were chloridized in 0.1M NaCl in MeOH for 0.67 hr at 5 mA following the procedure of MacInness and Beattie (1). The resulting electrodes were plum colored and were stored in dilute NaCl in water which had been degassed with argon. The procedure used to prepare the Ag/AgCl electrodes was selected based on recommendations from the review by Janz and Taniguchi (2).

The Ag/AgCl reference electrodes were enclosed in 7 mm dia. glass tubes with 5 mm dia. sintered glass frits at the tip as a precaution to improve the stability and life of the electrode. It was observed that the plum colored Ag/AgCl electrodes rapidly turned white in $TBAPF_6$/DMF solutions to which 30 mM of 1.8M $LiAlCl_4/SOCL_2$ had been added. It is not known if the white color was due to the white allotropic form of AgCl mentioned by Janz (2) or due to the oxidation of AgCl to some Ag (II) compound such as $AgCl_2$ by $SOCl_2$. The plum colored Ag/Cl electrodes protected by the frits did not turn white in DMF solutions containing $SOCl_2$ electrolytes.

The solubility of AgCl in DMF has been reported as 0.1M and $6.63 \, . \, 10^{-4}$M in references (3) and (4) respectively. In the eventuality that the AgCl solubility was as high as 0.1M, the AG/AgCl electrode was enclosed with a fritted tube. It was thought that enclosing the electrode would both increase its life and prevent erratic potentials due to natural convection during voltammetry or slow dissolution during the coulometry experiments which involve stirring with a magnetic stirrer. During an exploratory coulometry experiment it was found that stirring caused the OCP potential of the Ag/AgCl reference electrode to anodically polarize about 21 mV. The potential rapidly recovered as soon as the stirring was stopped. The potential of the Ag/AgCl electrode enclosed with a frit changed less than 2 mV from the unstirred to stirred condition.

A.2 Characteristics of the Ag/AgCl Reference Electrode in 0.1M $TBAPF_6$/DMF

The potential between two Ag/AgCl electrodes with frits was monitored in 0.1M $TBAPF_2$/DMF for 72 hrs at 25°C and the potential changed less than ± 1 mV. To characterize the behavior of the reference electrode under a prolonged galvanostatic load two Ag/AgCl electrodes without frits were discharged at 16 μA total current. Under these severe load conditions the potential between the electrodes increased only 15.9% from 0.038 V to 0.357 V in 20 minutes. These and other tests indicated that the Ag/AgCl reference electrode has acceptable stability, capacity, polarization characteristics and life for the present investigation.

The Ag/AgCl electrode witha 5 mm sintered glass frit as shown in Figure 1 were observed to have a potential of 3.42 ± 0.00 V vs a Li reference electrode in 0.1M $TBAPF_6$/DMF electrolyte.

REFERENCES (Appendix A)

1. D.A. MacInnes and J.A. Beattie, J. Am. Chem. Soc. 42, 117 (1920).
2. G.J. Janz and H. Taniguchi, Chem. Reviews 53, 397 (1953).
3. J.C. Synott and J.N. Butler, Anal. Chem. 41, 1890 (1969).
4. "*Dimethyl Formamide*," E.I. duPont Co. (Inc.) Product Bulletin, 1980. Editor, Volume III, Academic Press, N.Y. (1970).

☆U.S.Government Printing Office: 1984 - 759-062/919

F

8